REACHABLE SET CONTROL FOR PREFERRED AXIS HOMING MISSILES

By

DONALD J. CAUGHLIN, JR.

A DISSERTATION PRESENTED TO THE GRADUATE SCHOOL
OF THE UNIVERSITY OF FLORIDA IN
PARTIAL FULFILLMENT OF THE REQUIREMENTS
FOR THE DEGREE OF DOCTOR OF PHILOSOPHY

UNIVERSITY OF FLORIDA

1988

To Barbara

Amy

Jon

ACKNOWLEDGMENTS

The author wishes to express his gratitude to his committee chairman, Dr. T.E Bullock, for his instruction, helpful suggestions, and encouragement. Appreciation is also expressed for the support and many helpful comments from the other committee members, Dr. Basile, Dr. Couch, Dr. Smith, and Dr. Svoronos.

TABLE OF CONTENTS

LIST OF FIGURES

KEY TO SYMBOLS

$a(\cdot)$	Reference control input vector.
a_{Mx}	Missile inertial x axis acceleration.
a_{Tx}	Target inertial x axis acceleration.
A_x	Specific force (drag) along X body axis.
A_{zb}, A_{yb}	Desired linear acceleration about Z and Y body axes.
$B(\cdot)$	Reference control input matrix.
$C(\cdot)$	Reference state output matrix.
$D(\cdot)$	Feedforward state output matrix.
D_0	Stability parameter - Equilibrium drag coefficient.
$D0_{wt}$	Stability parameter - Change in drag due to weight.
D_u	Stability parameter - Change in drag due to velocity.
$D\alpha$	Stability parameter - Change in drag due to angle of attack.
$D\dot{\alpha}$	Stability parameter - Change in drag due to angle of attack rate.
D_q	Stability parameter - Change in drag due to pitch rate.
$D\theta$	Stability parameter - Change in drag due to pitch angle.
$D\delta_e$	Stability parameter - Change in drag due to pitch canard deflection angle.
$E(\cdot)$	Feedforward reference output matrix.
e_ϕ	Roll angle error.
$F(\cdot)$	System matrix describing the dynamic interaction between state variables.
$G(\cdot)$	System control input matrix.
$G^*(t_i)$	Optimal control feedback gain matrix.

$G1(t_i)$	Optimal system state feedback gain matrix.
$G2(t_i)$	Optimal target state feedback gain matrix.
$G3(t_i)$	Optimal reference state feedback gain matrix.
g	Acceleration due to gravity.
$H(\cdot)$	System state output matrix.
I_{xx}, I_{yy}, I_{zz}	Moment of inertial with respect to the given axis.
J	Cost to go function for the mathematical optimization.
$L(\cdot)$	System noise input matrix.
L_0	Stability parameter - Equilibrium change in Z axis velocity.
$L0_{wt}$	Stability parameter - Change in Z axis velocity due to weight.
L_u	Stability parameter - Change in Z axis velocity due to forward velocity.
$L\alpha$	Stability parameter - Change in Z axis velocity due to angle of attack.
$L\dot{\alpha}$	Stability parameter - Change in Z axis velocity due to angle of attack rate.
L_q	Stability parameter - Change in Z axis velocity due to pitch rate.
$L\theta$	Stability parameter - Change in Z axis velocity due to pitch angle.
$L\delta_e$	Stability parameter - Change in Z axis velocity due to pitch canard deflection angle.
L_0	Stability parameter - Equilibrium change in roll rate.
L_β	Stability parameter - Change in roll rate due to sideslip angle.
$L_{\dot{\beta}}$	Stability parameter - Change in roll rate due to sideslip angle rate.
L_p	Stability parameter - Change in roll rate due to roll rate.
L_r	Stability parameter - Change in roll rate due to yaw rate.
$L\delta_a$	Stability parameter - Change in roll rate due to roll canard deflection angle.
$L\delta_r$	Stability parameter - Change in roll rate due to yaw canard deflection angle.

M	Mass of the missile.
M_0	Stability parameter - Equilibrium pitch rate.
M_u	Stability parameter - Change in pitch rate due to forward velocity.
$M\alpha$	Stability parameter - Change in pitch rate due to angle of attack.
$M\dot{\alpha}$	Stability parameter - Change in pitch rate due to angle of attack rate.
M_q	Stability parameter - Change in pitch rate due to pitch rate.
$M\delta_e$	Stability parameter - Change in pitch rate due to pitch canard deflection angle.
N_0	Stability parameter - Equilibrium yaw rate.
N_β	Stability parameter - Change in yaw rate due to sideslip angle.
$N_{\dot{\beta}}$	Stability parameter - Change in yaw rate due to sideslip angle rate.
N_p	Stability parameter - Change in yaw rate due to roll rate.
N_r	Stability parameter - Change in yaw rate due to yaw rate.
$N\delta_a$	Stability parameter - Change in yaw rate due to roll canard deflection angle.
$N\delta_r$	Stability parameter - Change in yaw rate due to yaw canard deflection angle.
Nx,Ny,Nz	Components of applied acceleration on respective missile body axis.
P	Solution to the Riccati equation.
P,Q,R	Angular rates about the X,Y, and Z body axis respectively.
Q(·)	State weighting matrix.
R(·)	Control weighting matrix.
R(·)	Reference state vector.
S(·)	State-Control cross weighting matrix.
T(·)	Target disturbance state vector.
Tgo	Time-to-go.
U	System input vector.

U,V,W	Linear velocities with respect to the X,Y, and Z body axis respectively.
$V_x,V_y,V_z,$	State velocity.
V_s	System noise process.
W_s	Zero mean white Gaussian noise modeling uncorrelated state disturbances.
W_t	Zero mean white Gaussian noise driving first order Markov process modeling correlated state disturbances.
$\|V_{tot}\|$	Total missile velocity.
$X(\cdot)$	System state vector.
X,Y,Z	Body stabilized axis.
Y_0	Stability parameter - Equilibrium change in Y axis velocity.
$Y0_{wt}$	Stability parameter - Change in Y axis velocity due to weight.
Y_β	Stability parameter - Change in Y axis rate due to sideslip angle.
$Y_{\dot{\beta}}$	Stability parameter - Change in Y axis velocity due to sideslip angle rate.
Y_p	Stability parameter - Change in Y axis velocity due to roll rate.
Y_r	Stability parameter - Change in Y axis velocity due to yaw rate.
$Y\phi$	Stability parameter - Change in Y axis velocity due to roll angle.
$Y\delta_a$	Stability parameter - Change in Y axis velocity due to roll canard deflection angle.
$Y\delta_r$	Stability parameter - Change in Y axis velocity due to yaw canard deflection angle.
α	Angle of attack.
β	Angle of Sideslip.
Φ_n	System noise transition matrix.
Φ_r	Reference state transition matrix.
Φ_T	Target disturbance state transition matrix.
Φ_x	System state transition matrix.

λ_x	Target model correlation time.
θ_a	Target elevation aspect angle.
θ_g	Seeker elevation gimbal angle.
ψ_a	Target azimuth aspect angle.
ψ_g	Seeker azimuth gimbal angle.

Abstract of Dissertation Presented to the Graduate School
of the University of Florida in Partial Fulfillment of the
Requirements for the Degree of Doctor of Philosophy

REACHABLE SET CONTROL FOR PREFERRED AXIS HOMING MISSILES

By

Donald J. Caughlin, Jr.

April 1988

Chairman: T.E. Bullock
Major Department: Electrical Engineering

The application of modern control methods to the guidance and control of preferred axis terminal homing missiles is non-trivial in that it requires controlling a coupled, non-linear plant with severe control variable constraints, to intercept an evading target. In addition, the range of initial conditions is quite large and is limited only by the seeker geometry and aerodynamic performance of the missile. This is the problem: Linearization will cause plant parameter errors that modify the linear trajectory. In non-trivial trajectories, both Ny and Nz acceleration commands will, at some time, exceed the maximum value. The two point boundary problem is too complex to complete in real time and other formulations are not capable of handling plant parameter variations and control variable constraints.

Reachable Set Control directly adapts Linear Quadratic Gaussian (LQG) synthesis to the Preferred Axis missile, as well as a large class of nonlinear problems where plant uncertainty and control constraints prohibit effective fixed-final-time linear control. It is a robust control technique that controls a continuous system with sampled data and minimizes the effects of modeling errors. As a stochastic command generator/tracker, it specifies and maintains a minimum control trajectory to minimize the terminal impact of errors generated by plant parameter (transfer function) or target set uncertainty while rejecting system noise and target set disturbances. Also, Reachable Set Control satisfies the Optimality Principle by insuring that saturated control, if required, will occur during the initial portion of the trajectory. With large scale dynamics determined by a dual reference in the command generator, the tracker gains can be optimized to the response time of the system. This separation results in an "adaptable" controller because gains are based on plant dynamics and cost while the overall system is smoothly driven from some large displacement to a region where the relatively high gain controller remains linear.

CHAPTER I
INTRODUCTION

The application of modern control methods to the guidance and control of preferred axis terminal homing missiles has had only limited success [1,2,3]. This guidance problem is non-trivial in that it requires controlling a coupled, non-linear plant with severe control variable constraints, to intercept an evading target. In addition, the range of initial conditions is quite large and limited only by the seeker geometry and aerodynamic performance of the missile.

There are three major control issues that must be addressed: the coupled non-linear plant of the Preferred Axis Missile; the severe control variable constraints; and implementation in the missile where the solution is required to control trajectories lasting one (1) to two (2) seconds real time.

There have been a number of recent advances in non-linear control but these techniques have not reached the point where real time implementation in an autonomous missile controller is practical [4,5,6]. Investigation of non-linear techniques during this research did not improve the situation. Consequently, primarily due to limitations imposed by real time implementation, linear suboptimal control schemes were emphasized.

Bryson & Ho introduced a number of techniques for optimal control with inequality constraints on the control variables [7]. Each of these use variational techniques to generate constrained and unconstrained arcs that must be pieced together to construct the optimal trajectory.

In general, real time solution of optimal control problems with bounded control is not possible [8]. In fact, with the exception of space applications, the optimal control solution has not been applied [9,10]. When Linear Quadratic Gaussian (LQG) techniques are used, the problem is normally handled via saturated linear control, where the control is calculated as if no constraints existed and then simply limited. This technique has been shown to be seriously deficient. In this case, neither stability nor controllability can be assured. Also, this technique can cause an otherwise initially controllable trajectory to become uncontrollable [11].

Consequently, a considerable amount of time is spent adjusting the gains of the controller so that control input will remain below its maximum value. This adjustment, however, will force the controller to operate below its maximum capability [12]. Also, in the case of the terminal homing missile, the application of LQG controllers that do not violate an input constraint lead to an increasing acceleration profile and (terminally) low gain systems [13]. As a result, the performance of these controllers is not desirable.

While it is always possible to tune a regulator to control the system to a given trajectory, the variance of the initial conditions, the time to intercept the target (normally a few seconds for a short range high performance missile), and the lack of a globally optimal trajectory due to the nonlinear nature, the best policy is to develop a suboptimal real time controller.

The problem of designing a globally stable and controllable high performance guidance system for the preferred axis terminal homing missile is treated in this dissertation. Chapter 2 provides adequate background information on the missile guidance problem. Chapter 3 covers recent work on constrained

control techniques. Chapters 4 and 5 discuss Robust Control and introduce "Reachable Set" Control, while Chapter 6 applies the technique to control of a preferred axis homing missile. The performance of "Reachable Set" control is presented in Chapter 7.

CHAPTER II
BACKGROUND

The preferred axis orientation missile has significant control input constraints and complicated coupled angular dynamics associated with the maneuvering. In the generic missile considered, the Z axis acceleration (see Figure 2.1) was structurally limited to 100 "g" with further limits on "g" resulting from a maximum angle of attack as a function of dynamic pressure. Even though the Z axis was capable of 100 "g", the "skid-to-turn" capability of the Y axis was constrained to 5 "g" or less because of aerodynamic limitations - a 20:1 difference. In addition to pitch (Nz) and yaw (Ny) accelerations, the missile can roll up to 500 degrees per second to align the primary maneuver plane with the plane of intercept. Hence, bank-to-turn.

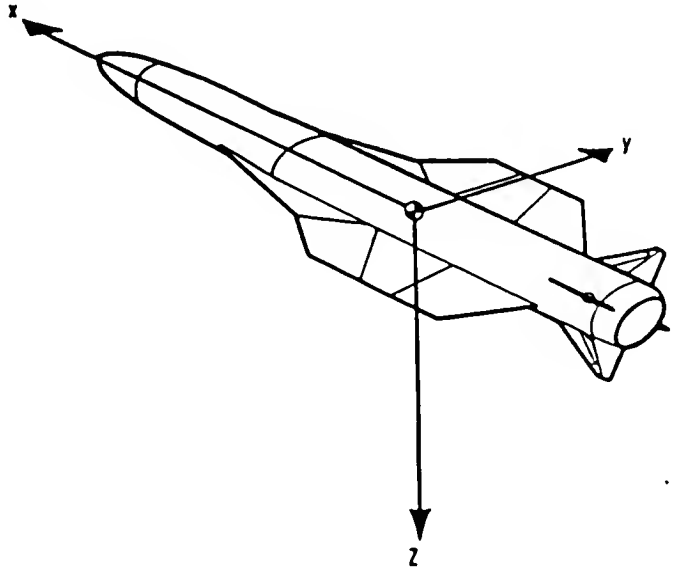

Figure 2.1 Missile Reference System.

The classical technique for homing missile guidance is proportional navigation (pro nav). This technique controls the seeker gimbal angle rate to zero which (given constant velocity) causes the missile to fly a straight line trajectory toward the target [14,15]. In the late 70's an effort was made to use modern control theory to improve guidance laws for air-to-air missiles. For recent research on this problem see, for example, [11]. As stated in the introduction, these efforts have not significantly improved the performance of the preferred axis homing missile.

Of the modern techniques, two basic methodologies have emerged: one was a body-axis oriented control law that used singular perturbation techniques to uncouple the pitch & roll axis [16,17]. This technique assumed that roll rate is the fast variable, an assumption that may not be true during the terminal phase of an intercept. The second technique was an inertial point mass formulation that controls inertial accelerations [18]. The acceleration commands are fixed with respect to the missile body; but, since these commands can be related to the inertial reference via the Euler Angles, the solution is straight forward. Both of these methods have usually assumed unlimited control available and the inertial technique has relied on the autopilot to control the missile roll angle, and therefore attitude, to derotate from the inertial to body axis.

Missile Dynamics

The actual missile dynamics are a coupled set of nonlinear forces and moments resolved along the (rotating) body axes of the missile [19]. Linearization of the equations about a "steady state" or trim condition,

neglecting higher order terms, results in the following set of equations (using standard notation, see symbol key in the preface):

$$\dot{\alpha} = Q - P\beta + A_{zb} / |V_{tot}| \tag{1}$$

$$\dot{\beta} = - R - P\alpha + A_{yb} / |V_{tot}| \tag{2}$$

Linear Accelerations

$$\dot{U} = RV - QW - \frac{1}{M} \{D_0 + D0_{wt}\} - D_u U - D_\alpha \alpha - D_{\dot{\alpha}} \dot{\alpha} - D_q Q - D_\theta \theta - D_{\delta e} \delta e + A_x/M \tag{3}$$

$$\dot{V} = PW - RU + \frac{1}{M} \{Y_0 + Y0_{wt}\} + Y_\beta \beta + Y_{\dot{\beta}} \dot{\beta} + Y_p P + Y_r R + Y_\phi \phi + Y_{\delta a} \delta a + Y\delta_r \delta r \tag{4}$$

$$\dot{W} = QU - PV + \frac{1}{M} \{L_0 + L0_{wt}\} - L_u U - L_\alpha \alpha - L_{\dot{\alpha}} \dot{\alpha} - L_q Q - L_\theta \theta - L_{\delta e} \delta e \tag{5}$$

Moment Equations

$$\dot{Q} = M_0/I_{yy} + M_u U + M_\alpha \alpha + M_{\dot{\alpha}} \dot{\alpha} + M_q Q + M_{\delta e} \delta e + \frac{(I_{zz}-I_{xx})}{I_{yy}} PR - (P^2 - R^2) \frac{I_{xz}}{I_{yy}} \tag{6}$$

$$\dot{R} = N_0/I_{zz} + N_\beta\beta + N_{\dot\beta}\dot\beta + N_pP + N_rR + N_{\delta a}\delta a + N_{\delta r}\delta r \qquad (7)$$

$$+ \frac{(I_{yy}-I_{xx})}{I_{zz}} PQ - (QR - \dot{P}) \frac{I_{xz}}{I_{zz}}$$

$$\dot{P} = L_0/I_{xx} + L_\beta\beta + L_{\dot\beta}\dot\beta + L_pP + L_rR + L_{\delta a}\delta a + L_{\delta r}\delta r \qquad (8)$$

$$+ \frac{(I_{xx}-I_{yy})}{I_{zz}} QR - (PQ - \dot{R}) \frac{I_{xz}}{I_{xx}}$$

Linear Quadratic Gaussian Control Law

For all of the modern development models, a variation of a fixed-final-time LQG controller was used to shape the trajectory. Also, it was expected that the autopilot would realize the commanded acceleration. First, consider the effect of the unequal body axis constraints. Assume that 100 "g" was commanded in each axis resulting in an acceleration vector 45 degrees from Nz. If Ny is only capable of 5 "g", the resultant vector will be 42 degrees in error, an error that will have to be corrected by succeeding guidance commands. Even if the missile has the time or capability to complete a successful intercept, the trajectory can not be considered optimal.

Now consider the nonlinear nature of the dynamics. The inertial linear system is accurately modeled as a double integrator of the acceleration to determine position. However, the acceleration command is a function of the missile state, equation (1), and therefore, it is not possible to arbitrarily assign the input acceleration. And, given a body axis linear acceleration, the inertial

component will be severely modified by the rotation (especially roll) of the reference frame. All of these effects are neglected in the linearization.

This then is the problem: In the intercept trajectories worth discussing, Ny, Nz, and roll acceleration commands will, at some time, saturate. High order linear approximations do not adequately model the effects of nonlinear dynamics, and the complete two point boundary value problem with control input dynamics and constraints is too difficult to complete in real time.

Although stochastic models are discussed in Bryson and Ho [7], and a specific technique is introduced by Fiske [18], the general procedure has been to use filtered estimates and a dynamic-programming-like definition of optimality (using the Principle of Optimality) with Assumed Certainty Equivalence to find control policies [20,21,22]. Therefore, all of the controllers actually designed for the preferred axis missiles are deterministic laws cascaded with a Kalman Filter. The baseline for our analysis is an advanced control law proposed by Fiske [18]. Given the finite dimensional linear system:

$$\dot{x}(t) = Fx(t) + Gu(t) \tag{9}$$

where

$$x = \begin{pmatrix} x \\ y \\ z \\ Vx \\ Vy \\ Vz \end{pmatrix} \qquad u = \begin{pmatrix} Ax \\ Ay \\ Az \end{pmatrix}$$

and

$$F = \begin{pmatrix} 0 & I \\ 0 & 0 \end{pmatrix} \qquad G = \begin{pmatrix} 0 \\ -I \end{pmatrix}$$

with the cost functional:

$$J=x_f P_f x_f + \gamma \int_{t_0}^{t_f} u^T R u d\tau \tag{10}$$

$$P = \begin{bmatrix} I & 0 \\ 0 & 0 \end{bmatrix} \qquad R = I$$

Application of the Maximum principle results in a linear optimal control law:

$$u_i(t) = \frac{3(Tgo)}{3\gamma + (Tgo)^3} x_i(t) + \frac{3(Tgo)^2}{3\gamma + (Tgo)^3} V_i(t) \tag{11}$$

Coordinates used for this system are "relative inertial." The orientation of the inertial system is established at the launch point. The distances and velocities are the relative measures between the missile and the target. Consequently, the set point is zero, with the reference frame moving with the missile similar to a "moving earth" reference used in navigation.

Since Fisk's control law was based on a point mass model, the control law did not explicitly control the roll angle PHI (ø). The roll angle was controlled by a bank-to-turn autopilot [23]. Therefore, the guidance problem was decomposed into two components, trajectory formation and control. The autopilot attempted to control the roll so that the preferred axis (the -Z axis) was directed toward the plane of intercept. The autopilot used to control the missile was designed to use proportional navigation and is a classical combination of single loop systems.

Recently, Williams and Friedland have developed a new bank-to-turn autopilot based on modern state space methods [24]. In order to accurately control the banking maneuver, the missile dynamics are augmented to include the kinematic relations describing the change in the commanded specific force

vector with bank angle. To determine the actual angle through which the vehicle must roll, define the roll angle error:

$$e_{\phi} = \tan^{-1}\{\frac{A_{yb}}{A_{zb}}\} \tag{12}$$

Using the standard relations for the derivative of a vector in a rotating reference frame, the following relationships follow from the assumption that $A|_I << A|_B$:

$$\dot{A}_{zb} = - P(A_{yb}) \tag{13}$$

$$\dot{A}_{yb} = + P(A_{zb}) \tag{14}$$

The angle e_{ϕ} represents the error between the actual and desired roll angle of the missile. Differentiating e_{ϕ} yields:

$$\dot{e}_{\phi} = \frac{(A_{zb})(\dot{A}_{yb}) - (A_{yb})(\dot{A}_{zb})}{(A_{zb})^2 + (A_{yb})^2} \tag{15}$$

which, after substituting components of A x w, shows that

$$\dot{e}_{\phi} = P \tag{16}$$

Simplifying the nonlinear dynamics of (1) - (8), the following model was used:

$$\dot{\alpha} = Q - P\beta + A_{zb} / |V_{tot}| \tag{17}$$

$$\dot{\beta} = - R - P\alpha + A_{yb} / |V_{tot}| \tag{18}$$

$$\dot{Q} = M_{\alpha}\alpha + M_q Q + M_{\delta e}\delta e + \frac{(I_{zz} - I_{xx})}{I_{yy}} PR \tag{19}$$

$$\dot{R} = N_{\beta}\beta + N_{r}R + N\delta_{r}\delta r + \frac{(Iy_{y} - I_{xx})}{I_{zz}} PQ \tag{20}$$

$$\dot{P} = L_{p}P + L_{\delta a}\delta a \tag{21}$$

where

$$A_{z} = Z_{\alpha}\alpha + Z_{\delta q}\delta q \tag{22}$$

$$A_{y} = Z_{\beta}\beta + Z_{\delta q}\delta q \tag{23}$$

Using this model directly, the autopilot would be designed as an eighth-order system with time-varying coefficients. However, even though these equations contain bilinear terms involving the roll rate P as well as pitch/yaw cross-coupling terms, the roll dynamics alone, represent a second order system that is independent of pitch and yaw. Therefore, using an "Adiabatic Approximation" where the optimal solution of the time-varying system is approximated by a sequence of solutions of the time-invariant algebraic Riccati equation for the optimum control law at each instant of time, the model was separated into roll and pitch/yaw subsystems [25]. Now, similar to a singular perturbations technique, the function of the roll channel is to provide the necessary orientation of the missile so that the specific force acceleration lies on the Z (preferred) axis of the missile. Using this approximation, the system is assumed to be in steady state, and all coefficients--including roll rate--are assumed to be constant. Linear Quadratic Gaussian (LQG) synthesis is used, with an algebraic Riccati equation, on a second and sixth order system. And, when necessary, the gains are scheduled as a function of the flight condition.

While still simplified, this formulation differs significantly from previous controllers in two respects. First, the autopilot explicitly controls the roll angle; and second, the pitch and yaw dynamics are coupled.

Even though preliminary work with this controller demonstrated improved tracking performance by the autopilot, overall missile performance, measured by miss distance and time to intercept, did not improve. However, the autopilot still relies on a trajectory generated by the baseline controller (e.g. A_{zb} in 17). Consequently, the missile performance problem is not in the autopilot, the error source is in the linear optimal control law which forms the trajectory. "Reachable Set Control" is a LQG formulation that can minimize these errors.

CHAPTER III
CONSTRAINED CONTROL

In Chapters I and II, we covered the non-linear plant, the dynamics neglected in the linearization, the impact of control variable constraints, and the inability of improved autopilots to reduce the terminal error. To solve this problem, we must consider the optimal control of systems subject to input constraints. Although a search of the constrained control literature did not provide any suitable technique for real time implementation, some of the underlying concepts were used in the formulation of "Reachable Set Control." This Chapter reviews some of these results to focus on the constrained control problem and illustrate the concepts.

Much of the early work was based on research reported by Tufts and Shnidman [26] which justified the use of saturated linear control. However, as stated in the introduction, with saturated linear control, controllability is not assured. If the system, boundary values and final time are such that there is no solution with any allowable control (If the trajectory is not controllable), then the boundary condition will not be met by either a zero terminal error or penalty function controller. While constrained control can be studied in a classical way by searching for the effect of the constraint on the value of the performance function, this procedure is not suitable for real time control of a system with a wide range of initial conditions [27]. Some of the techniques that could be implemented in real time are outlined below.

Lim used a linearized gain to reduce the problem to a parameter optimization [8]. Given the system model:

$$\dot{x} = Fx + Gu + Lw \tag{1}$$

with state x, constant F, G, and L, scaler control u, and Lw representing zero mean Gaussian white noise with covariance LL^T. Consider the problem of choosing a feedback law such that in steady state, assuming it exists, the expected quadratic cost

$$J = E\{ \lim_{t_f \to \infty} [\int_{t_0}^{t_f} (x(t)^T Q x(t) + \lambda u(t)^2)\, dt + x(t_f)^T P(t_f) x(t_f)] \} \tag{2}$$

is minimized. The weighting matrix Q is assumed to be positive semidefinite and $\lambda \geq 0$. Dynamic programming leads to Bellman's equation:

$$\min_{|u| \leq 1} \{ \tfrac{1}{2} \mathrm{tr}[L^T V_{xx}(x) L] + (Fx + Gu)^T V_x(x) + x^T Q x + \lambda u^2 \} = \alpha^* \tag{3}$$

and, assuming a V(x) satisfying (3), the optimal solution

$$u(x) = \mathrm{SAT} \{ (1/2\lambda) G^T V_x(x) \} \qquad \lambda \neq 0 \tag{4}$$

$$= \mathrm{SGN} \{ G^T V_x(x) \} \qquad \lambda = 0$$

However, (3) cannot be solved analytically, and V_x in general is a nonlinear function of x. Consider a <u>modified problem</u> by assuming a control of the form:

$$u(x) = \mathrm{SAT} \{ g^T x \} \qquad \lambda \neq 0 \tag{5a}$$

$$= \mathrm{SGN} \{ g^T x \} \qquad \lambda = 0 \tag{5b}$$

where g is a constant (free) vector.

Assume further that x is Gaussian with known covariance W (positive definite). Using statistical linearization, a linearized gain k can be obtained by minimizing

$$E\{u(x) - k^T x\}^2 \tag{6}$$

which results in

for (5a): $$k = \Phi\{(g^T W g)^{-\frac{1}{2}}\}\, g, \tag{7a}$$

where

$$\Phi(z) = (2/\pi)^{\frac{1}{2}} \int_0^z \exp\{-\tfrac{1}{2}y^2\}\, dy$$

for (5b): $$k = (2/\pi)^{\frac{1}{2}} \cdot (g^T W g)^{-\frac{1}{2}} \cdot g \tag{7b}$$

From (1), with $u = k^T x$, the stable covariance matrix W and steady state P are determined by

$$(F + Gk^T)W + W(F + Gk^T)^T + LL^T = 0 \tag{8}$$

and

$$(F + Gk^T)^T P + P(F + Gk^T) + P + \lambda k k^T = 0 \tag{9}$$

The solution to (3), without the minimum, is

$$V(x) = x^T P x \tag{10}$$

and

$$\propto = \mathrm{tr}\{L^T P L\} \tag{11}$$

The problem is to choose g such that the expected cost $\propto$ by statistical linearization is a minimum. However, a minimum may not exist. In fact, from [8], a minimum does not exist when the noise disturbance is large. Since we are considering robust control problems with plant uncertainty or significant modeling errors, the noise will be large and the minimum will be replaced by a greatest lower bound. As $\propto$ approached the greatest lower bound, the control approached bang-bang operation. A combination of plant errors and the rapid dynamics of some systems (such as the preferred axis missile) would preclude acceptable performance with bang-bang control.

Frankena and Sivan suggested a criterion that reduce the two-point boundary problem to an initial value problem [12]. They suggest controlling the plant while minimizing this performance index:

$$J = \int_{t_0}^{t_1} \{(1/2)\|x(t)\|^2_{Q(t)} + \|x(t)\|_{S(t)}\}dt + (1/2)\|x(t_1)\|^2_{P(t)} \tag{12}$$

With the constraint

$$\|u(t)\|_{R(t)} \leq 1$$

Applying the maximum principle to the Hamiltonian developed from

$$\dot{x}(t) = F(t)x(t) + G(t)u(t) \qquad t_0 < t < t_1 \tag{13}$$

with

$$x(t_0) = x_0$$

provides the adjoint differential equation

$$\dot{\lambda}(t) = Q(t)x(t) + \frac{S(t)x(t)}{\|x(t)\|_{S(t)}} - F^T(t)\lambda(t) \quad \lambda(t_1) = -P_1 x(t_1) \tag{14}$$

With $u(t) = R^{-1}(t)G^T(t)\lambda$ found by maximizing the Hamiltonian, the constraint in (12) can be expressed as

$$u(t) = \frac{R^{-1}(t)G^T(t)\lambda(t)}{\|R^{-1}(t)G^T(t)\lambda(t)\|_{R(t)}} \tag{15}$$

The desired control exists if a matrix P(t) can be defined such that

$$\lambda(t) = P(t)x(t) \tag{16}$$

and from (14)

$$P(t_1) = -P_1 < 0 \tag{17}$$

For $G^T Px \neq 0$ and $\|x\|_S \neq 0$, P will be the solution of

$$\dot{P} + PF + \frac{PGR^{-1}G^TP}{\|R^{-1}G^TPx\|_R} = Q + \frac{S}{\|x\|_S} - F^TP \qquad (18)$$

Now choosing $S = PGR^{-1}G^TP$ results in a Lyapunov equation and will insure negative definite P(t) if F is a stability matrix. Therefore, with this choice of weighting functions to transform the problem to a single boundary condition, a stable F matrix is required. This is a significant restriction and not applicable to the system under consideration.

Gutman and Hagander developed a design for saturated linear controllers for systems with control constraints [9,28]. The design begins with a low-gain stabilizing control, solves a Lyapunov equation to find a region of stability and associated stability matrix, and then sums the controls in a saturation function to form the constrained control. Begin with the stabilizable continuous linear time invariant system

$$\dot{x} = Fx + Gu \qquad x(0) = x_0 \qquad (19)$$

with admissible control inputs u_i, such that

$$g_i \leq u_i \leq h_i \qquad i = 1,...,m$$

where g_i and h_i are the control constraints. Consider an n x m matrix

$$L \equiv [\ l_1 \mid l_2 \mid \cdots \mid l_m\ ] \qquad (20)$$

such that

$$F_c \equiv F_c(L) \equiv (F + GL^T) \qquad (21)$$

is a stability matrix.

Associated with each of the controls are sets that define allowable conditions. The set D is the set of initial conditions from which it is desired to stabilize the system to the origin. The low gain stabilizing control L defines the set E:

$$E \equiv E(L) \equiv \{\ z \mid\ z \in R \quad \text{and } g_i \le l_i^T z \le h_i\ \} \qquad i=1,\ldots,m \tag{22}$$

which is the set of states at which the stabilizing linear feedback does not initially exceed the constraints. Another set is F:

$$F \equiv F(L) \equiv \bigcap_{t\in[0,\infty)} \{\ (e^{Fct})^{-1}\ E\ \} \tag{23}$$

F is a subset of E such that along all trajectories emanating from F, the stabilizing linear state feedback does not exceed the constraint. The region of stability for the solution of the Lyapunov equation is defined by

$$\Omega \equiv \Omega(L,P,c) \equiv \{\ x \mid\ x^T P x \le c\} \tag{24}$$

where $V(x) = x^T P x$ is the Lyapunov function candidate for the stability matrix F_c, and c is to be determined.

The control technique follows:

Step 1: Determine D.

Step 2: Find L by solving a LQG problem. The control penalty is increased until the control $L^T x$ satisfies the constraint in (19) for x in D. If D is such that the control constraint can not be satisfied, then this design is not appropriate.

Step 3: Find P and c. First find a $P = P^T > 0$ such that the Lyapunov equation $PF_c + F_c^T P > 0$. Now determine Ω by choosing c in (24) such that $D \subseteq \Omega \subseteq E$:

$$\sup_{x\in D} x^T P x \le c \le \min_{x\in \delta E} x^T P x \tag{25}$$

where δE designates the boundary of E. If this fails, choose another P, or select a "lower gain" in order to enlarge E, or finally, a reduction in the size of D might be considered.

Step 4: Set up the control according to

$$u = SAT[\ (L^T - KG^TP)x\ ] \tag{26}$$

where K is defined

$$K = \begin{pmatrix} k_i & & 0 \\ & \ddots & \\ 0 & & k_m \end{pmatrix} \quad k_i \geq 0,\ i = 1,2,\ldots,m \tag{27}$$

and tune the parameters k_i by simulations.

A sufficient condition for the algorithm to work is

$$D \subseteq \Omega \subseteq E. \tag{28}$$

Unfortunately, determining the stability region was trial and error; and, once found, further tuning of a diagonal gain matrix is required. In essence, this was a technique for determining a switching surface between a saturated and linear control. Also, when the technique was applied to an actual problem, inadequacies in the linear model were not compensated for. Given the nonlinear nature of the preferred axis missile, range of initial conditions, and the trial and error tuning required for each of these conditions, the procedure would not be adequate for preferred axis terminal homing missile control. A notable feature of the control scheme, however, was the ability to maintain a stable system with a saturated control during much of the initial portion of the trajectory.

Another technique for control with bounded input was proposed by Spong et al. [29]. This procedure used an optimal decision strategy to develop a pointwise optimal control that minimized the deviation between the actual and

desired vector of joint accelerations, subject to input constraints. The computation of the control law is reduced to the solution of a weighted quadratic programming problem. Key to this solution is the availability of a desired trajectory in state space. Suppose that a dynamical system can be described by

$$\dot{x}(t) = f(x(t)) + G(x(t))u(t) \tag{29}$$

with

$$|u_i| \leq u_{i,max}$$

which can be written as

$$Nu \leq c$$

Fix time $t \geq 0$, let $s(t,x_0,t_0,u(t))$ (or $s(t)$ for short), denote the solution to (29) corresponding to the given input function $u(t)$. At time t, ds/dt is the velocity vector of the system, and is given explicitly by the right hand side of (29). Define the set $C_t = C(s(t))$

$$C(s(t)) = \{ \alpha(t,\omega) \in R^N \mid \alpha = f(s(t)) + G(s(t))\omega,\ \omega \in \Omega \} \tag{30}$$

with

$$\Omega = \{ \omega \mid N\omega \leq c \}$$

Therefore, for each t and any allowable $u(t)$, ds/dt lies in the set C_t. In other words, the set C_t contains the allowable velocities of the solution $s(t)$. Assume that there exists a desired trajectory y^d, and an associated vector field $v(t) = v(s(t),y^d(t),t))$, which is the desired (state) velocity of $s(t)$ to attain y^d.

Consider the following "optimal decision strategy" for a given positive definite matrix Q: Choose the input $u(t)$ so that the corresponding solution $s(t)$ satisfies $(d/dt)s(t,u(t)) = s^*(t)$, where $s^*(t)$ is chosen at each t to minimize

$$\min_{\alpha \in C_t} \{ (\alpha - v(s(t),y^d(t),t))^T Q(\alpha - v(s(t),y^d(t),t)) \} \tag{31}$$

This is equivalent to the minimization

$$\min_{u} \{ \tfrac{1}{2} u^T G^T Q G u - (G^T Q (v-f))^T u \} \text{ subject to, } Nu(t) \leq c \qquad (32)$$

We may now solve the quadratic programming problem to yield a pointwise optimal control law for (29).

At each time t, the optimal decision strategy attempts to "align" the closed loop system with the desired velocity v(t) as nearly as possible in a least squares sense. In this way the authors retain the desirable properties of v(t) within the constraints imposed by the control. Reachable Set Control builds on this technique: it will determine the desired trajectory and optimally track it.

Finally, minimum-time control to the origin using a constrained acceleration has also been solved by a transformation to a two-dimensional unconstrained control problem [30]. By using a trigonometric transformation, the control is defined by an angular variable, u(t) = f{cos(ß),sin(ß)}, and the control problem was modified to the control of this angle. The constrained linear problem is converted to an unconstrained nonlinear problem that forces a numerical solution. This approach removes the effect of the constraints at the expense of the continuous application of the maximum control. Given the aerodynamic performance (range and velocity) penalty of maximum control and the impact on attainable roll rates due to reduced stability at high angle of attack, this concept did not fit preferred axis homing missiles.

An important assumption in the previous techniques was that the constrained system was controllable. In fact, unlike (unconstrained) linear systems, controllability becomes a function of the set admissible controls, the initial state, the time-to-go, and the target state. To illustrate this, some of the relevant points from [31,32] will be presented. An admissible control is one

that satisfies the condition $u(\cdot) : [0,\infty) \rightarrow \Omega \in R^m$ where Ω is the control restraint set. The collection of all admissible controls will be denoted by $M(\Omega)$. The target set X is a specified subset in R^n. A system is defined to be Ω-controllable from an initial state $x(t_0) = x_0$ to the target set X at T if there exists $U(\cdot) \in M(\Omega)$ such that $x(T,u(\cdot),x_0) \in X$. A system would be globally Ω-controllable to X if it is Ω-controllable to X from every $x(t_0) \in R^n$.

In order to present the necessary and sufficient conditions for Ω-controllability, consider the following system:

$$\dot{x}(t) = F(t)x(t) + G(t,u(t)) \qquad x(t_0) = x_0 \tag{33}$$

and the adjoint defined by:

$$\dot{z}(t) = -F(t)^T z(t) \qquad z(t_0) = z_0 \qquad t \in [0,\infty) \tag{34}$$

with the state transition matrix $\Phi(t,\tau)$ and solution

$$z(t) = \Phi(t_0,t)^T z_0 \tag{35}$$

The interior B and surface S of the unit ball in R^n are defined as

$$B = \{ z_0 \in R^n : \|z_0\| \leq 1 \} \tag{36}$$

$$S = \{ z_0 \in R^n : \|z_0\| = 1 \} \tag{37}$$

The scaler function $J(\cdot)$: $R^n \times R \times R^n \times R^n \rightarrow R$ is defined by

$$J(x_0,t,x,z_0) = x_0^T z_0 + \int_0^t \max_{\omega \in \Omega} [\, G^T(\tau,\omega)z(\tau) \,]d\tau - x(t)^T z(t) \tag{38}$$

Given the relatively mild assumptions of [32], a necessary condition for (33) to be Ω-controllable to X from $x(t_0)$ is

$$\max_{x \in X} \min_{z_0 \in B} J(x_0,T,x,z_0) = 0 \tag{39}$$

while a sufficient condition is

$$\sup_{x \in X} \min_{z_0 \in S} J(x_0,T,x,z_0) > 0 \tag{40}$$

The principle behind the conditions arises from the definition of the adjoint system -- Z(t). Using reciprocity, the adjoint is formed by reversing the role of the input and output, and running the system in reverse time [33]. Consider

$$\begin{aligned} \dot{x}(t) &= F(t)x(t) + G(t)u(t) \qquad x(t_0) = x_0 \qquad (41) \\ y(t) &= H(t)x(t) \end{aligned}$$

and:

$$\begin{aligned} \dot{z}(t) &= -F(t)^T z(t) + H^T(t)\mu(t) \qquad z(t_0) = z_0 \qquad (42) \\ o(t) &= G^T(t)z(t) \end{aligned}$$

Therefore

$$z^T(t)\dot{x}(t) = z^T(F(t)x(t) + G(t)u(t)) \qquad (43)$$

and

$$\begin{aligned} (d/dt)(z^T(t)x(t)) &= \dot{z}^T(t)x(t) + z^T(t)\dot{x}(t) \qquad (44) \\ &= \mu^T(t)H(t)x(t) + z^T(t)G(t)u(t) \end{aligned}$$

Integrating both sides from t_0 to t_f yields the adjoint lemma:

$$z^T(t_f)x(t_f) - z^T(t_0)x(t_0) = \int_{t_0}^{t_f} (\mu^T(t)H(t)x(t) + z^T(t)G(t)u(t))\, dt \qquad (45)$$

The adjoint defined in (31) does not have an input. Consequently, the integral in (35) is a measure of the effect of the control applied to the original system. By searching for the maximum $G^T(\tau,\omega)z(\tau)$, it provides the <u>boundary</u> of the effect of allowable control on the system (33). Restricting the search over the target set to the min { $J(x_0,t,x,z_0)$: $t \in [0,T]$, $z_0 \in S$ } or min { $J(x_0,t,x,z_0)$: $t \in [0,T]$, $z_0 \in B$ } minimizes the effect of the specific selection of z_0 on the reachable set and insures that the search is over a function that is jointly continuous in (t,x). Consequently, (35) compares the autonomous growth of the system, the reachable boundary of the allowable input, and the desired target set and time. Therefore, if J = 0, the adjoint lemma is be

identically satisfied at the boundary of the control constraint set (necessary); $J > 0$ guarantees that a control can be found to satisfy the lemma. If the lemma is satisfied, then the initial and final conditions are connected by an allowable trajectory. The authors [32] go on to develop a zero terminal error steering control for conditions where the target set is closed and

$$\max_{x \epsilon X} \min_{z_0 \epsilon S} J(x_0,T,x,z_0) \geq 0 \tag{46}$$

But their control technique has two shortcomings: First; it requires the selection of z_0. The initial condition z_0 is not specified but limited to $\|z_0\| = 1$. A particular z_0 must be selected to meet the prescribed conditions and the equality in (43) for a given boundary condition, and is therefore not suitable for real time applications. And second; the steering control searched $M(\Omega)$ for the supremum of J, making the control laws bang-bang in nature, again not suitable for homing missile control.

While a direct search of Ω_x is not appropriate for a preferred axis missile steering control, a "dual" system, similar to the adjoint system used in the formulation of the controllability function J, can be used to determine the amount of control required to maintain controllability. Once controllability is assured, then a cost function that penalizes the state deviation (as opposed to a zero terminal error controller) can be used to control the system to an arbitrarily small distance from the reference.

CHAPTER IV
CONSTRAINED CONTROL WITH UNMODELED SETPOINT AND PLANT VARIATIONS

Chapter III reviewed a number of techniques to control systems subject to control variable constraints. While none of the techniques were judged adequate for real time implementation of a preferred-axis homing missile controller, some of the underlying concepts can be used to develop a technique that can function in the presence of control constraints: (1) Use of a "dual system" that can be used to maintain a controllable system (trajectory); (2) an "optimal decision strategy" to minimize the deviation between the actual and desired trajectory generated by the "dual system;" and (3) initially saturated control and optimal (real time) selection of the switching surface to linear control with zero terminal error.

However, in addition to, and compounding the limitations imposed by control constraints, we must also consider the sensitivity of the control to unmodeled disturbances and robustness under plant variations. In the stochastic problem, there are three major sources of plant variations. First, there will be modeling errors (linearization/reductions) that will cause the dynamics of the system to evolve in a different or "perturbed" fashion. Second, there may be the unmodeled uncertainty in the system state due to Gaussian assumptions. And finally, in the fixed final time problem, there may be errors in the final time, especially if it is a function of the uncertain state or impacted by the modeling reductions. Since the primary objective of this research is the zero error control of a dynamical system in fixed time, most of the more recent

optimization techniques (eg. LQG/LTR,H^{∞}) did not apply. At this time, these techniques seemed to be more attuned to loop shaping or robust stabilization questions.

A fundamental proposition that forms the basis of Reachable Set Control is that excessive terminal errors encountered when using an optimal feedback control for an initially controllable trajectory (a controllable system that can meet the boundary conditions with allowable control values) are caused by the combination of control constraints and uncertainty (errors) in the target set stemming from unmodeled plant perturbations (modeling errors) or set point dynamics.

First, a distinction must be made between a feedback and closed-loop controller. Feedback control is defined as a control system with real-time measurement data fed back from the actual system but no knowledge of the form, precision, or even the existence of future measurements. Closed-loop control exploits the knowledge that the loop will remain closed throughout the future interval to the final time. It adds to the information provided to a feedback controller, anticipates that measurements will be taken in the future, and allows prior assessment of the impact of future measurements. If Certainty Equivalence applies, the feedback law is a closed-loop law. Under the Linear Quadratic Gaussian (LQG) assumptions, there is nothing to be gained by anticipating future measurements. In the mathematical optimization, external disturbances can be rejected, and the mean value of the terminal error can be made arbitrarily close to zero by a suitable choice of control cost.

For the following discussion, the "system" consists of a controllable plant and an uncontrollable reference or target. The system state is the relative difference between the plant state and reference. Since changes in the system

boundary condition can be caused by either a change in the reference point or plant output perturbations similar to those discussed in Chapter II, some definitions are necessary. The set of boundary conditions for the combined plant and target system, allowing for unmodeled plant and reference perturbations, will be referred to as the target set. Changes, or potential for change, in the target set caused only by target (reference) dynamics will be referred to as variations in the set point. The magnitude of these changes is assumed to be bounded. Admissible plant controls are restricted to a control restraint set that limits the input vector. Since there are bounds on the input control, the system becomes non-linear in nature, and each trajectory must be evaluated for controllability. Assume that the system (trajectory) is pointwise controllable from the initial to the boundary condition.

Before characterizing the effects of plant and set point variations, we must consider the form of the plant and it's perturbations. If we assume that the plant is nonlinear and time-varying, there is not much that can be deduced about the target set perturbations. However, if have a reduced order linear model of a combined linear and nonlinear process, or a reasonable linearization of a nonlinear model, then the plant can be considered as linear and time-varying. For example, in the case of a Euclidean trajectory, the system model (a double integrator) is exact and linear. Usually, neglected higher order or nonlinear dynamics or constraints modify the accelerations and lead to trajectory (plant) perturbations. Consequently, in this case, the plant can be accurately represented as a Linear Time Invariant System with (possibly) time varying perturbations.

Consider the feedback interconnection of the systems K and P where K is a sampled-data dynamic controller and P the (continuous) controlled system:

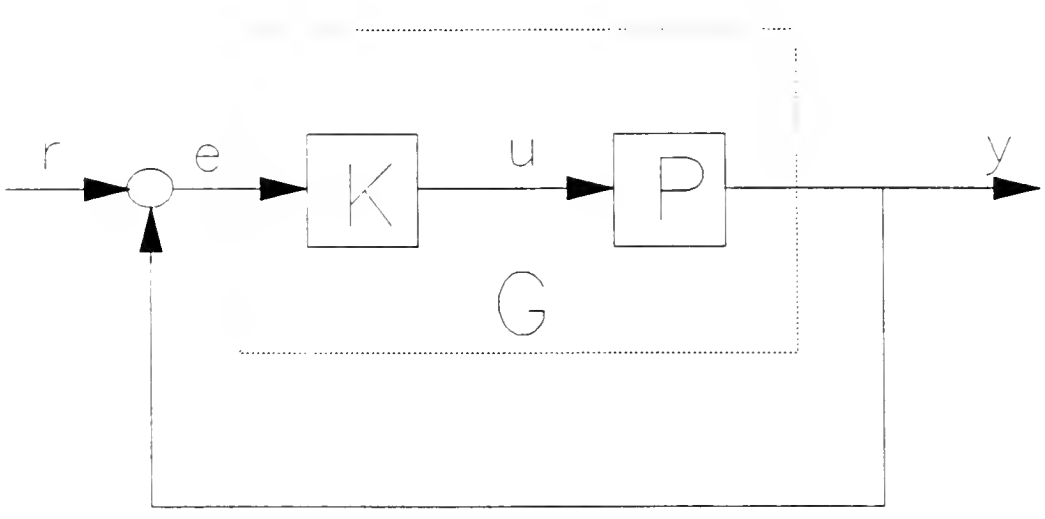

Figure 4.1 Feedback System and Notation

Assuming that the feedback system is well defined and Bounded Input Bounded Output (BIBO) stable, at any sample time t_i, the system can be defined in terms of the following functions:

$$e(t_i) = r(t_i) - y(t_i) \quad (1)$$

$$u(t_i) = Ke(t_i) \quad (2)$$

$$y(t_i) = Pu(t_i) \quad (3)$$

with the operator G = G[K,P] as the operator that maps the input $e(t_i)$ to the output $y(t_i)$ [34].

At any time, the effect of a plant perturbation ΔP can also be characterized as a perturbation in the target set.

$$\text{If } P = P_0 + \Delta P \tag{4a}$$

or

$$P = P(I+\Delta P) \tag{4b}$$

then

$$y(t_i) = y_0(t_i) + \Delta y(t_i) \tag{5}$$

where $\Delta y(t_i)$ represents the deviation from the "nominal" output caused by either the additive or multiplicative plant perturbation. Therefore,

$$e(t_i) = r(t_i) - (y_0(t_i) + \Delta y(t_i)) \tag{6}$$

$$= (r(t_i) + \Delta y(t_i)) - y_0(t_i) \tag{7}$$

$$= \Delta r(t_i) - y_0(t_i) \tag{8}$$

with $\Delta r(t_i)$ representing a change in the target set that was unknown to the controller. These changes are then fed back to the controller but could be handled a priori in a closed loop controller design as target set uncertainty.

Now consider the effect of constraints. If the control is not constrained, and target set errors are generated by plant variations or target maneuvers, the feedback controller can recover from these intermediate target set errors by using large (impulsive) terminal controls. The modeled problem remains linear. While the trajectory is not the optimal closed-loop trajectory, the trajectory is optimal based on the model and information set available.

Even with unmodeled control variable constraints, and a significant displacement of the initial condition, an exact plant model allows the linear stochastic optimal controller to generate an optimal trajectory. The switching time from saturated to linear control is properly (automatically) determined and,

as in the linear case, the resulting linear control will drive the state to within an arbitrarily small distance from the estimate of the boundary condition.

If the control constraint set covers the range of inputs required by the control law, the law will always be able to accommodate target set errors in the remaining time-to-go. This is, in effect, the unconstrained case. If, however, the cost-to-go is higher and/or the deviation from the boundary condition is of sufficient magnitude relative to the time remaining to require inputs outside the boundary of the control constraint set, the system will not follow the trajectory assumed by the system model. If this is the case as time-to-go approaches zero, the boundary condition will not be met, the system is not controllable (to the boundary condition). As time-to-go decreases, the effects of the constraints become more important.

With control input constraints, and intermediate target set errors caused by unmodeled target maneuvers or plant variations, it may not be possible for the linear control law to recover from the midcourse errors by relying on large terminal control. In this case, an optimal trajectory is not generated by the feedback controller, and, at the final time, the system is left with large terminal errors.

Consequently, if external disturbances are adequately modeled, terminal errors that are orders of magnitude larger than predicted by the open loop optimal control are caused by the combination of control constraints and target set uncertainty.

Linear Optimal Control with Uncertainty and Constraints

An optimal solution must meet the boundary conditions. To accomplish this, plant perturbations and constraints must be considered a priori. They should be included as a priori information in the system model, they must be physically realizable, and they must be deterministic functions of a priori information, past controls, current measurements, and the accuracy of future measurements.

From the control point of view, we have seen that the effect of plant parameter errors and set point dynamics can be grouped as target set uncertainty. This uncertainty can cause a terminally increasing acceleration profile even when an optimal feedback control calls for a decreasing input (see Chapter 5). With the increasing acceleration caused by midcourse target set uncertainty, the most significant terminal limitation becomes the control input constraints. (These constraints not only affect controllability, they also limit how quickly the system can recover from errors.) If the initial control is saturated while the terminal portion linear, the control is still optimal. If the final control is going to be saturated, however, the controller must account for this saturation.

The controller could anticipate the saturation and correct the linear portion of the trajectory to meet the final boundary condition. This control, however, requires a closed form solution for x(t), carries an increased cost for an unrealized constraint, and is known to be valid for monotonic (single switching time) trajectories only [11].

Another technique available is LQG synthesis. However, LQG assumes controllability in minimizing a quadratic cost to balance the control error and

input magnitudes. As we have seen, the effects of plant parameter and reference variations, combined with control variable constraints, can adversely impact controllability. The challenge of LQG is the proper formulation of the problem to function with control variable constraints while compensating for unmodeled set point and plant variations. Reachable Set Control uses LQG synthesis and overcomes the limitations of an anticipative control to insure a controllable trajectory.

Control Technique

Reachable Set Control can be thought of as a fundamentally different robust control technique based on the concepts outlined above. The usual discussion of robust feedback control (stabilization) centers on the development of controllers that function even in the presence of plant variations. Using either a frequency domain or state space approach, and modeling the uncertainty, bounds on the allowable plant or perturbations are developed that guarantee stability [35]. These bounds are determined for the specific plant under consideration and a controller is designed so that expected plant variations are contained within the stability bounds. Building on ideas presented above, however, this same problem can be approached in an entirely different way. This new approach begins with the same assumptions as standard techniques, specifically a controllable system and trajectory. But, with Reachable Set Control, we will not attempt to model the plant or parameter uncertainty, nor the set point variation. We will, instead, reformulate the problem so that the system remains controllable, and thus stable, throughout the trajectory even in the presence of plant perturbations and severe control input constraints.

Before we develop an implementable technique, consider the desired result of Reachable Set Control (and the origin of the name) by using a two-dimensional missile intercept problem as an example. At time $t = t_1$, not any specific time during the intercept, the target is at some location T_1 and the missile is at M_1 as shown in Figure 4.2. Consider these locations as origins of two independent, target and missile centered, reference systems. From these initial locations, given the control inputs available, reachable sets for each system can be defined as a function of time (not shown explicitly). The target set is circular because is maneuver direction is unknown but its capability bounded, and the missile reachable set exponential because the x axis control is constant and uncontrollable while the z axis acceleration is symmetric and bounded. The objective of Reachable Set Control is to maintain the reachable target set in the interior of the missile reachable set. Hence, Reachable Set Control.

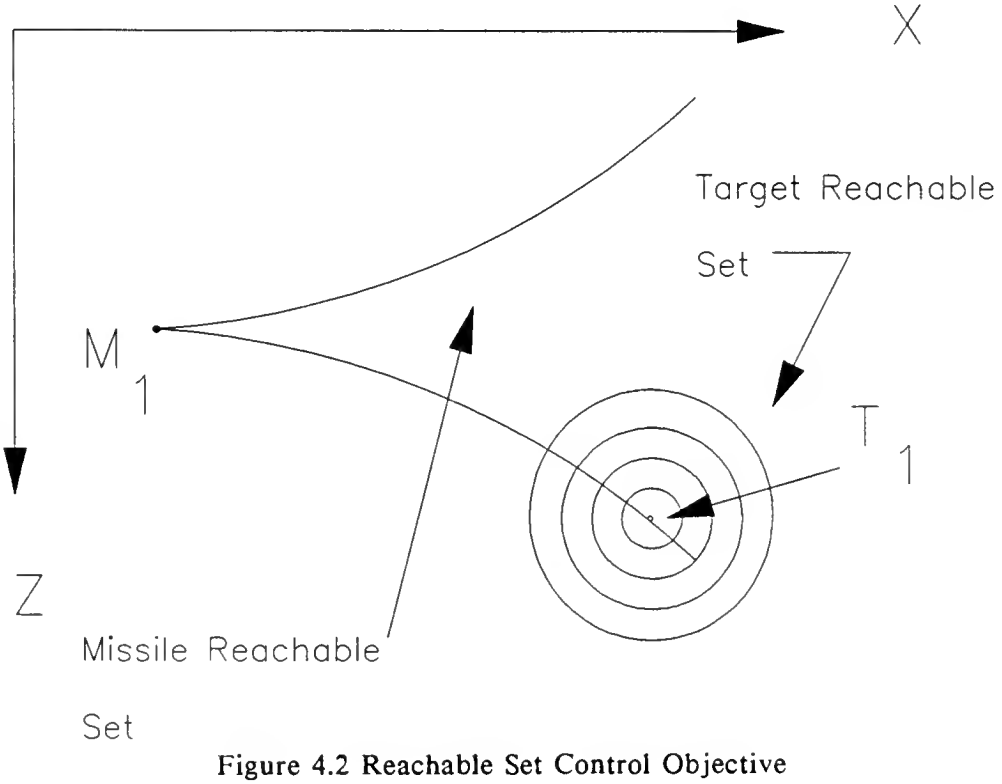

Figure 4.2 Reachable Set Control Objective

As stated, Reachable Set Control would be difficult to implement as a control strategy. Fortunately, however, further analysis leads to a simple, direct, and optimal technique that is void of complicated algorithms or ad-hoc procedures.

First, consider the process. The problem addressed is the control of fixed--terminal-time systems. The true cost is the displacement of the state at the final time and only at the final time. In the terminal homing missile problem, this is the closest approach, or miss distance. In another problem, it may be fuel remaining at the final time, or possibly a combination of the two. In essence, with respect to the direct application of this technique, there is no preference for one trajectory over another or no intermediate cost based on the displacement of the state from the boundary condition. The term "direct application" was used because constrained path trajectories, such as those required by robotics, or the infinite horizon problem, like the control of the depth of a submarine can be addressed by separating the problem into several distinct intervals--each with a fixed terminal time--or a switching surface when the initial objective is met [36].

Given a plant with dynamics

$$\dot{x}(t) = f(x,t) + g(u(w),t) \qquad x(t_0) = x_0 \tag{9}$$

$$y(t) = h(x(t),t)$$

modeled by

$$\dot{x}(t) = F(t)x(t) + G(t)u(t) \tag{10}$$

$$y_x(t) = H(t)x(t)$$

with final condition $x(t_f)$ and a compact control restraint set Ω_x. Let Ω_x denote the set of controls u(t) for which $u(t) \in \Omega_x$ for $t \in [0,\infty)$. The reachable set

$$X(t_0,t_f,x_0,\Omega_x) \equiv \{ x: x(t_f) = \text{solution to (10) with } x_0 \text{ for some } u(\cdot) \in M(\Omega_x) \} \quad (11)$$

is the set of all states reachable from x_0 in time t_f.

In addition to the plant and model in (9 & 10), we define the reference

$$\dot{r}(t) = a(x,t) + b(a(w),t) \qquad r(t_0) = r_0 \quad (12)$$

$$y(t) = c(x(t),t)$$

modeled by

$$\dot{r}(t) = A(t)r(t) + B(t)a(t) \quad (13)$$

$$y_r(t) = C(t)r(t)$$

and similarly defined set $R(t_0,t_f,r_0,\Omega_r)$,

$$R(t_0,t_f,r_0,\Omega_r) \equiv \{ r: r(t_f) = \text{solution to (13) with } r_0 \text{ for some } a(\cdot) \in M(\Omega r) \} \quad (14)$$

as the set of all reference states reachable from r_0 in time t_f.

Associated with the plant and reference, at every time t, is the following system:

$$e(t) = y_x(t) - y_r(t) \quad (15)$$

From (10 & 13), we see that $y_x(t)$ and $y_r(t)$ are output functions that incorporate the significant characteristics of the plant and reference that will be controlled.

The design objective is

$$e(t_f) = 0 \quad (16)$$

and we want to maximize the probability of success and minimize the effect of errors generated by the deviation of the reference and plant from their associated models. To accomplish this with a sampled-data feedback control law,

we will select the control $u(t_i)$ such that, at the next sample time (t_{i+1}), the target reachable set will be covered by the plant reachable set and, in steady state, if $e(t_f) = 0$, the control will not change.

Discussion

Recalling that the performance objective at the final time is the real measure of effectiveness, and assuming that the terminal performance is directly related to target set uncertainty, this uncertainty should be reduced with time-to-go. Now consider the trajectory remembering that the plant model is approximate (linearized or reduced order), and that the reference has the capability to change and possibly counter the control input. (This maneuverability does not have to be taken in the context of a differential game. It is only intended to allow for unknown set point dynamics.) During the initial portion of the trajectory, the target set uncertainty is the highest. First, at this point, the unknown (future) reference changes have the capability of the largest displacement. Second, the plant distance from the uncertain set point is the greatest and errors in the plant model will generate the largest target set errors because of the autonomous response and the magnitude of the control inputs required to move the plant state to the set point.

Along the trajectory, the contribution of the target (reference) maneuverability to set point uncertainty will diminish with time. This statement assumes that the target (reference) capability to change does not increase faster than the appropriate integral of its' input variable. Regardless of the initial maneuverability of the target, the time remaining is decreasing, and consequently, the

ability to move the set point decreases. Target motion is smaller and it's position is more and more certain.

Selection of the control inputs in the initial stages of the trajectory that will result in a steady state control (that contains the target reachable set within the plant reachable set) reduces target set uncertainty by establishing the plant operating point and defining the effective plant transfer function.

At this point, we do not have a control procedure, only the motivation to keep the target set within the reachable set of the plant along with a desire to attain steady state performance during the initial stages of the trajectory. The specific objectives are to minimize target set uncertainty, and most importantly, to maintain a controllable trajectory. The overall objective is better performance in terms of terminal errors.

Procedure

A workable control law that meets the objectives can be deduced from Figure 4.3. Here we have the same reachable set for the uncertain target, but this time, several missile origins are placed at the extremes of target motion. From these origins, the system is run backward from the final time to the current time using control values from the boundary of the control constraint set to provide a unique set of states that are controllable to the specific origin. If the intersection of these sets is non-empty, any potential target location is reachable from this intersection. Figure 4.4 is similar, but this time the missile control restraint set is not symmetric. Figure 4.4 shows a case where the missile acceleration control is constrained to the set

$$A = [Amin, Amax] \text{ where } 0 \leq Amin \leq Amax \qquad (17)$$

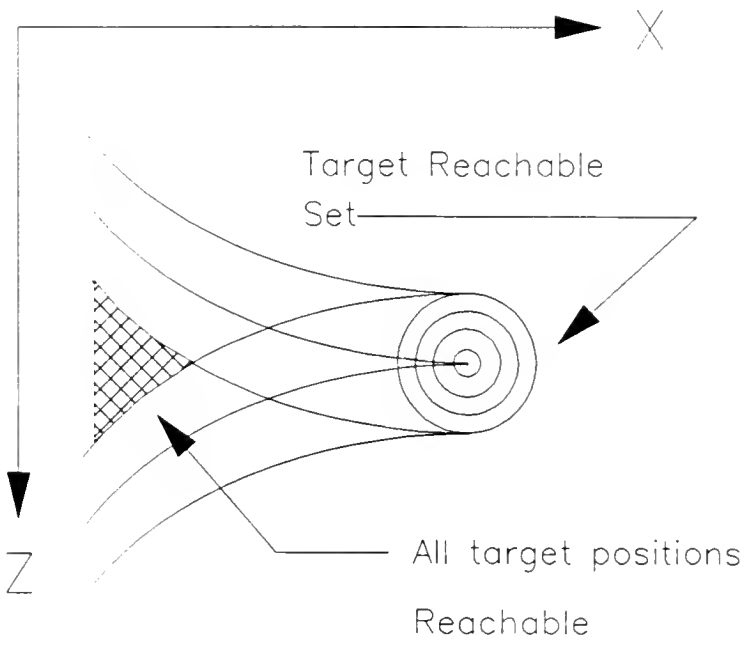

Figure 4.3 Intersection of Missile Reachable Sets Based on Uncertain Target Motion and Symmetric Constraints

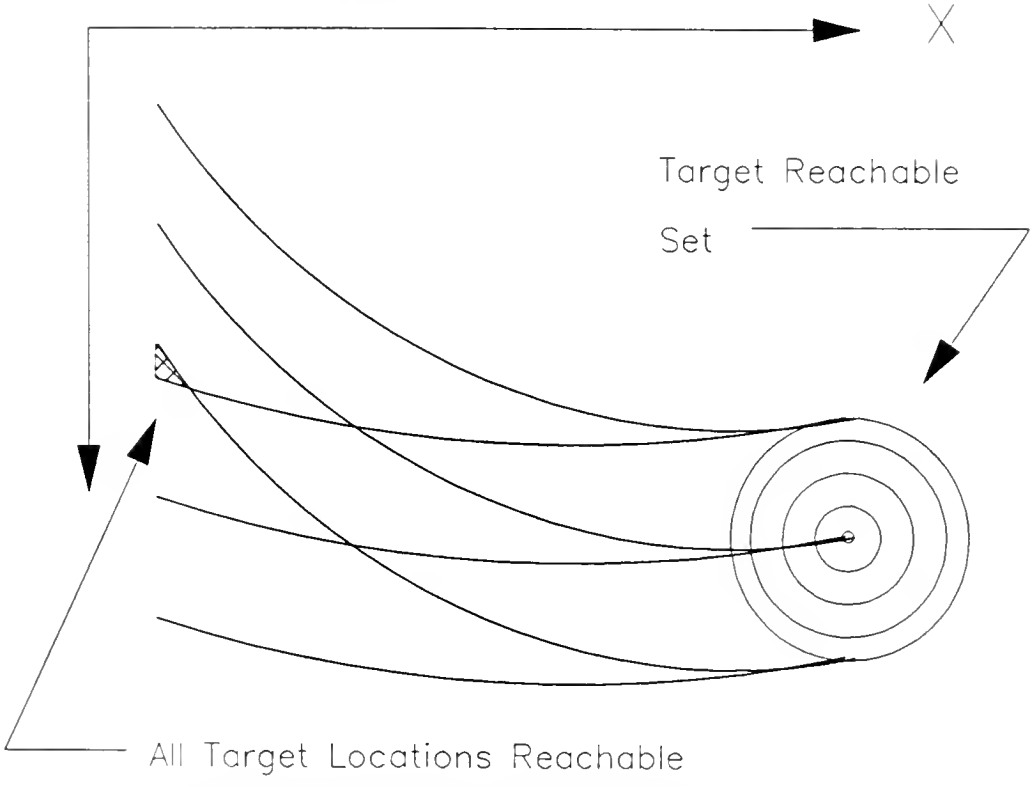

Figure 4.4 Intersection of Missile Reachable Sets Based on Uncertain Target Motion and Unsymmetric Constraints

Since controllability is assumed, which for constrained control includes the control bounds and the time interval, the extreme left and right (near and far) points of the set point are included in the set drawn from the origin.

To implement the technique, construct a dual system that incorporates functional constraints, uncontrollable modes, and uses a suitable control value from the control constraint set as the input. From the highest probability target position at the final time, run the dual system backward in time from the final boundary condition. Regulate the plant (system) to the trajectory defined by the dual system. In this way, the fixed-final-time zero terminal error control is accomplished by re-formulating the problem as optimal regulation to the dual trajectory.

In general, potential structures of the constraint set preclude a specific point (origin, center, etc.) from always being the proper input to the dual system.

Regulation to a "dual" trajectory from the current target position will insure that the origin of the target reachable set remains within the reachable set of the plant. Selection of a suitable interior point from the control restraint set as input to the dual system will insure that the plant has sufficient control power to prevent the target reachable set from escaping from the interior of the plant reachable set.

Based on unmodeled set point uncertainty, symmetric control constraints, and a double integrator for the plant, a locus exists that will keep the target in the center of the missile reachable set. If the set point is not changed, this trajectory can be maintained without additional inputs. For a symmetric control restraint set, especially as the time-to-go approaches zero, Reachable Set Control is control to a "coasting" (null control) trajectory.

If the control constraints are not symmetric, such as Figure 4.4, a locus of points that maintains the target in the center of the reachable set is the trajectory based on the system run backward from the final time target location with the acceleration command equal to the midpoint of the set A. Pictured in Figures 4.2 to 4.4 were trajectories that are representative of the double integrator. Other plant models would have different trajectories.

Reachable Set Control is a simple technique for minimizing the effects of target set uncertainty and improving terminal the performance of a large class of systems. We can minimize the effects of modeling errors (or target set uncertainty) by a linear optimal regulator that controls the system to a steady state control. Given the well known and desirable characteristics of LQG synthesis, this technique can be used as the basis for control to the desired "steady state control" trajectory. The technique handles constraints by insuring an initially constrained trajectory. Also, since the large scale dynamics are controlled by the "dual" reference trajectory, the tracking problem be optimized to the response time of the system under consideration. This results in an "adaptable" controller because gains are based on plant dynamics and cost while the overall system is smoothly driven from some large displacement to a region where the relatively high gain LQG controller will remain linear.

CHAPTER V
REACHABLE SET CONTROL EXAMPLE

Performance Comparison - Reachable Set and LQG Control

In order to demonstrate the performance of "Reachable Set Control" we will contrast its performance with the performance of a linear optimal controller when there is target set uncertainty combined with input constraints.

Consider, for example, the finite dimensional linear system:

$$\frac{d^2x}{dt^2} = u \qquad x(t_0) = x_0 \tag{1}$$

with the quadratic cost

$$J = \frac{1}{2} x_f^T P_f x_f + \gamma \int_{t_0}^{t_f} u(\tau)^T u(\tau) d\tau \tag{2}$$

where

$$t_f \in [0,\infty)$$

and

$$\gamma \geq 0$$

Application of maximum principle yields the following linear optimal control law:

$$u = + \frac{1}{\gamma} x(t_f)(t-t_f) \tag{3}$$

where

$$x(tf) = \frac{x_0 + \dot{x}_0 * t_f}{1 + \frac{(t_f)^3}{3\gamma}} \tag{4}$$

Appropriately defining t, t_0, and t_f, the control law can be equivalently expressed in an open loop or feedback form with the latter incorporating the usual disturbance rejection properties. The optimal control will tradeoff the cost of the integrated square input with the final error penalty. Consequently, even in the absence of constraints, the terminal performance of the control is a function of the initial displacement, time allowed to drive the state to zero, and the weighting factor γ. To illustrate this, Figure 5.1 presents the terminal states (miss distance and velocity) of the linear optimal controller. This plot is a composite of trajectories with different run times ranging from 0 to 3.0 seconds. The figure presents the values of position and velocity at the final time $t = t_f$ that result from an initial position of 1000 feet and with velocity of 1000 feet/sec with $\gamma = 10^{-4}$. Figure 5.2 depicts, as a function of the run time, the initial acceleration (at $t = 0.$) associated with each of the trajectories shown in Figure 5.1. From these two plots, the impact of short run times is evident: the miss distance will be higher, and the initial acceleration command will be greater. Since future set point (target) motion is unknown, the suboptimal feedback controller is reset at each sample time to accommodate this motion. The word reset is significant. The optimal control is a function of the initial condition at time $t = t_0$, time, and the final time. A feedback realization becomes a function of the initial condition and time to go only. In this case, set point motion (target set uncertainty) can place the controller in a position where the time-to-go is small but the state deviation is large.

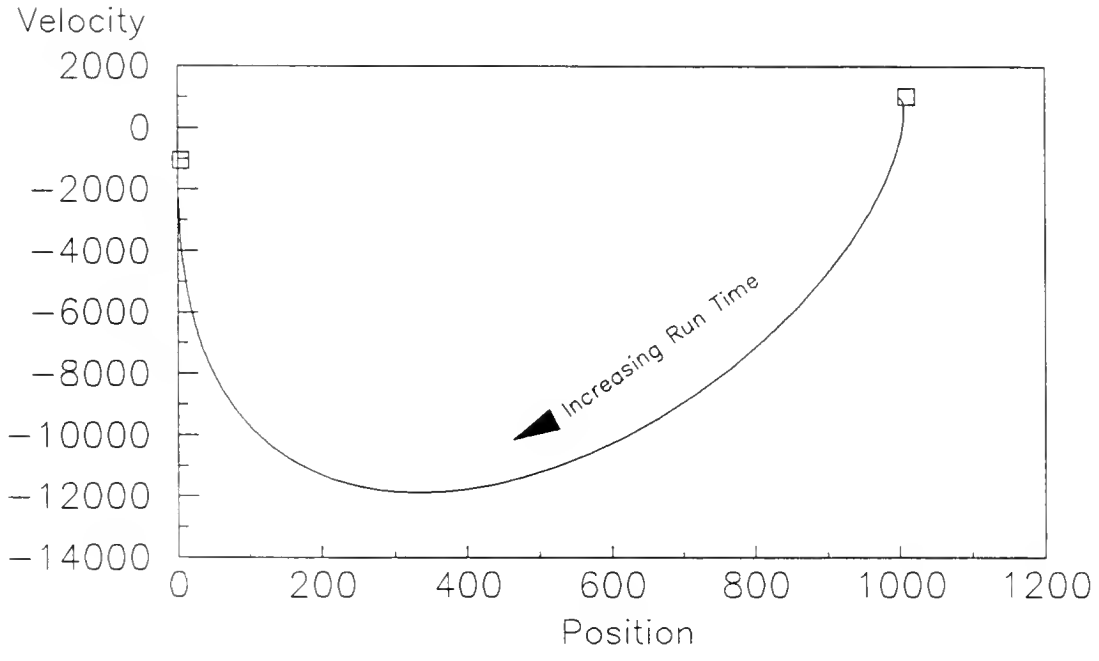

Figure 5.1 Terminal Performance of Linear Optimal Control

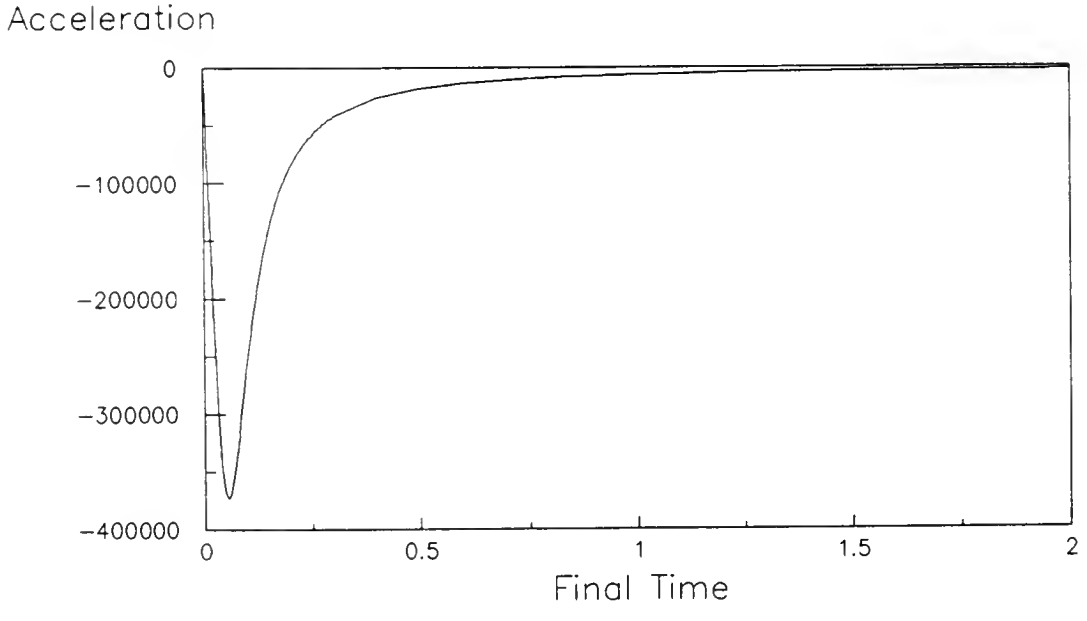

Figure 5.2 Initial Acceleration of Linear Optimal Control

While short control times will result in poorer performance and higher accelerations, it does not take a long run time to drive the terminal error to near zero. Also, from (4) we see that the terminal error can be driven to an arbitrarily small value by selection of the control weighting. Figure 5.1 presented the final values of trajectories running from 0 to 3 seconds. Figures 5.3 through 5.5 are plots of the trajectory parameters for the two second trajectory (with the same initial conditions) along with the zero control trajectory values. These values are determined by starting at the boundary conditions of the optimal control trajectory and running the system backward with zero acceleration. For example, if we start at the final velocity and run backwards in time along the optimal trajectory, for each point in time, there is a velocity (the null control velocity) that will take the corresponding position of the optimal control trajectory to the boundary without additional input. The null control position begins at the origin at the final time, and moving backward in time, is the position that will take the system to the boundary condition at the current velocity. Therefore, these are the positions and velocities (respectively) that will result in the boundary condition without additional input. As $t \Rightarrow t_f$ the optimal trajectory acceleration approaches zero. Therefore, the zero control trajectory converges to the linear optimal trajectory. If the system has a symmetric control constraint set, Reachable Set Control will control the system position to the zero control (constant velocity) trajectory.

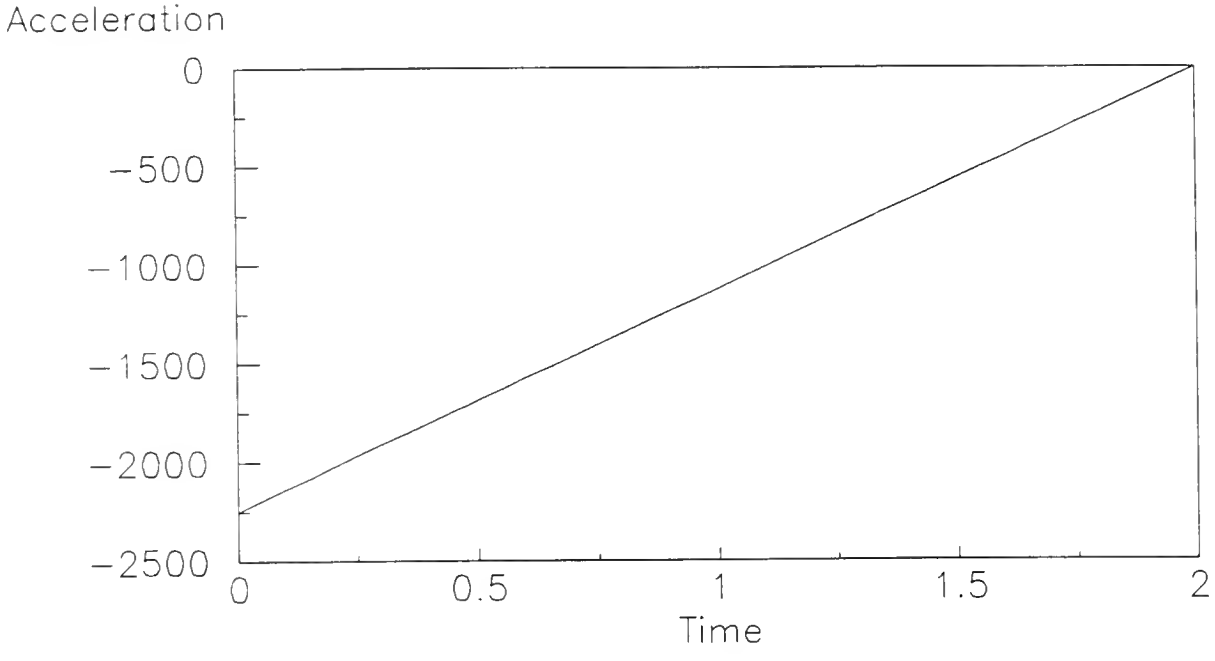

Figure 5.3 Linear Optimal Acceleration vs Time

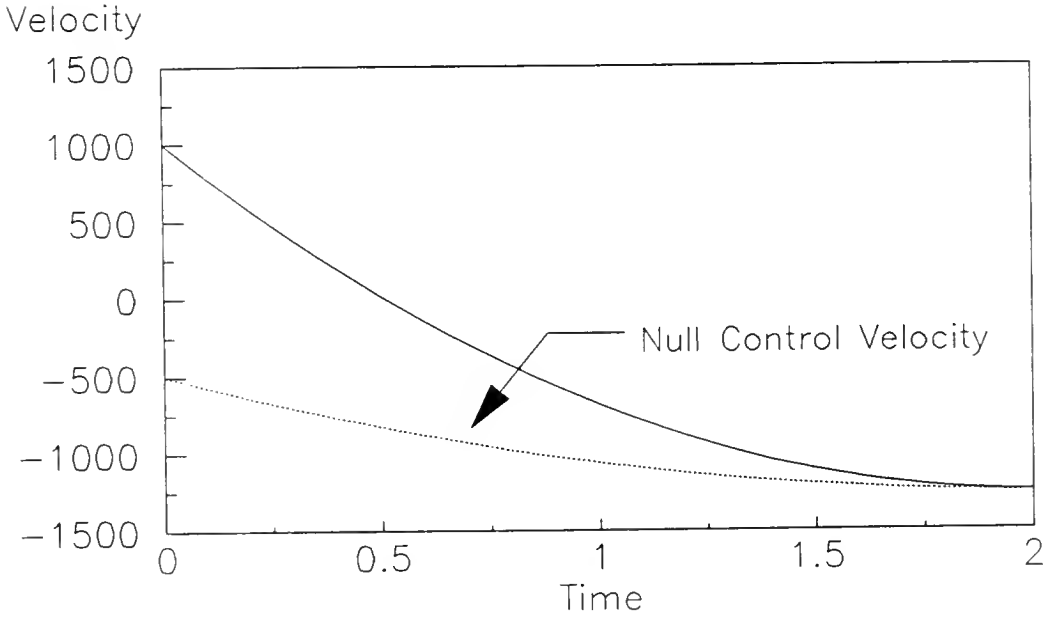

Figure 5.4 Linear Optimal Velocity vs Time

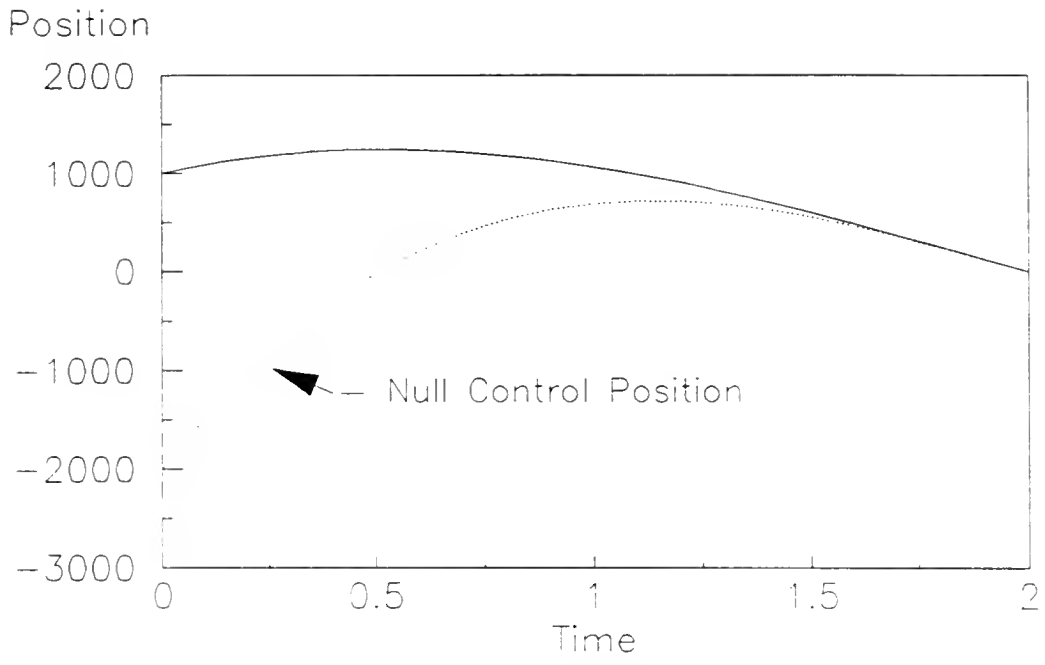

Figure 5.5 Linear Optimal Position vs Time

Consider now the same problem with input constraints. Since U(t) is a linear function of time and the final state, it is monotonic and the constrained optimal control is

$$u = SAT(\frac{1}{\gamma} x(t_f)(t-t_f)) \tag{5}$$

In this case, controllability is in question, and is a function of the initial conditions and the time-to-go. Assuming controllability, the final state will be given by:

$$x(t_f) = \frac{x_0 + \dot{x}_0 t_f - a(t_1)SGN(x(t_f)[t_f-(t_1/2)]}{1 + \frac{(t_f-t_1)^3}{3\gamma}} \tag{6}$$

where t_1 is the switching time from saturated to linear control. The open loop switch time can be shown to be

$$t_1 = t_f \pm \{ 3(t_f)^2 - 6(x_0+\dot{x}_0 t_f)/a \}^{\frac{1}{2}} \quad (7)$$

or the closed loop control can be used directly. In either case, the optimal control will correctly control the system to a final state $X(t_f)$ near zero. Figures 5.6 through 5.8 illustrate the impact of the constraint on the closed loop optimal control. In each plot, the optimal constrained and unconstrained trajectory is shown.

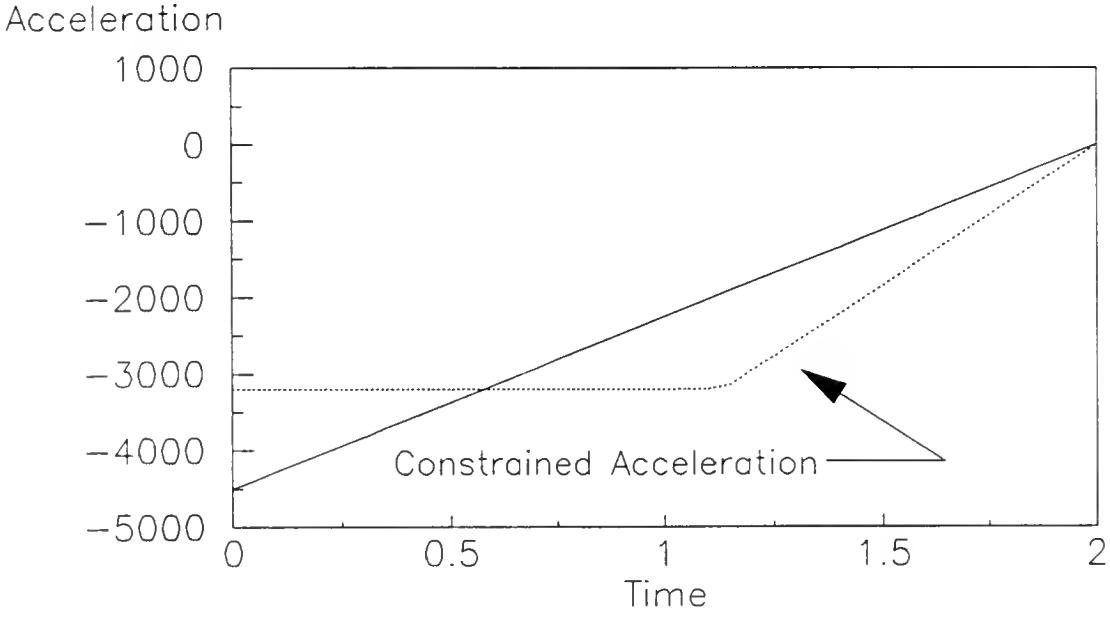

Figure 5.6 Unconstrained and Constrained Acceleration

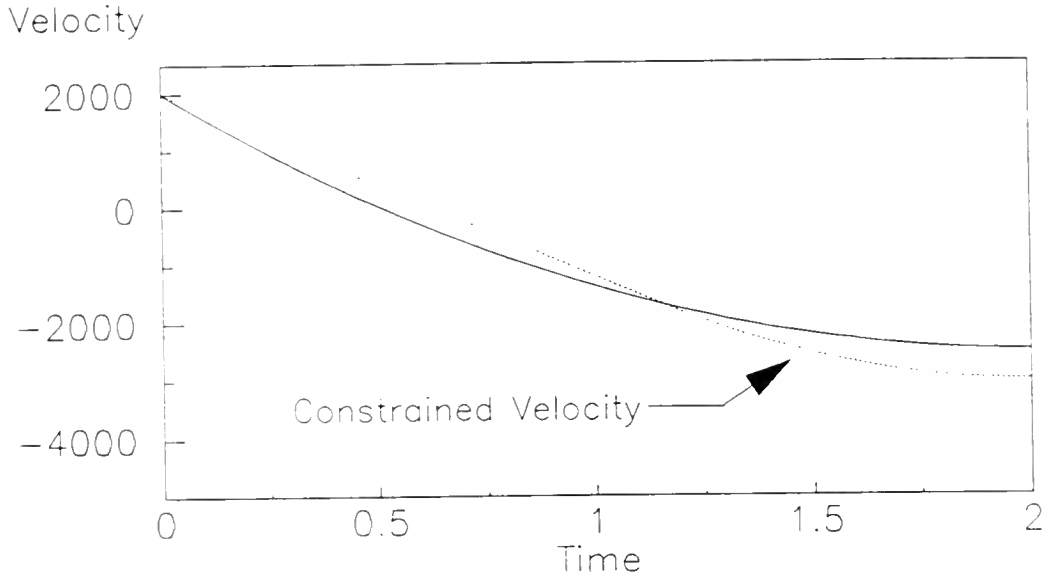

Figure 5.7 Unconstrained and Constrained Velocity vs Time

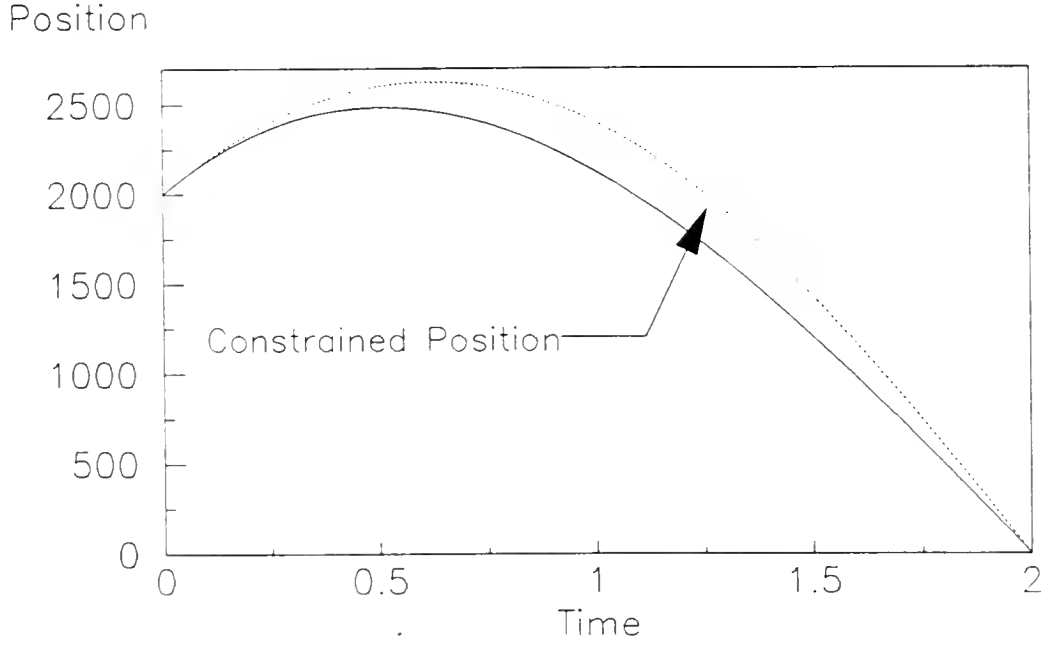

Figure 5.8 Unconstrained and Constrained Position vs Time

Now consider the effects of target set uncertainty on the deterministic optimal control by using the same control law for a 2.0 second trajectory where the boundary condition is not constant but changes. The reason for the target uncertainty and selection of the boundary condition can be seen by analyzing the components of the modeled system. Assume that system actually consists of an uncontrollable reference (target) plant as well as controlled (missile) plant with the geometry modeled by the difference in their states. Therefore, the final set point (relative distance) is zero, but the boundary condition along the controlled (missile) trajectory is the predicted target position at the final time. This predicted position at the final time is the boundary condition for the controlled plant.

Figures 5.9 through 5.11 are plots of linear optimal trajectories using the control law in (5,6). There are two trajectories in each plot. The boundary condition for one trajectory is fixed at zero, the set point for the other trajectory is the pointwise zero control value (predicted target state at the final time). Figures 5.9 through 5.11 demonstrate the impact of this uncertainty on the linear optimal control law by comparing the uncertain constrained control with the constrained control that has a constant boundary condition.

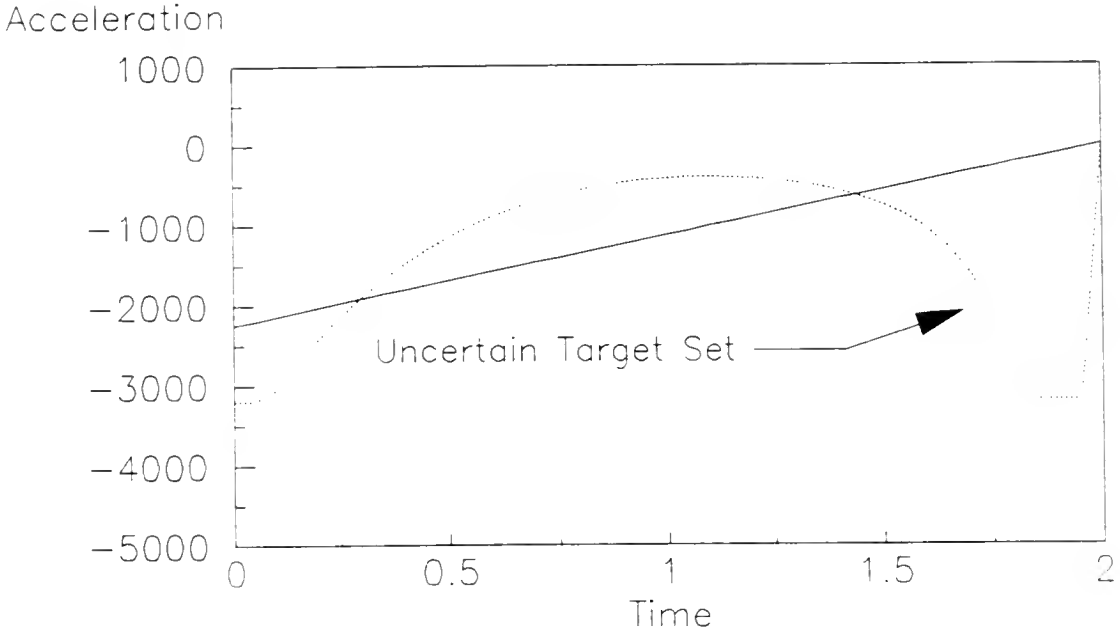

Figure 5.9 Acceleration Profile
With and Without Target Set Uncertainty

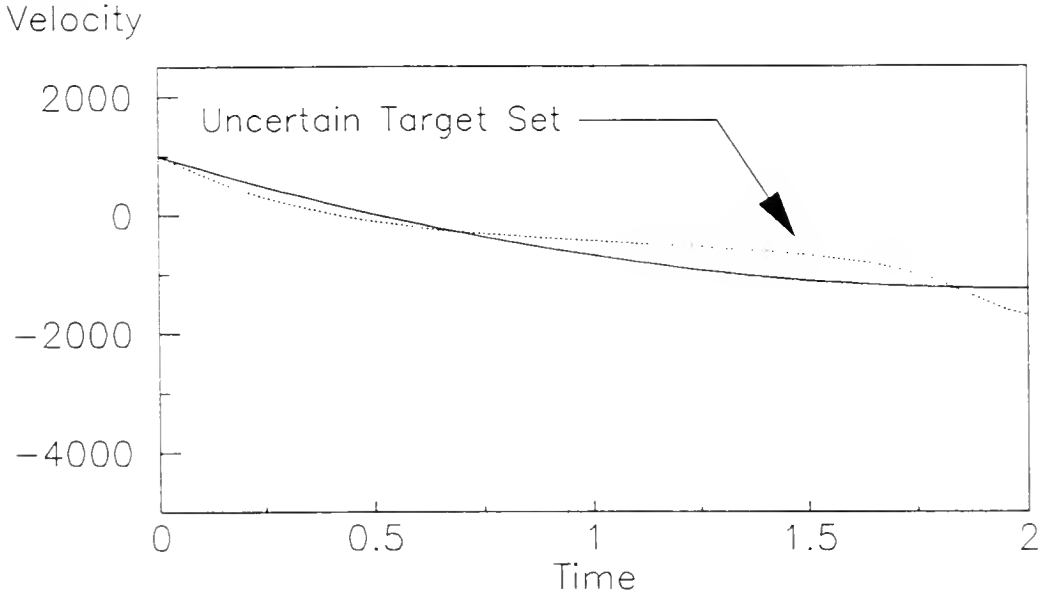

Figure 5.10 Velocity vs Time
With and Without Target Set Uncertainty

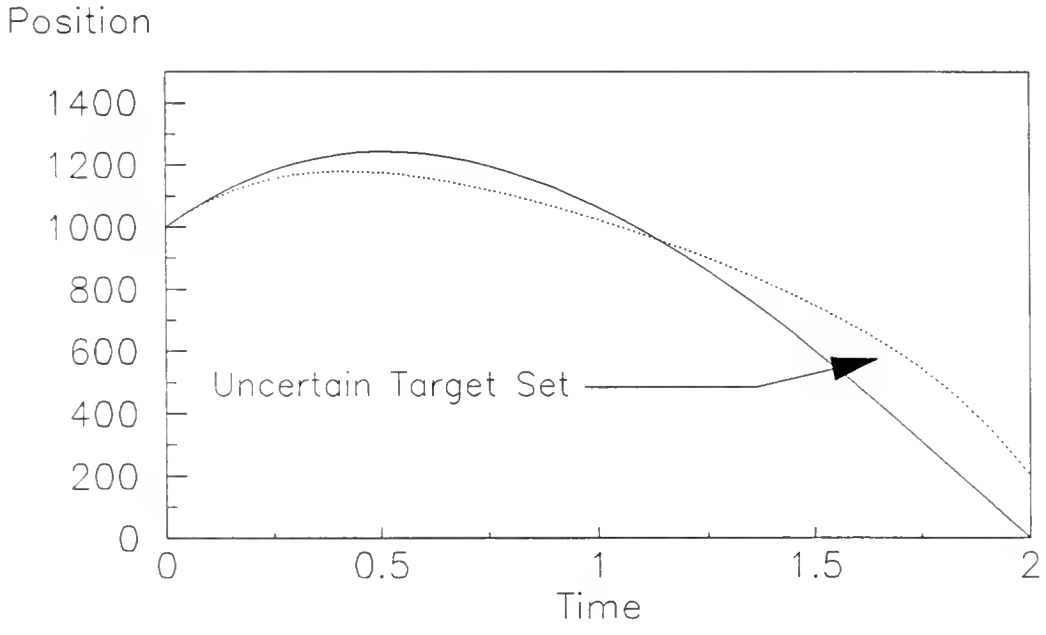

Figure 5.11 Position vs Time
With and Without Target Set Uncertainty

When there is target set uncertainty, simulated by the varying set point, the initial acceleration is insufficient to prevent saturation during the terminal phase. Consequently, the boundary condition is not met.

The final set of plots, Figures 5.12 through 5.14, contrast the performance of the optimal LQG closed loop controller that we have been discussing and the Reachable Set Control technique. In these trajectories, the final set point is zero but there is target set uncertainty again simulated by a time varying boundary condition (predicted target position) that converges to zero. Although properly shown as a fixed final time controller, the Reachable Set Control results in Figures 5.12 through 5.14 are from a simple steady state (fixed gain) optimal tracker referenced to the zero control trajectory r.

The system model for each technique is

$$\frac{d^2x}{dt^2} = u \tag{8}$$

with $x(t_0) = (x-r)_0$

The linear optimal controller has a quadratic cost of

$$J = \frac{1}{2}(x-r)_f^T P_f (x-r)_f + \gamma \int_{t_0}^{t_f} u(\tau)^T u(\tau) d\tau \tag{9}$$

The reachable set controller minimizes

$$J = \int_{t_0}^{t_f} [(x-r)^T Q (x-r) + u(\tau)^T u(\tau)] d\tau \tag{10}$$

And, in either case, the value for r(t) is the position that will meet the boundary condition at the final time without further input.

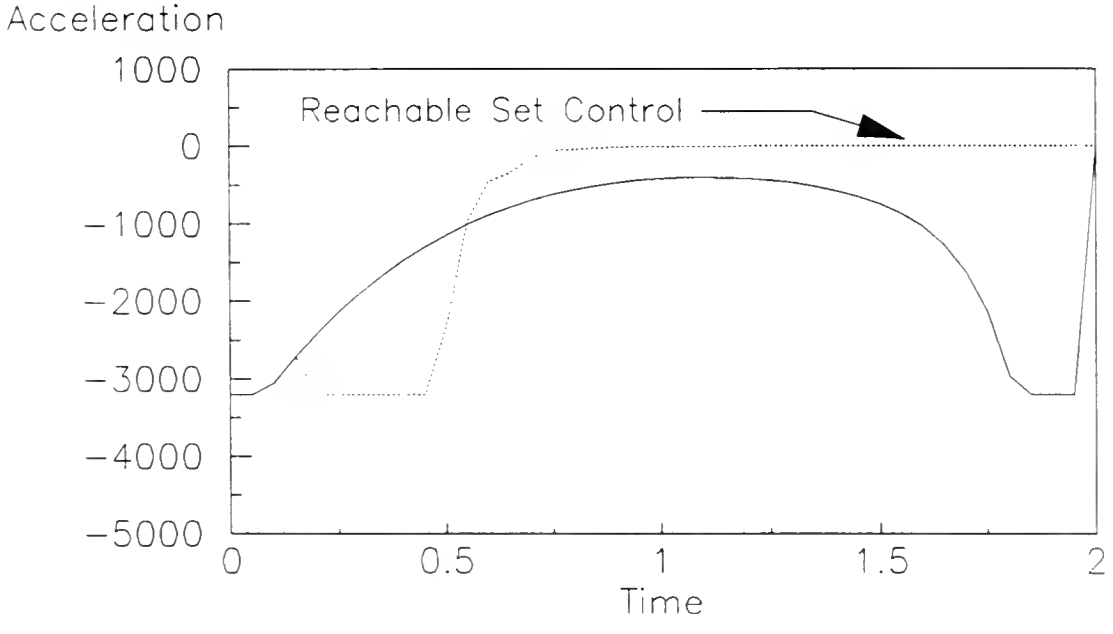

Figure 5.12 Acceleration vs Time
LQG and Reachable Set Control

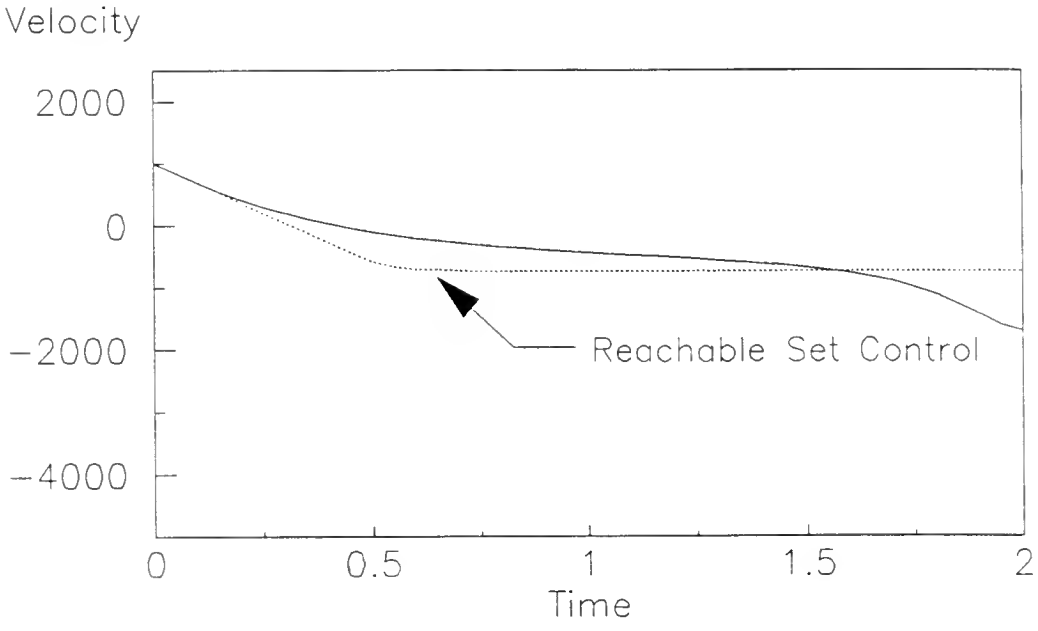

Figure 5.13 Velocity vs Time
LQG and Reachable Set Control

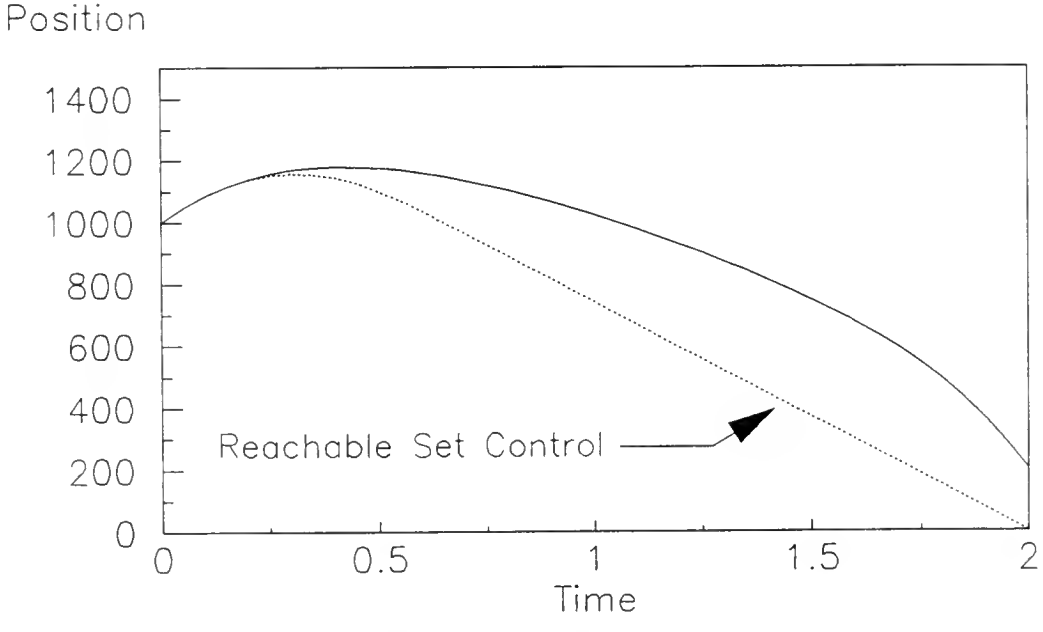

Figure 5.14 Position vs Time
LQG and Reachable Set Control

Summary

The improved performance of Reachable Set Control is obvious from Figure 5.14. While demonstrated for a specific plant, and symmetric control constraint set, Reachable Set Control is capable of improving the terminal performance of a large class of systems. It minimized the effects of modeling errors (or target set uncertainty) by regulating the system to the zero control state. The technique handled constraints and insured an initially constrained trajectory. The tracking problem could be optimized to the response time of the system under consideration by smoothly driving the system from some large displacement to a region where the relatively high gain LQG controller remained linear.

CHAPTER VI
REACHABLE SET CONTROL FOR PREFERRED AXIS HOMING MISSILES

As stated in Chapter II, the most promising techniques that can extend the inertial point mass formulation are based on singular perturbations [37,38,39]. When applied to the preferred axis missile, each of these techniques leads to a controller that is optimal in some sense. However, a discussion of "optimality" notwithstanding, the best homing missile intercept trajectory is the one that arrives at the final "control point" with the highest probability of hitting the target. This probability can be broken down into autonomous and forced events. If nothing is changed, what is the probability of a hit or what is the miss distance? If the target does not maneuver, can additional control inputs result in a hit? And, in the worse case, if the target maneuvers (or an estimation error is corrected) will the missile have adequate maneuverability to correct the trajectory? None of the nonlinear techniques based on singular perturbations attempt to control uncertainty or address the terminally constrained trajectories caused by increasing acceleration profile.

Unfortunately, an increasing acceleration profile has been observed in all of the preferred axis homing missile controllers. In many cases, the generic bank-to-turn missile of [11,18] was on all three constraints (Ny,Nz,P) during the latter portion of the trajectory. If the evading target is able to put the missile in this position without approaching it's own maneuver limits, it will not be possible for the missile to counter the final evasive maneuver. The missile is no longer controllable to the target set. The "standard" solution to the increasing acceleration profile is a varying control cost. However, without additional

additional modifications, this type of solution results in a trajectory dependent control. As we have seen, Reachable Set Control is an LQG control implementation that moves the system to the point where further inputs are not required. A Reachable Set Controller that will reject target and system disturbances, can satisfy both the mathematical and heuristic optimality requirements by minimizing the cost yet maintaining a controllable system.

Since the roll control has different characteristics, the discussion of the preferred axis homing missile controller using the Reachable Set Control technique will be separated into translational and roll subsystems. The translational subsystem has a suitable null control trajectory defined by the initial velocity and uncontrollable acceleration provided by the rocket motor. The roll subsystem, however, is significantly different. In order for the preferred axis missile to function, the preferred axis must be properly aligned. Consequently, both roll angle error and roll rate should be zero at all times. In this case, the null control trajectory collapses to the origin.

Acceleration Control

System Model

Since we want to control the relative target-missile inertial system to the zero state, the controller will be defined in this reference frame. Each of the individual system states are defined (in relative coordinates) as target state minus missile state.

Begin with the deterministic system:

$$\dot{x}(t) = Fx(t) + Gu(t) \tag{1}$$

where

$$x = \begin{bmatrix} x \\ y \\ z \\ Vx \\ Vy \\ Vz \end{bmatrix} \qquad u = \begin{bmatrix} Nx \\ Ny \\ Nz \end{bmatrix}$$

and

$$F = \begin{bmatrix} 0 & I \\ 0 & 0 \end{bmatrix} \qquad G = \begin{bmatrix} 0 \\ -I \end{bmatrix}$$

Since the autopilot model is a linear approximation and the inertial model assumes instantaneous response, modeling errors will randomly affect the trajectory. Atmospheric and other external influences will disturb the system. Also, the determination of the state will require the use of noisy measurements. Consequently, the missile intercept problem should be approached via a stochastic optimal control law. Because the Reachable Set Control technique will minimize the effect of plant parameter variations (modeling errors) and unmodeled target maneuvers to maintain controllability, we can use an LQG controller. Assuming Certainty Equivalence, this controller consists of an optimal linear (Kalman) filter cascaded with the optimal feedback gain matrix of the corresponding deterministic optimal control problem. Disturbances and modeling errors can be accounted for by suitably extending the system description [40]:

$$\dot{x}(t) = F(t)x(t) + G(t)u(t) + V_S(t) \tag{2}$$

by adding a noise process $V_S(\cdot,\cdot)$ to the dynamics equations with

$$V_S(t,\omega) \in R^n \tag{3}$$

Therefore, let the continuous time state description be formally given by the linear stochastic differential equation

$$dx(t) = F(t)x(t)dt + G(t)u(t)dt + L(t)d\beta(t) \tag{4}$$

(with $\beta(\cdot,\cdot)$ a Wiener process) that has the solution:

$$x(t) = \Phi(t,t_0)x(t_0) + \int_{t_0}^{t} \Phi(t,\tau)G(\tau)u(\tau)d\tau + \int_{t_0}^{t} \Phi(t,\tau)L(\tau)d\beta(\tau) \tag{5}$$

characterized by a covariance and mean whose trajectory can be adequately represented as:

$$\dot{x}(t) = F(t)x(t) + G(t)u(t) + Lw_S(t) \tag{6}$$

where $w_S(\cdot,\cdot)$ is a zero mean white Gaussian noise of strength $W_S(t)$ for all t.

$$E\{w_S(t)w_S(t)^T\} = W_S(t) \tag{7}$$

Disturbance Model

In the process of the intercept, it is expected that the target will attempt to counter the missile threat. While it is theoretically possible to have an adequate truth model and sufficiently sophisticated algorithms to adapt system parameters or detect the maneuvers, the short time of flight and maneuver detection delays make this approach unrealistic at this time. Even though the actual evasive maneuvers will be discretely initiated and carried out in finite time, the effect of these maneuvers, combined with unmodeled missile states, appear as continuous, correlated and uninterrupted disturbances on the system. Therefore, even though a minimum square error, unbiased estimate can be made of the system state it would be very unusual for the estimates of the target

state to converge with zero error. Since the optimal solution to the linear stochastic differential equation is a Gauss-Markov process, time correlated processes can be included by augmenting the system state to include the disturbance process.

Let the time-correlated target (position) disturbance be modeled by the following:

$$\dot{T}(t) = N(t)T(t) + w_t(t) \tag{8}$$

with

$$T(t) = \begin{bmatrix} Tx(t) \\ Ty(t) \\ Tz(t) \end{bmatrix}$$

and

$$E\{w_t(t)w_t(t)^T\} = W_t(t)$$

While the target disturbance resulting from an unknown acceleration is localized to a single plane with respect to the body axis of the target, the target orientation is unknown to the inertial model. Consequently, following the methodology of the Singer Model, each axis will be treated equally [41]. Since the disturbance is first order Markov, it's components will be:

$$N(t) = -(1/T_c)[I] \tag{9}$$

and

$$W_t(t) = (2\sigma_t^2/T_c)[I] \tag{10}$$

where T_c is the correlation time, and σ_T is the RMS value of the disturbance process. The Power Spectral Density of the disturbance is:

$$\Psi_{tt}(\omega) = \frac{2\sigma_t^2/T_c}{\omega^2 + (1/T_c)^2} \tag{11}$$

Figure 6.1 summarizes the noise interactions with the system.

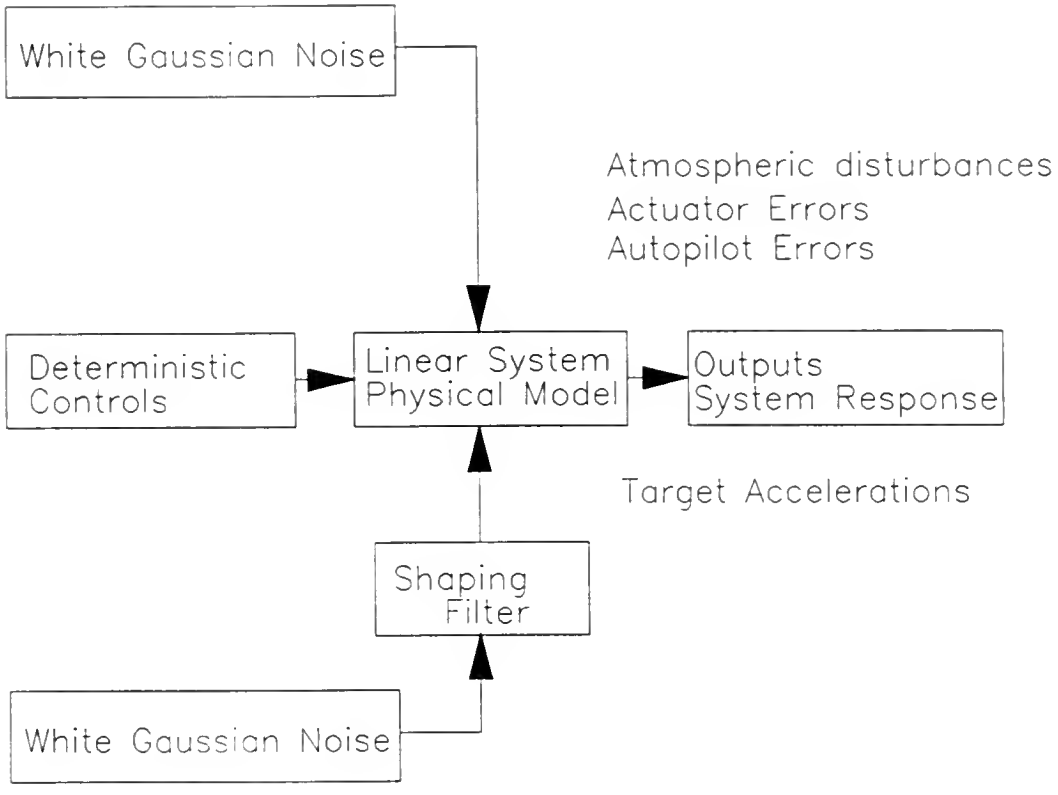

Figure 6.1 Reachable Set Control Disturbance processes.

With appropriate dimensions, the nine state (linear) augmented system model becomes:

$$\begin{bmatrix} \dot{x}(t) \\ \dot{T}(t) \end{bmatrix} = \begin{bmatrix} F(t) & I \\ O & N(t) \end{bmatrix} \begin{bmatrix} x(t) \\ T(t) \end{bmatrix} + \begin{bmatrix} G(t) \\ O \end{bmatrix} u(t) + \begin{bmatrix} L & O \\ O & M \end{bmatrix} \begin{bmatrix} w_s(t) \\ w_t(t) \end{bmatrix} \quad (12)$$

Reference Model

Reachable Set Control requires a supervisory steering control (reference) that includes the environmental impact on the controlled dynamic system. Recalling the characteristics of the dual system, one was developed that explicitly ran (1) backward in time after determining the terminal conditions. However, in developing this control for this preferred axis missile a number of factors actually simplify the computation of the reference trajectory:

(1) The control constraint set for this preferred axis missile is symmetric. Consequently, the reference trajectory for an intercept condition, is a null control (coasting) trajectory.

(2) The body axis X acceleration is provided by the missile motor, and is not controllable but known. This uncontrollable acceleration will contribute to the total inertial acceleration vector, must be considered by the controller, and is the only acceleration present on an intercept (coasting) trajectory.

(3) The termination of the intercept is the closest approach, which now becomes the fixed-final-time (t_f). The time-to-go (tgo) is defined with respect to the current time (t) by:

$$t = t_f - tgo \tag{13}$$

(4) The final boundary condition for the system state (target minus missile) is zero.

In summary, the intercept positions are zero, the initial velocity is given, and the average acceleration is a constant. Therefore, it is sufficient to reverse the direction of the initial velocity and average acceleration then run the system forward in time for tgo seconds from the origin to determine the current position of the coasting trajectory. Let:

$$\dot{r}(t) = A(t)r(t) + B(t)a(t) \tag{14}$$

with

$$r(0) = r_0 = 0$$

and

$$A(t) = F(t) \quad \text{and} \quad B(t) = G(t)$$

then r(t) is the point from which the autonomous system dynamics will take the system to desired boundary condition.

Because of the disturbances, target motion, and modeling errors, future control inputs are random vectors. Therefore, the best policy is not to

determine the input over the control period $[t_0,t_f]$ a priori but to reconsider the situation at each instant t on the basis of all available information. At each update, if the system is controllable, the reference (and system state) will approach zero as tgo approaches zero.

Since the objective of the controller is to drive the system state to zero, we do not require a tracker that will maintain the control variable at a desired non-zero value with zero steady state error in the presence of unmodeled constant disturbances. There are disturbances, but the final set point is zero, and therefore, a PI controller is not required.

Roll Control

Definition

The roll mode is most significant source of modeling errors in the preferred axis homing missile. While non-linear and high order dynamics associated with the equations of motion, autopilot, and control actuators are neglected, the double integrator is an exact model for determining inertial position from inertial accelerations. The linear system, however, is referenced with respect to the body axis. Consequently, to analyze the complete dynamics, the angular relationship between the body axis and inertial references must be considered. Recall Friedland's linearized (simplified) equations. The angular relationships determine the orientation of the body axis reference and the roll rate appeared in the dynamics of all angular relationships. Yet, to solve the system using linear techniques, the system must be uncoupled via a steady state (Adiabatic) assumption. Also, the roll angle is inertially defined and the effect of the linear accelerations on the error is totally neglected.

From a geometric point of view, this mode controls the range of the orthogonal linear acceleration commands and the constrained controllability of the trajectory. With a 20:1 ratio in the pitch and yaw accelerations, the ability to point the preferred axis in the "proper" direction is absolutely critical. Consequently, effective roll control is essential to the performance of the preferred axis homing missile.

The first problem in defining the roll controller, is the determination of the "proper" direction. There are two choices. The preferred axis could be aligned with the target position or the direction of the commanded acceleration. The first selection is the easiest to implement. The seeker gimbal angles provide a direct measure of intercept geometry (Figure 6.2), and the roll angle error is defined directly:

$$\phi_e = \mathrm{Tan}^{-1}\{\sin(\psi_g)/\tan(\theta_g)\} \qquad (15)$$

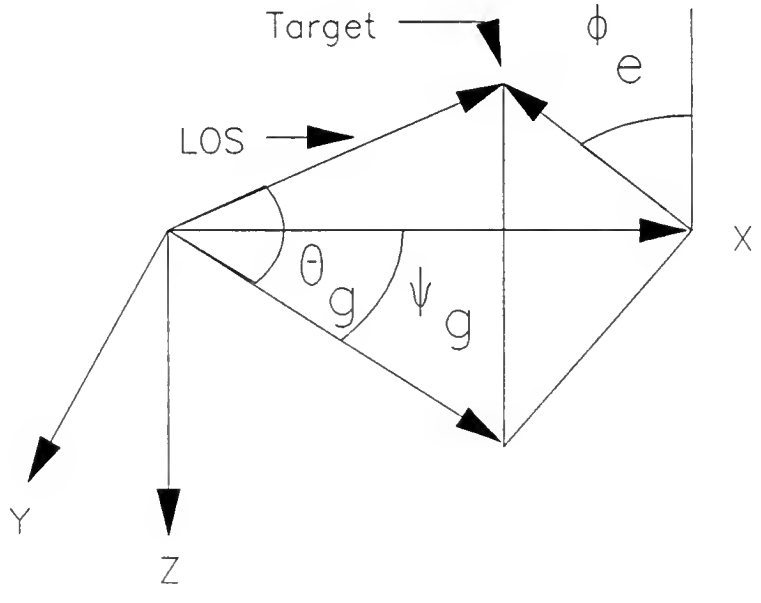

Figure 6.2. Roll Angle Error Definition from Seeker Angles.

This selection, however, is not the most robust. Depending on the initial geometry, the intercept point may not be in the plane defined by the current

line of sight (LOS) and longitudinal axis of the missile. In this case, the missile must continually adjust its orientation (roll) to maintain the target in the preferred plane. As range decreases the angular rates increase, with the very real possibility of saturation and poor terminal performance.

Consequently, the second definition of roll angle error should be used. Considering the dynamics of the intercept, however, aligning the preferred axis with the commanded acceleration vector is not as straightforward as it seems. Defining the roll angle error as

$$\phi_e = \mathrm{Tan}^{-1}\{A_y/A_z\} \tag{16}$$

leads to significant difficulties. From the previous discussion, it is obvious that roll angle errors must be minimized so that the preferred axis acceleration can be used to control the intercept. The roll controller must have a high gain. Assume, for example, the missile is on the intercept trajectory. Therefore, both A_y and A_z will be zero. Now, if the target moves slightly in the Y_b direction and the missile maneuvers to correct the deviation, the roll angle error instantaneously becomes 90 degrees. High gain roll control inputs to correct this situation are counter productive. The small A_y may be adequate to completely correct the situation before the roll mode can respond. Now, the combination of linear and roll control leads to instability as the unnecessary roll rate generates errors in future linear accelerations.

The problems resulting from the definition of equation 16 can be overcome be re-examining the roll angle error. First, A_y and A_z combine to generate a resultant vector at an angle from the preferred axis. In the process of applying constraints, the acceleration angle that results from the linear accelerations can be increased or decreased by the presence of the constraint. If the angle is decreased, the additional roll is needed to line up the preferred axis and the

desired acceleration vector. If the constrained (actual) acceleration angle is increased beyond the (unconstrained) desired value by the unsymmetric action of the constraints, then the roll controller must allow for this "over control" caused by the constraints.

Define the roll angle error as the difference between the actual and desired acceleration vectors after the control constraints are considered. This definition allows for the full skid to turn capability of the missile in accelerating toward the intercept point and limits rolling to correct large deviations in acceleration angle from the preferred axis that are generated by small accelerations.

Referring to Figure 6.3, three zones can be associated with the following definitions:

$$\phi_{ec} = \text{Tan}^{-1}\{A_y/A_z\} \tag{17}$$

$$\phi_{ea} = \text{Tan}^{-1}\{N_y/N_z\} \tag{18}$$

$$\phi_{er} = \phi_{ec} - \phi_{ea} \tag{19}$$

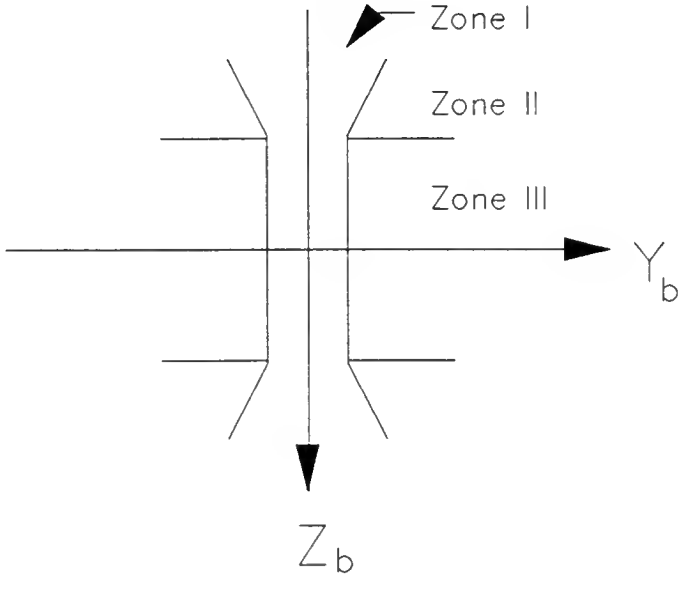

Figure 6.3. Roll Control Zones.

Here N_y and N_z are the constrained acceleration values. In Zone I, $\phi_{er} = 0$. The linear acceleration can complete the intercept without further roll angle change. This is the desired locus for the roll controller. Both A_y and A_z are limited in Zone II. This is the typical situation for the initial position of a demanding intercept. The objective of the roll controller is to keep the intercept acceleration out of Zone III where only A_y is limited. In this case, the A_y acceleration is insufficient to complete the intercept yet significant roll angle change may be required to make the trajectory controllable.

Controller

A dual mode roll controller was developed to accommodate the range of situations and minimize roll angle error. Zone I requires a lower gain controller that will stabilize the roll rate and maintain ϕ_{er} small. Zones II and III require high gain controllers. To keep Zone II trajectories from entering Zone III, the ϕ_{ec} will be controlled to zero rather than the roll angle error. Since the linear control value is also a function of the roll angle error, roll angle errors are determined by comparing the desired and actual angles of a fixed high gain reachable set controller. If the actual linear commands are used and a linear acceleration is small because of large roll angle errors, the actual amount of roll needed to line up the preferred axis and the intercept point, beyond the capability of the linear accelerations, will not be available because they have been limited by the existing roll angle error that must be corrected.

Unlike the inertial motions, the linear model for the roll controller accounts for the (roll) damping and recognizes that the input is a roll rate change command:

$$\ddot{\phi} = -\omega\dot{\phi} + \omega P \tag{20}$$

Therefore, the roll mode elements (that will be incorporated into the model are) are:

$$F_r = \begin{bmatrix} O & 1 \\ O & -\omega \end{bmatrix} \qquad G_r = \begin{bmatrix} O \\ \omega \end{bmatrix} \tag{21}$$

Also, the dual mode controller will require an output function and weighting matrix that includes both roll angle and roll rate.

Kalman Filter

The augmented system model (13) is not block diagonal. Consequently, the augmented system filter will not decouple into two independent system and reference filters. Rather, a single, higher order filter was required to generate the state and disturbance estimates.

A target model (the Singer model) was selected and modified to track maneuvering targets from a Bank-To-Turn missile [41,42]. Using this model, a continuous-discrete Extended Kalman Filter was developed. The filter used a 9 state target model for the relative motion (target - missile):

$$\begin{bmatrix} \dot{x}(t) \\ \dot{a}_T(t) \end{bmatrix} = \begin{bmatrix} F & -G \\ O & N \end{bmatrix} \begin{bmatrix} x(t) \\ a_T(t) \end{bmatrix} + \begin{bmatrix} G \\ O \end{bmatrix} u(t) + \begin{bmatrix} O \\ -N \end{bmatrix} \begin{bmatrix} O \\ w_t(t) \end{bmatrix} \tag{22}$$

with u(t) the known missile acceleration, N the correlation coefficient, and $w_t(t)$ an assumed Gaussian white noise input with zero mean.

Azimuth, elevation, range, and range rate measurements were available from passive IR, semi-active, analog radar, and digitally processed radar sensors. The four measurements are seeker azimuth (ψ), seeker elevation (θ), range (r), and range rate (dr/dt):

$$\theta = -\text{Tan}^{-1}\{z(x^2+y^2)^{-1/2}\} \tag{23}$$

$$\psi = +\text{Tan}^{-1}\{y/x\} \qquad x \geq 0$$

$$= \pi + \text{Tan}^{-1}\{y/x\} \qquad x \leq 0$$

$$r = \{x^2+y^2+z^2\}^{-1/2}$$

$$\dot{r} = \{x\dot{x}+y\dot{y}+z\dot{z}\}\{x^2+y^2+z^2\}^{-1/2}$$

Noise statistics for the measurements are a function of range, and are designed to simulate glint and scintillation in a relatively inexpensive missile seeker. In contrast to the linear optimal filter, the order of the measurements for the extended filter is important. In this simulation, the elevation angle (θ) was processed first, followed by azimuth (ψ), range (r), and range rate (dr/dt). In addition, optimal estimates were available from the fusion of the detailed (digital) radar model and IR seeker.

Reachable Set Controller

Structure

The Target-Missile System is shown in Figure 6.4. The combination of the augmented system state and the dual reference that generates the minimum control trajectory for the reachable set concept is best described as a Command Generator/Tracker and is shown in Figure 6.5. In a single system of equations the controller models the system response, including time correlated position disturbances, and provides the reference trajectory. Since only noise-corrupted measurements of the controlled system are available, optimal estimates of the actual states were used.

Because of the processing time required for the filter and delays in the autopilot response, a continuous-discrete Extended Kalman Filter, and a sampled

data (discrete) controller was used. This controller incorporated discrete cross-coupling terms to control the deviations between the sampling times as well the capability to handle non-coincident sample and control intervals (Appendices B and C).

Combining the linear and roll subsystems with a first order roll mode for the roll angle state, the model for the preferred axis homing missile becomes:

$$\begin{bmatrix} \dot{x}(t) \\ \dot{T}(t) \end{bmatrix} = \begin{bmatrix} F(t) & I \\ O & N(t) \end{bmatrix} \begin{bmatrix} x(t) \\ T(t) \end{bmatrix} + \begin{bmatrix} G(t) \\ O \end{bmatrix} u(t) + \begin{bmatrix} L & O \\ O & M \end{bmatrix} \begin{bmatrix} w_s(t) \\ w_t(t) \end{bmatrix} \tag{24}$$

the reference:

$$\dot{r}(t) = A(t)r(t) + B(t)a(t) \tag{25}$$

with the tracking error:

$$e(t) = [\ y_x(t) - y_r(t)\ ] = [\ H(t) \mid 0 \mid -C(t)\ ] \begin{bmatrix} x(t) \\ T(t) \\ r(t) \end{bmatrix} \tag{26}$$

The initial state is modeled as an n-dimensional Gaussian random variable with mean x_0 and covariance P_0. $E\{w_s(t)w_s(t)^T\} = Ws(t)$ is the strength of the system (white noise) disturbances to be rejected, and $E\{w_t(t)w_t(t)^T\} = Wt(t)$ is an input to a stationary first order Gauss-Markov process that models target acceleration. The positions are the primary variables of interest, and the output matrices will select these terms. Along with the roll rate, these are the variables that will be penalized by the control cost and the states where disturbances will directly impact the performance of the system.

The components of the controlled system are: (27)

$$x(t) = \begin{bmatrix} x(t) \\ y(t) \\ z(t) \\ \phi(t) \\ \dot{x}(t) \\ \dot{y}(t) \\ \dot{z}(t) \\ \dot{\phi}(t) \end{bmatrix} \qquad T(t) = \begin{bmatrix} Tx(t) \\ Ty(t) \\ Tz(t) \end{bmatrix} \qquad r(t) = \begin{bmatrix} r_x(t) \\ r_y(t) \\ r_z(t) \\ r_\phi(t) \\ \dot{r}_x(t) \\ \dot{r}_y(t) \\ \dot{r}_z(t) \\ \dot{r}_\phi(t) \end{bmatrix}$$

$$u(t) = \begin{bmatrix} Nx(t) \\ Ny(t) \\ Nz(t) \\ \dot{P}(t) \end{bmatrix} \qquad e(t) = \begin{bmatrix} x(t) \\ y(t) \\ z(t) \\ \phi(t) \\ 0 \\ 0 \\ 0 \\ \dot{\phi}(t) \end{bmatrix} - \begin{bmatrix} r_x(t) \\ r_y(t) \\ r_z(t) \\ r_\phi(t) \\ 0 \\ 0 \\ 0 \\ \dot{r}_\phi(t) \end{bmatrix}$$

$$a(t) = \begin{vmatrix} \cos(\theta)\cos(\psi) \\ \cos(\theta)\sin(\psi) \\ -\sin(\theta) \end{vmatrix} \hat{A}$$

where $\hat{A}$ is the average acceleration from the rocket motor.

In block form, with appropriate dimensions, the system matrices are:

$$F(t) = A(t) = F = \begin{bmatrix} O & I \\ O & O_w \end{bmatrix} \qquad G(t) = B(t) = G = \begin{bmatrix} O \\ I_w \end{bmatrix} \tag{28}$$

$$N(t) = -(1/T_c)[I]$$

$$H(t) = C(t) = [\, I \;\; h_w \,] \qquad L(t) = I \qquad M(t) = I$$

where the O_w, I_w, and h_w terms are required to specify the roll axis system and control terms:

$$(O_w)_{ij} = \begin{cases} -\omega & i=j=8 \\ 0 & \text{otherwise} \end{cases} \qquad (h_w)_{ij} = \begin{cases} 1 & i=j=8 \\ 0 & \text{otherwise} \end{cases}$$

$$(I_w)_{ij} = \begin{cases} +\omega & i=8, j=4 \\ I & \text{otherwise} \end{cases}$$

The performance objective for the LQG synthesis is to minimize an appropriate continuous-time quadratic cost:

$$J_s(t) = E\{J_d(t)|I(t)\} \tag{29}$$

where J_s is the stochastic cost, I(t) is the information set available at time t, and J_d a deterministic cost function:

$$J_d = e_f{}^T P_f e_f + \int_{t_0}^{t_f} \{e(\tau)^T Q(\tau) e(\tau) + u(\tau)^T R(\tau) u(\tau)\} d\tau \tag{30}$$

Dividing the interval of interest into N+1 intervals for discrete time control, and summing the integral cost generates the following (see Appendix C):

$$J_d = e(t_{N+1})^T P(t_{N+1}) e(t_{N+1}) \tag{31}$$
$$+ \sum_{i=0}^{N} \begin{bmatrix} e(t_i)^T \\ u(t_i) \end{bmatrix} \begin{bmatrix} Wxx(t_i) & Wxu(t_i) \\ Wxu(t_i)^T & Wuu(t_i) \end{bmatrix} \begin{bmatrix} e(t_i) \\ u(t_i) \end{bmatrix}$$

which can be related to the augmented state $\chi = [\, x\ T\ r \,]^T$ by:

$$J_d = \chi(t_{N+1})^T P(t_{N+1}) \chi(t_{N+1}) \tag{32}$$
$$+ \sum_{i=0}^{N} \begin{bmatrix} \chi(t_i)^T \\ u(t_i) \end{bmatrix} \begin{bmatrix} Q(t_i) & S(t_i) \\ S(t_i)^T & R(t_i) \end{bmatrix} \begin{bmatrix} \chi(t_i) \\ u(t_i) \end{bmatrix}$$

In general, with the cost terms defined for the augmented state (Appendix C), the optimal (discrete) solution to the LQG tracker can be expressed as:

$$u^*(t_i) = -[G^*(t_i)] \begin{bmatrix} x(t_i) \\ T(t_i) \\ r(t_i) \end{bmatrix} \tag{33}$$

where

$$G^*(t_i) = [\, R(t_i) + G^T(t_i)P(t_{i+1})G(t_i) \,]^{-1} \tag{34}$$
$$[\, G^T(t_i)P(t_{i+1})\Phi(t_{i+1},t_i) + S^T(t_i) \,]$$

and

$$P(t_i) = Q(t_i) + \Phi^T(t_{i+1},t_i)P(t_{i+1})\Phi(t_{i+1},t_i) \tag{35}$$
$$- [\, G^T(t_i)P(t_{i+1})\Phi(t_{i+1},t_i) + S^T(t_i) \,]^T G^*(t_i)$$

Since only the positions (and roll rate) are penalized, the Riccati recursion is quite sparse. Consequently, by partitioning the gain and Riccati equations, and explicitly carrying out the matrix operations, considerable computational improvements are possible over the straightforward implementation of a 19 by 19 tracker (Appendix D).

Application

The tracking error and control costs were determined from the steady state tracker used in the example in Chapter 5. First, missile seeker and aerodynamic limitations were analyzed to determine the most demanding intercept attainable by the simulated hardware. Then, autopilot delays were incorporated to estimate that amount of time that a saturated control would require to turn the missile after correcting a 90 degree (limit case) roll angle error. The steady state regulator was used to interactively place the closed loop poles and select a control cost combination that generated non zero control for the desired length of time. These same values were used in the time varying Reachable Set Controller with the full up autopilot simulation to determine the

terminal error cost and control delay time. To maintain a basis of comparison, the Kalman Filter parameters were not modified for this controller. Appendix E contains initial conditions for the controller and estimator dynamics.

During the initialization sequence (safety delay) for a given run, time varying fixed-final-time LQG regulator gains are calculated (via 36) based on the initial estimate of the time to go. Both high and low roll control gains were computed. These solutions used the complete Riccati recursion and cost based on the sampled data system, included a penalty on the final state (to control transient behavior as tgo approaches zero), and allowed for non-coincident sample and control.

Given an estimated tgo, at each time t, the Command Generator / Tracker computed the reference position and required roll angle that leads to an intercept without additional control input. The high or low roll control gain was selected based on the mode. Then the precomputed gains (that are a function of tgo) are used with the state and correlated disturbance estimate from the filter, roll control zone, and the reference r to generate the control (which is applied only to the missile system). Because of symmetry, the tracker gain for the state term equaled the reference gain, so that, in effect, except for the correlated noise, the current difference between the state x and the reference r determined the control value.

During the intercept, between sample times when the state is extrapolated by the filter dynamics, tgo was calculated based on this new extrapolation and appropriate gains used. This technique demonstrated better performance than using a constant control value over the duration of the sample interval and justified the computational penalty of the continuous - discrete implementation of the controller and filter.

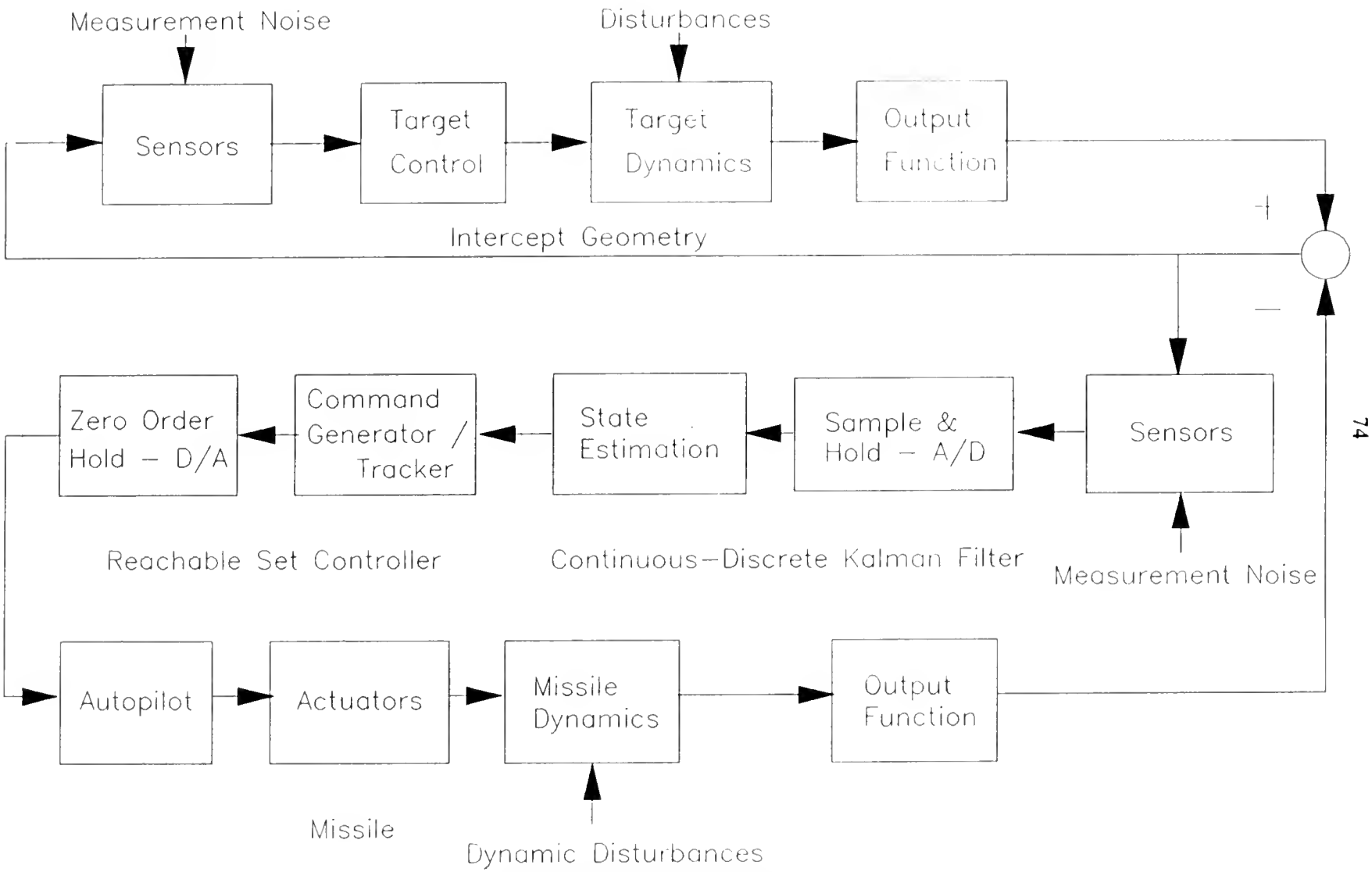

Figure 6.4 Target - Missile System

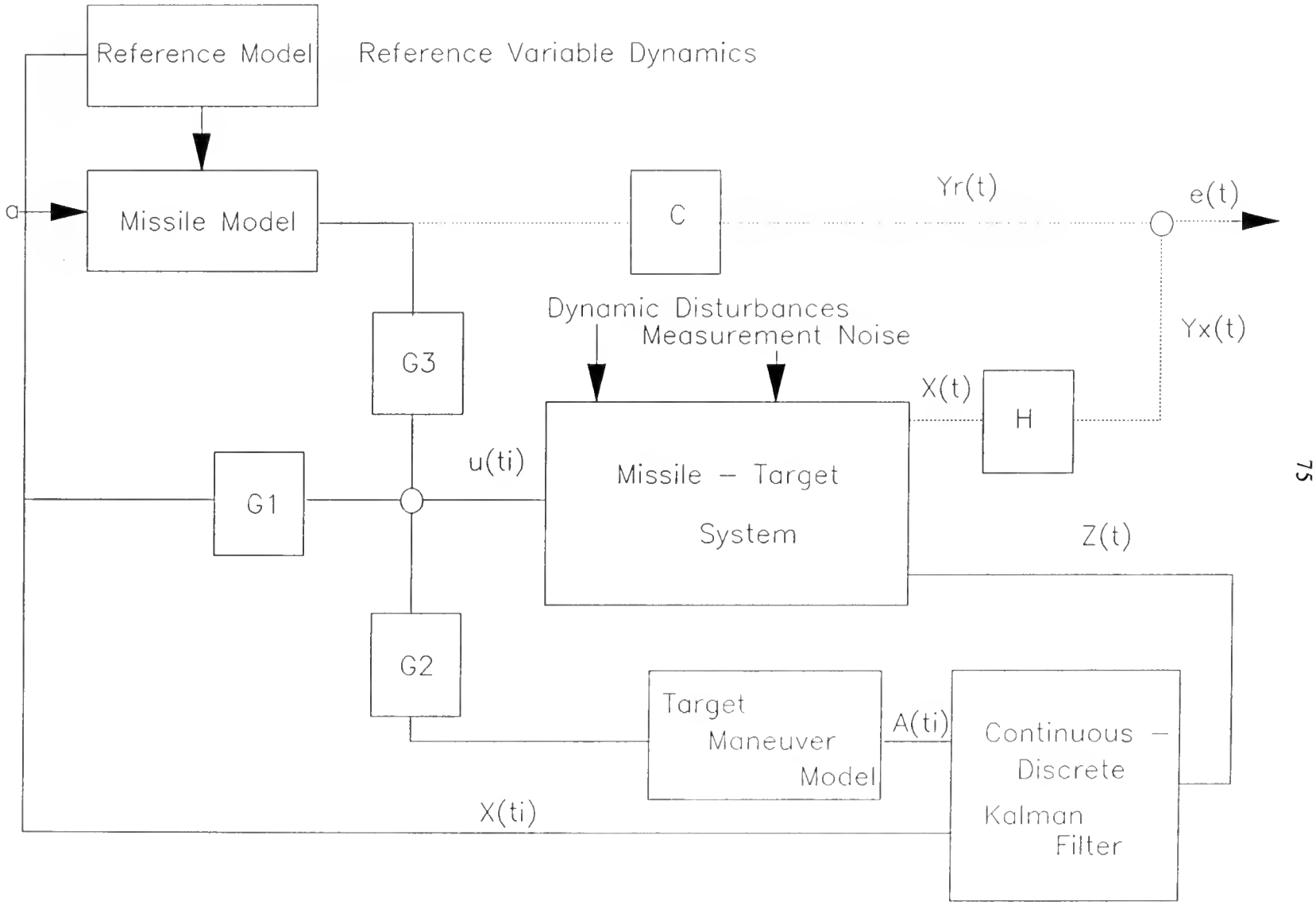

Figure 6.5 Command Generator / Tracker

CHAPTER VII
RESULTS AND DISCUSSION

As an additional reference, before comparing the results of Reachable Set Control to the baseline control, consider an air-to-air missile problem from [13]. In this example, the launch direction is along the line of sight, the missile velocity is constant, and the autopilot response to commands is instantaneous. The controller has noisy measurements of target angular location, a priori knowledge of the time to go, and stochastically models the target maneuver. Even with this relatively simple problem, the acceleration profile increases sharply near the final time. Unfortunately, this acceleration profile is typical, and has been observed in all previous optimal control laws. Reachable Set Control fixes this problem.

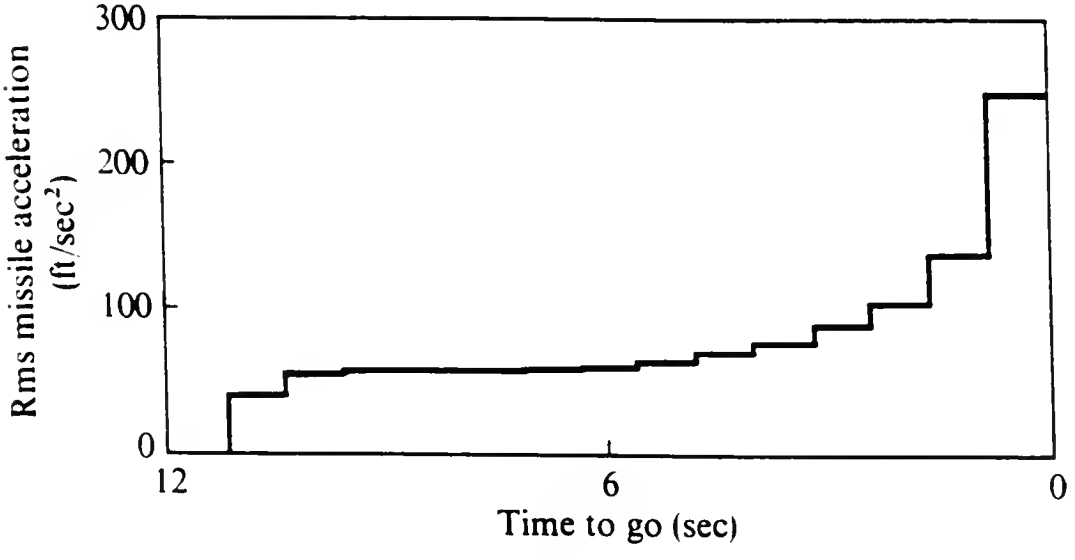

Figure 7.1 RMS Missile Acceleration

Simulation

The performance of Reachable Set Control was determined via a high fidelity Bank-To-Turn simulation developed at the University of Florida and used for a number of previous evaluations. The simulation is based on the coupled non-linear missile dynamics of chapter II equations (1) to (8) and is a continuous-discrete system that has the capability of comparing control laws and estimators at any sample time. In addition to the non-linear aerodynamic parameters, the simulation models the Rockwell Bank-To-Turn autopilot, sensor (seeker and accelerometer) dynamics, has a non-standard atmosphere, and mass model of the missile to calculate time-varying moments of inertia and the missile specific acceleration from the time varying rocket motor.

Figure 7.2 presents the engagement geometry and some of the variables used to define the initial conditions.

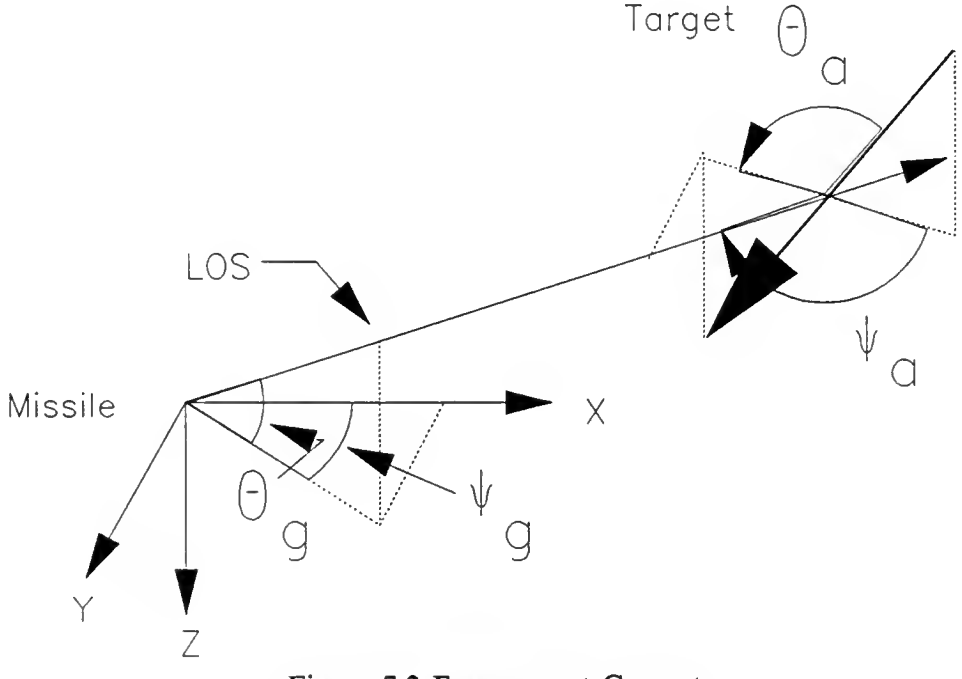

Figure 7.2 Engagement Geometry

The simulated target is a three (3) dimensional, nine (9) "g" maneuvering target. Initially, the target trajectory is a straight line. Once the range from the missile to target is less than 6000 feet, the target initiates an instantaneous 9 "g" evasive maneuver in a plane determined by the target roll angle, an input parameter. If the launch range is within 6000 feet, the evasive maneuver begins immediately. There is a .4 second "safety" delay between missile launch and autopilot control authority.

Trajectory Parameters

The performance of the control laws was measured with and without sensor noise using continuous and sampled data measurements. The integration step was .005 seconds and the measurement step for the Extended Kalman Filter was .05 seconds. The trajectory presented for comparison has an initial offset angle of 40 degrees (ψ_g) and 180 degree aspect (ψ_a), and a target roll of 90 degrees away from the missile. This angle off and target maneuver is one of the most demanding intercept for a preferred axis missile since it must roll through 90 degrees before the preferred axis is aligned with the target. Other intercepts were run with different conditions and target maneuvers to verify the robustness of Reachable Set Control and the miss distances were similar or less that this trajectory.

Results

Deterministic Results

These results are the best comparison of control concepts since both Linear Optimal Control and Reachable Set Control are based on assumed Certainty Equivalence.

Representative deterministic results are presented in Table 7.1 and Figure 7.3. Figures A.1 through A.9 present relevant parameters for the 4000 foot deterministic trajectories.

Table 7.1 Deterministic Control Law Performance

Initial Range (feet)	Control	Time (sec)	Miss Distance (feet)
5500	Baseline	2.34	8
	Reachable	2.34	6
5000	Baseline	2.21	13
	Reachable	2.21	10
4800	Baseline	2.17	15
	Reachable	2.17	4
4600	Baseline	2.13	29
	Reachable	2.13	6
4400	Baseline	2.06	38
	Reachable	2.08	7
4200	Baseline	2.02	35
	Reachable	2.05	5
4000	Baseline	1.98	54
	Reachable	2.00	13
3900	Baseline	1.98	43
	Reachable	1.98	8
3800	Baseline	1.98	40
	Reachable	1.98	8
3700	Baseline	2.02	44
	Reachable	1.99	10
3600	Baseline	1.99	136
	Reachable	1.99	65

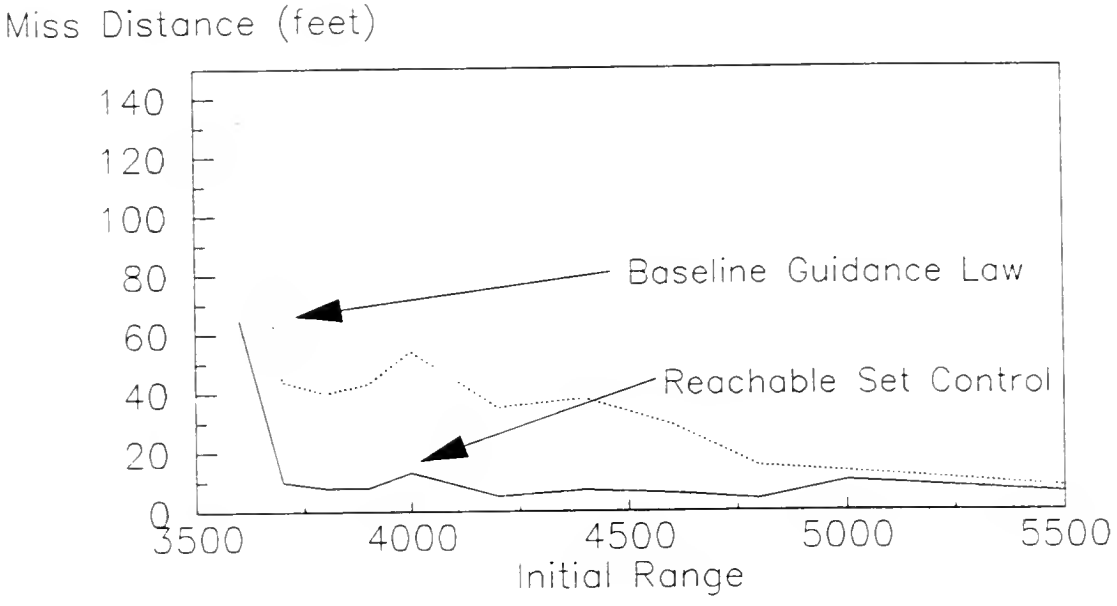

Figure 7.3 Deterministic Results

An analysis of trajectory parameters revealed that one of the major performance limitations was the Rockwell autopilot. Designed for proportional navigation with noisy (analog) seeker angle rates, the self adaptive loops in the autopilot penalized a high gain control law such as Reachable Set Control. This penalty prevented Reachable Set Control from demonstrating quicker intercepts and periodic control that were seen with a perfect autopilot on a similar simulation used during the research. However, even with the autopilot penalty, Reachable Set Control was able to significantly improve missile performance near the inner launch boundary. This verifies the theoretical analysis, since this is the region where the target set errors, control constraints, and short run times affect the linear law most significantly.

Stochastic Results

Stochastic performance was determined by 100 runs at each initial condition. At the termination of the run, the miss distance and Time of Flight (TOF) was recorded. During each of these runs, the estimator and seeker (noise) error sequences were tracked. Both sequences were analyzed to insure gaussian seeker noise, and an unbiased estimator (with respect to each axis). From the final performance data, the mean and variance of the miss distance was calculated. Also, from the estimator and seeker sequences, the root mean square (RMS) error and variance for each run was determined to identify some general characteristics of the process. The average of these numbers is presented. Care must be taken in interpreting these numbers. Since the measurement error is a function of the trajectory as well as instantaneous trajectory parameters, a single number is not adequate to completely describe the total process. Table 7.2 and Figure 7.4 present average results using the guidance laws with noisy measurements and the Kalman filter.

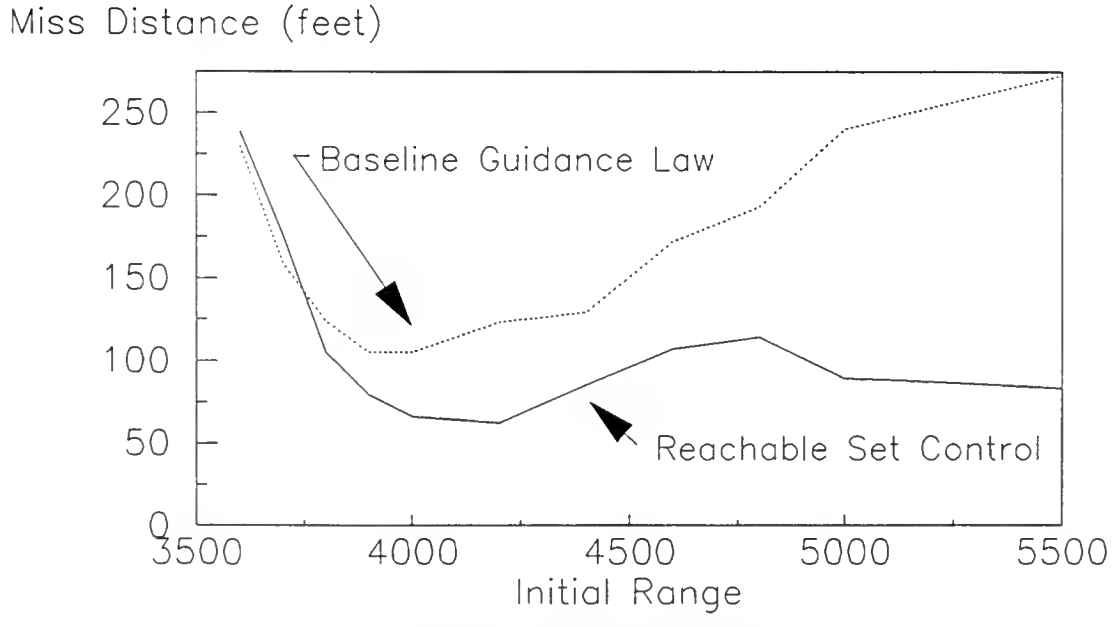

Figure 7.4 Stochastic Results

Table 7.2 Stochastic Control Law Performance

Initial Control Range (feet)		Time (sec)	Miss Distance Mean (feet)	Miss Distance Variance	RMS Error EKF (feet)	RMS Error Seeker (deg)
5500	Baseline	2.38	273	11470	11	1.3
	Reachable	2.41	83	2677	11	1.5
5000	Baseline	2.23	240	7874	11	1.4
	Reachable	2.25	89	3937	10	1.6
4800	Baseline	2.18	193	7540	10	1.4
	Reachable	2.19	114	3708	10	1.6
4600	Baseline	2.13	172	5699	10	1.4
	Reachable	2.13	107	1632	10	1.5
4400	Baseline	2.08	129	4324	10	1.5
	Reachable	2.07	85	1421	10	1.6
4200	Baseline	2.04	123	3375	10	1.6
	Reachable	2.03	62	673	10	1.7
4000	Baseline	2.01	105	2745	10	1.7
	Reachable	2.01	66	1401	10	1.8
3900	Baseline	2.00	105	3637	10	1.8
	Reachable	2.00	79	4356	10	1.8
3800	Baseline	2.00	124	5252	10	1.8
	Reachable	1.99	105	10217	10	2.0
3700	Baseline	1.98	159	5240	10	1.8
	Reachable	1.98	176	13078	9	1.8
3600	Baseline	1.95	230	6182	10	1.7
	Reachable	1.95	239	14808	10	1.7

The first runs made with Reachable Set Control were not as good as the results presented. Reachable Set Control was only slightly (10 to 20 feet) superior to the baseline guidance law and was well below expectations. Yet, the performance of the filter with respect to position error was reasonable, many of the individual runs had miss distances near 20 feet, and most of the errors were in the Z axis. Analyzing several trajectories from various initial conditions led to two main conclusions. First, the initial and terminal seeker errors were quite large, especially compared to the constant 5 mrad tracking accuracy assumed by many studies [2,3,18]. Second, the non-linear coupled nature of the preferred axis missile, combined with range dependent seeker errors, and the system (target) model, makes the terminal performance a strong function of the particular sequence of seeker errors. For example, Figure 7.5 compares the actual and estimated Z axis velocity (Target - Missile) from a single 4000 foot run. The very first elevation measurement generated a 14 foot Z axis position error. A reasonable number considering the range. The Z axis velocity error, however, was quite large, 409 feet per second, and never completely eliminated by the filter. Recalling that the target velocity is 969 feet per second, is approximately co-altitude with the missile and maneuvers primarily in the XY plane, this error is significant when compared to the actual Z axis velocity (2 feet per second). Also, this is the axis that defines the roll angle error and, consequently, roll rate of the missile. Errors of this magnitude cause the primary maneuver plane of the missile to roll away from the target limiting (via the constraints) the ability of the missile to maneuver.

Further investigation confirmed that the filter was working properly. Although the time varying noise prevents a direct comparison for an entire trajectory, these large velocity errors are consistent with the covariance ratios

in [41]. The filter model was developed to track maneuvering targets. The penalty for tracking maneuvering targets is the inability to precisely define all of the trajectory parameters (ie. velocity). More accurate (certain) models track better, but risk losing track (diverging) when the target maneuvers unexpectedly. The problem with the control then, was the excessive deviations in the velocity. To verify this, the simulation was modified to use estimates of position, but to use actual velocities. Figure 7.6 and Table 7.3 has these results. As seen from the table, the control performance is quite good considering the noise statistics and autopilot.

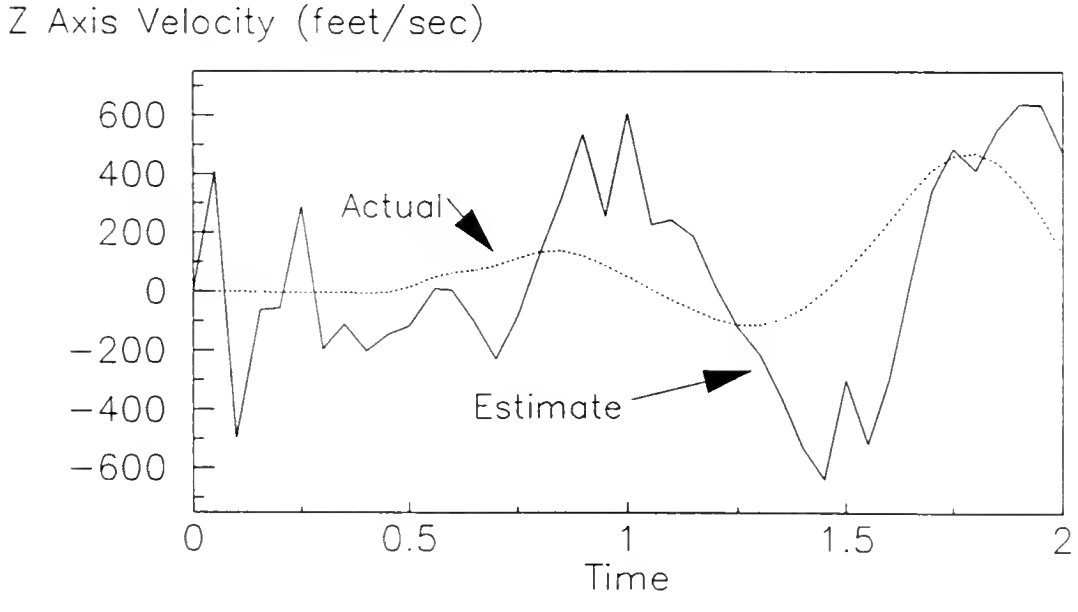

Figure 7.5 Measured vs Actual Z Axis Velocity

Table 7.5 Stochastic Control Law Performance
Using Actual Velocities

Initial Range (feet)	Control	Time (sec)	Miss Distance Mean (feet)	Miss Distance Variance (feet)	RMS Error EKF (feet)	RMS Error Seeker (deg)
5500	Baseline	2.35	34	318	10	1.5
	Reachable	2.37	38	504	11	1.5
5000	Baseline	2.21	50	506	10	1.7
	Reachable	2.23	38	623	10	1.6
4800	Baseline	2.17	55	367	10	1.6
	Reachable	2.19	48	526	10	1.5
4600	Baseline	2.12	61	366	10	1.6
	Reachable	2.14	52	326	10	1.6
4400	Baseline	2.06	62	333	10	1.7
	Reachable	2.10	45	415	10	1.7
4200	Baseline	2.02	60	277	10	1.7
	Reachable	2.06	44	463	10	1.8
4000	Baseline	1.98	62	330	10	1.9
	Reachable	2.02	53	1011	9	1.9
3900	Baseline	1.98	55	436	10	1.9
	Reachable	2.00	64	2052	10	1.9
3800	Baseline	1.98	53	400	9	2.0
	Reachable	1.99	91	2427	10	1.8
3700	Baseline	1.99	63	235	10	2.0
	Reachable	1.99	140	3110	10	1.7
3600	Baseline	1.98	138	354	10	1.8
	Reachable	1.96	213	4700	10	1.6

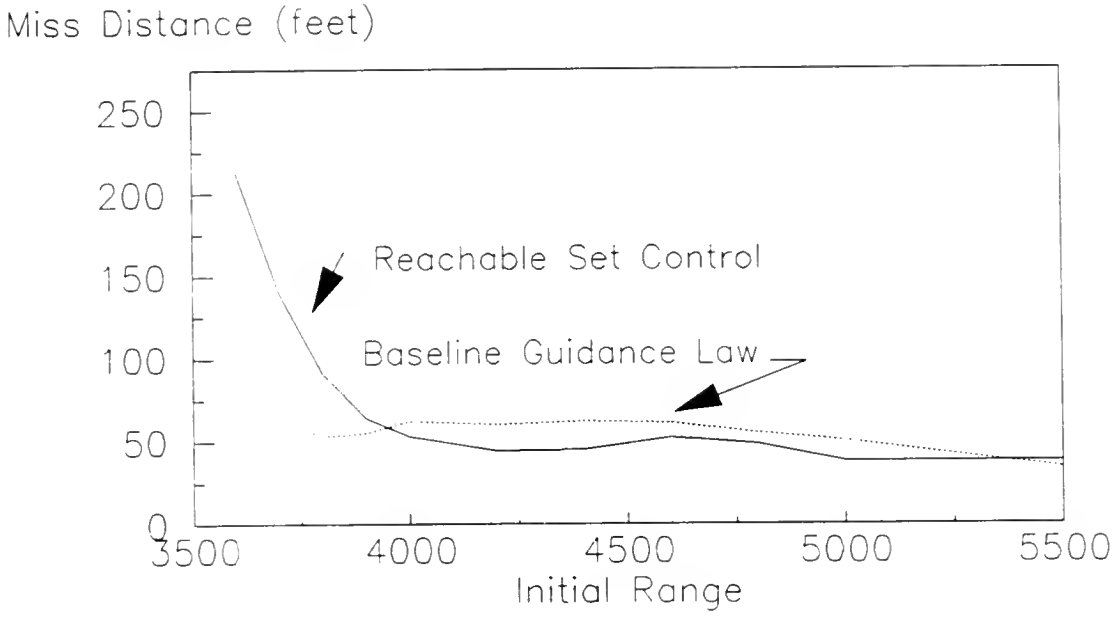

Figure 7.6 Performance Using Position Estimates and Actual Velocities

While the long term solution to the problem is a better target model that will accommodate both tracking and control requirements, the same model was used in order to provide a better comparison with previous research. For the same reason, the Kalman filter was not tuned to function better with the higher gain reachable set controller. However, target velocity changes used for the generation of the roll angle error were limited to the equivalent of a 20 degree per second target turn rate. This limited the performance on a single run, but precluded the 300 foot miss that followed a 20 foot hit.

Conclusions

Reachable Set Control

As seen from the Tables 7.1 and 7.2, Reachable Set Control was inherently more accurate than the baseline linear law, especially in the more realistic case where noise is added and sampled data measurements are used.

In addition, Reachable set control did insure an initially constrained trajectory for controllable trajectories, and required minimal accelerations during the terminal phase of the intercept.

Unlike previous constrained control schemes, Reachable Set Control was better able to accommodate unmodeled non-linearities and provide adequate performance with a suboptimal sampled data controller.

While demonstrated with a Preferred Axis Missile, Reachable Set Control is a general technique that could be used on most trajectory control problems.

Singer Model

Unmodified, the Singer model provides an excellent basis for a maneuvering target tracker, but it is not a good model to use for linear control. Neither control law penalized velocity errors. In fact, the baseline control law did not define a velocity error. Yet the requirements of linearity, and the integration from velocity to position, require better velocities estimates than are provided by this model (for this quality seeker).

APPENDIX A
SIMULATION RESULTS

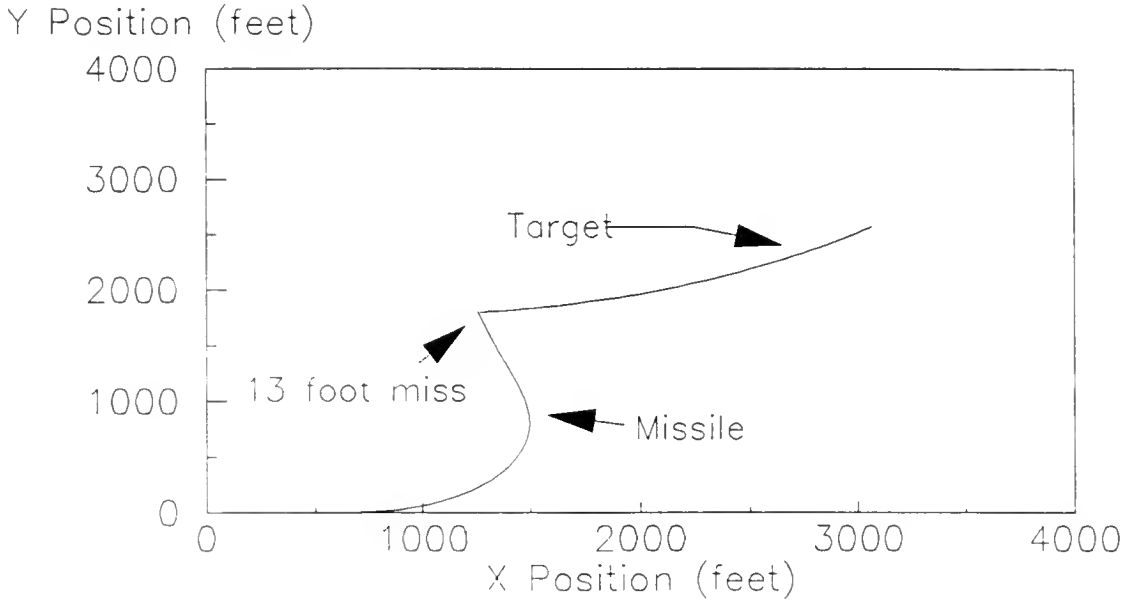

Figure A.1 XY Missile & Target Positions
Reachable Set Control

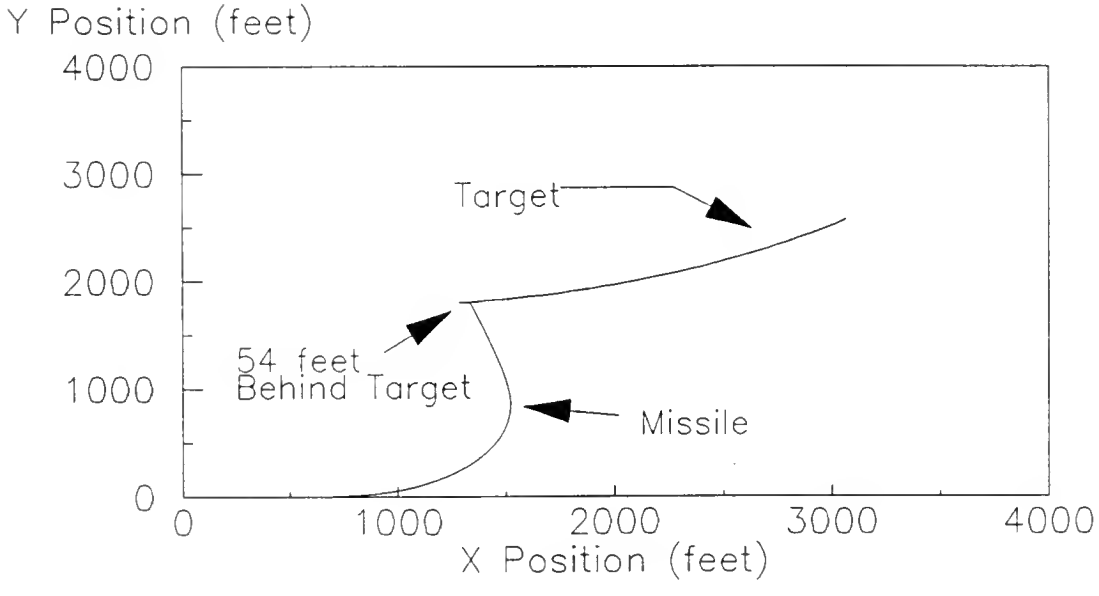

Figure A.2 XY Missile & Target Positions
Baseline Control Law

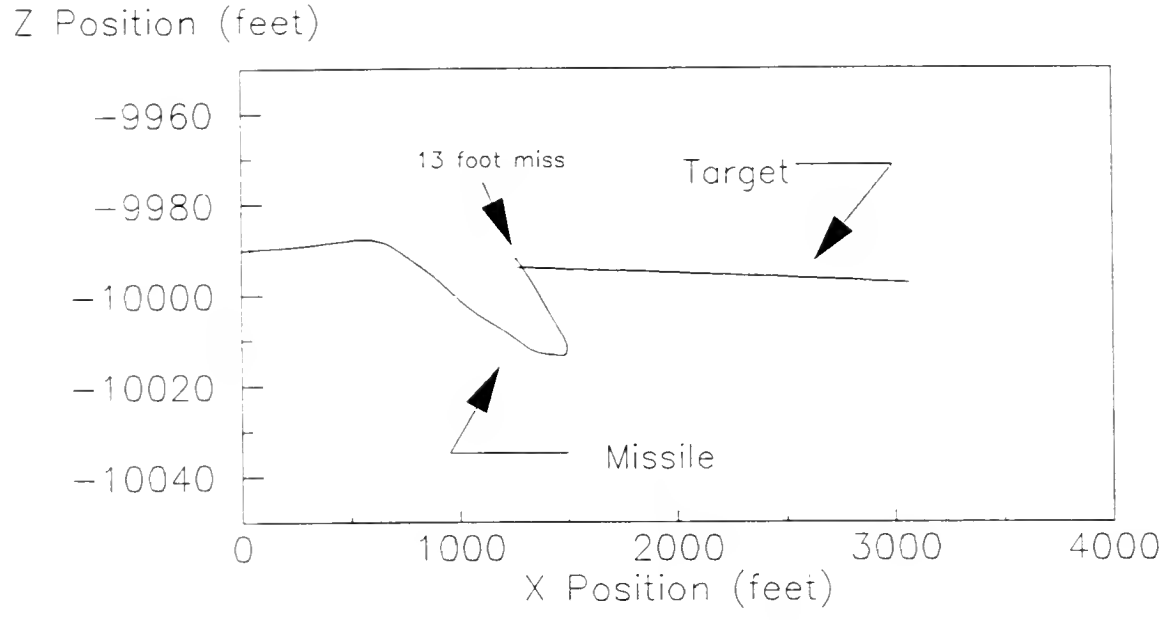

Figure A.3 XZ Missile & Target Positions
Reachable Set Control

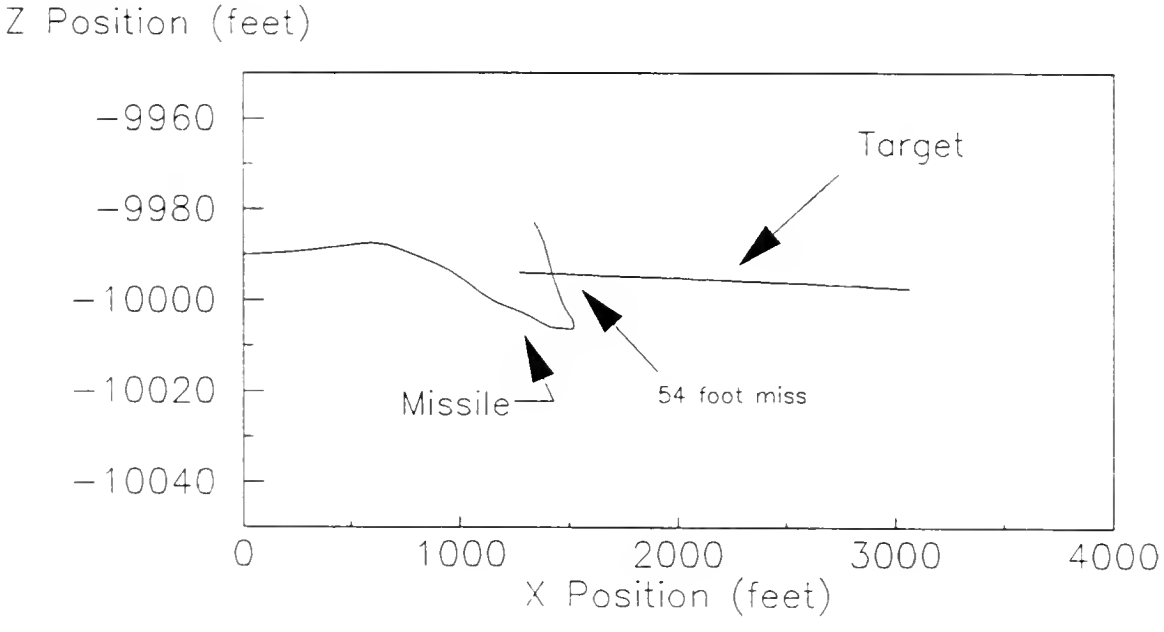

Figure A.4 XZ Missile & Target Positions
Baseline Control Law

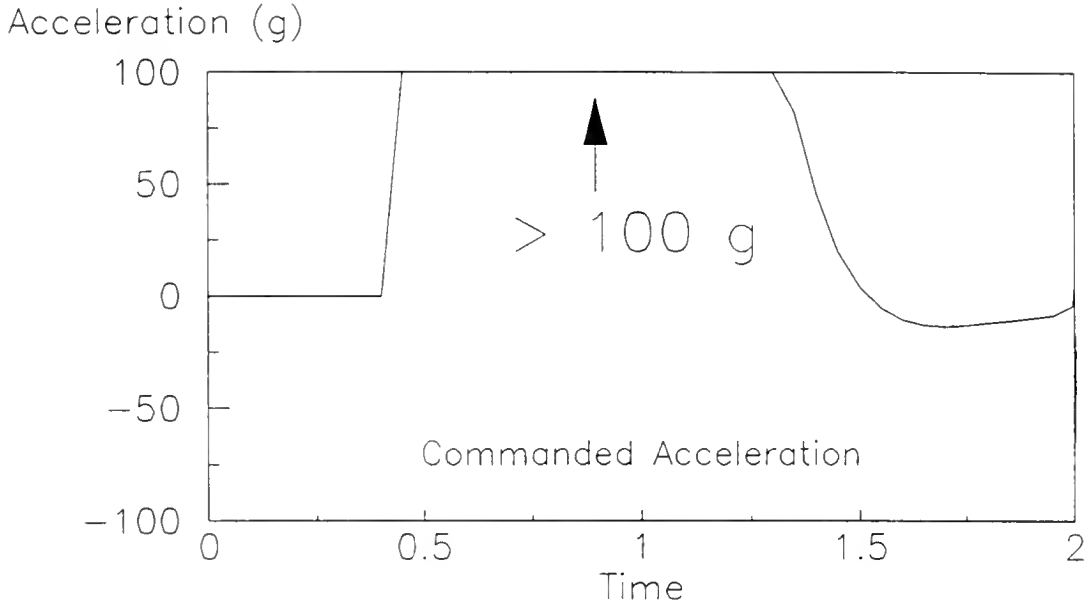

Figure A.5 Missile Acceleration - Reachable Set Control

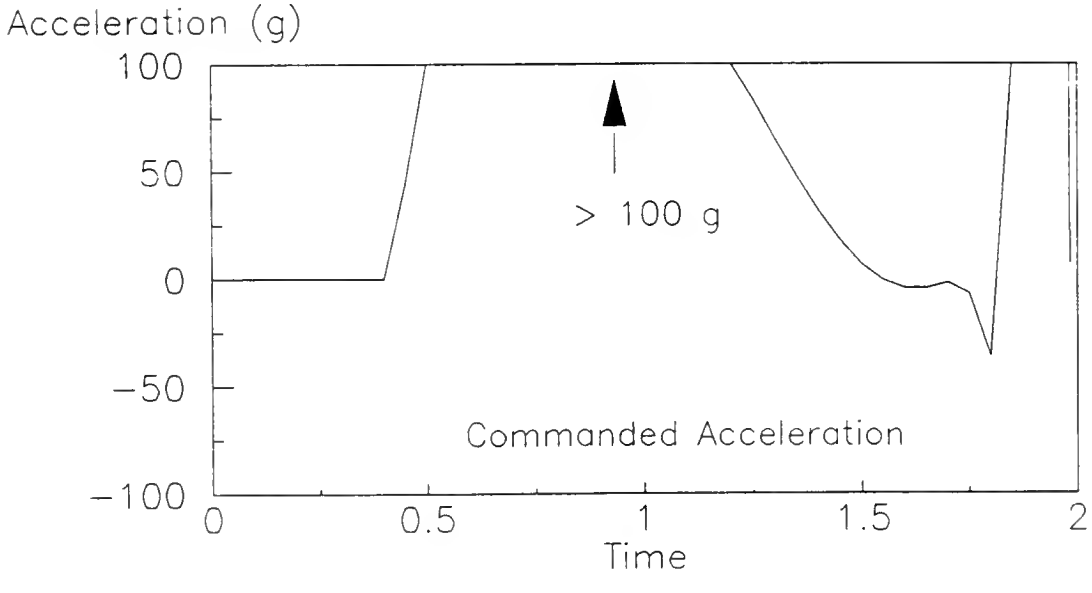

Figure A.6 Missile Acceleration - Baseline Control Law

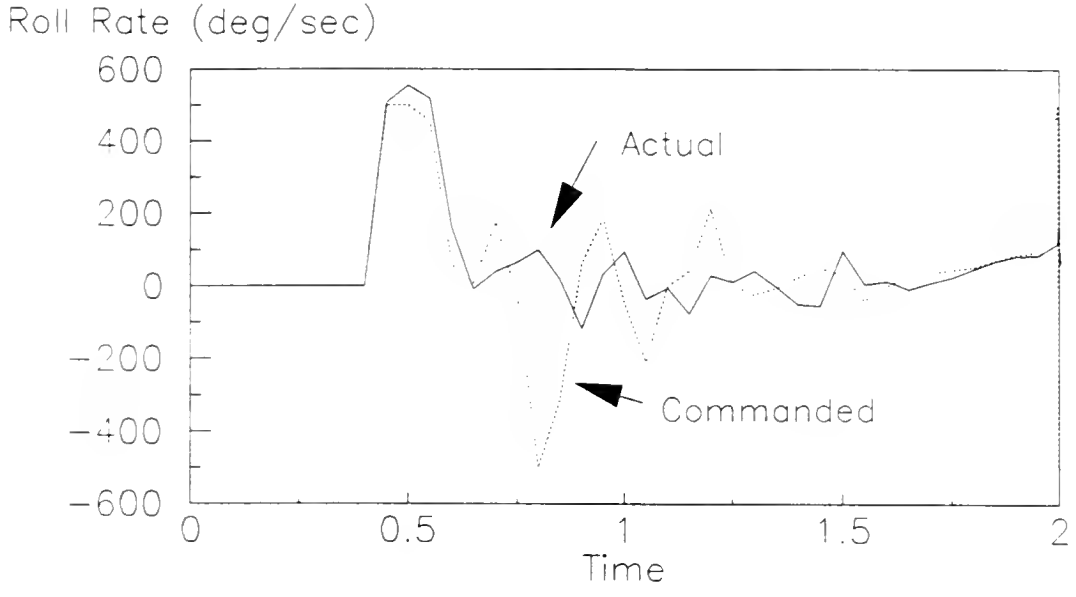

Figure A.7 Missile Roll Commands & Rate - Reachable Set Control

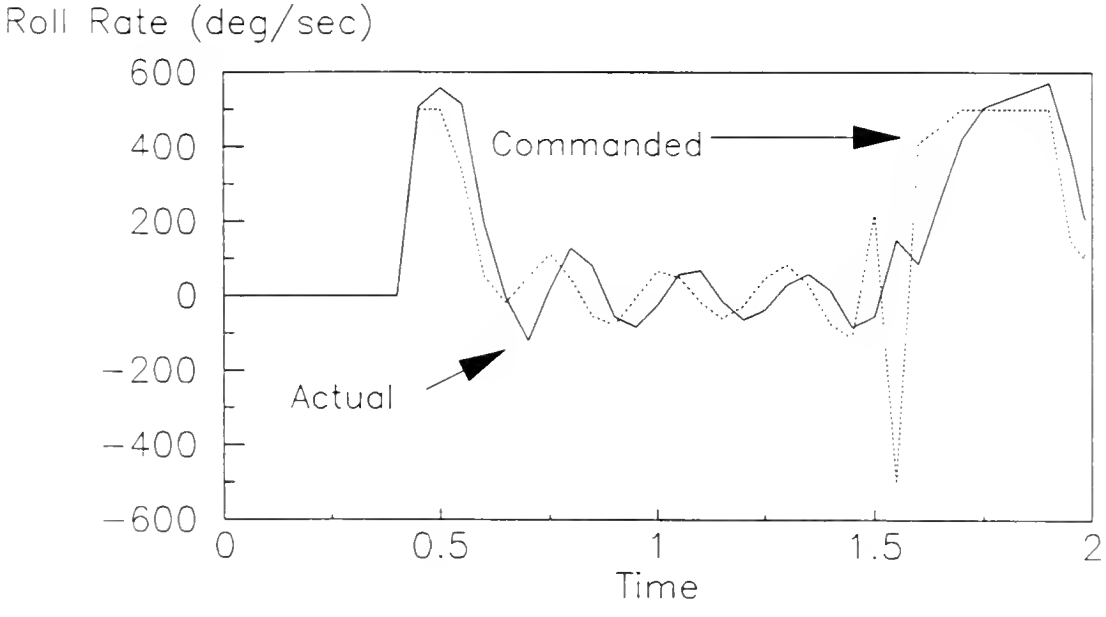

Figure A.8 Missile Roll Commands & Rate - Baseline Control Law

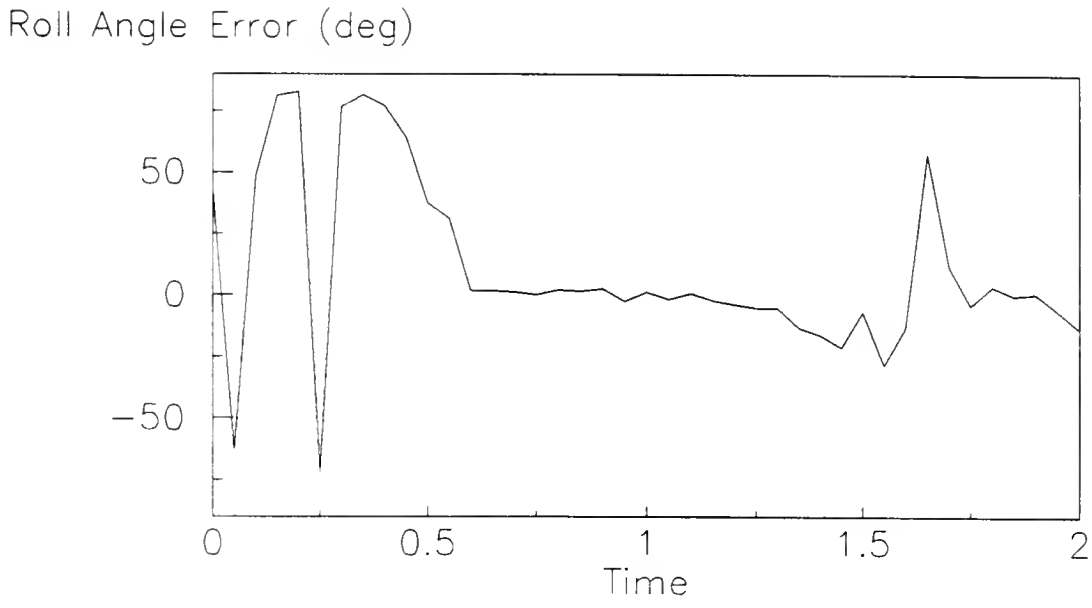

Figure A.9 Missile Roll Angle Error

APPENDIX B
SAMPLED-DATA CONVERSION

System Model

The system model for the formulation of the sampled-data control law consists of the plant dynamics with time correlated and white disturbances:

$$\begin{bmatrix} \dot{x}(t) \\ \dot{T}(t) \end{bmatrix} = \begin{bmatrix} F(t) & I \\ O & N(t) \end{bmatrix} \begin{bmatrix} x(t) \\ T(t) \end{bmatrix} + \begin{bmatrix} G(t) \\ O \end{bmatrix} u(t) + \begin{bmatrix} L & O \\ O & M \end{bmatrix} \begin{bmatrix} w_s(t) \\ w_t(t) \end{bmatrix} \quad (1)$$

the reference:

$$\dot{r}(t) = A(t)r(t) + B(t)a(t) \quad (2)$$

with the tracking error:

$$e(t) = [\, y_x(t) - y_r(t) \,] = [\, H(t) \mid 0 \mid -C(t) \,] \begin{bmatrix} x(t) \\ T(t) \\ r(t) \end{bmatrix} \quad (3)$$

and quadratic cost $J_s(t) = E\{J_d(t)|I(t)\}$, where

$$J_d = e_f^T P_f e_f + \int_{t_0}^{t_f} \{e(\tau)^T Q(\tau) e(\tau) + u(\tau)^T R(\tau) u(\tau)\} d\tau \quad (4)$$

$E\{w_s(t)w_s(t)^T\} = Ws(t)$ is the strength of the system (white noise) disturbances to be rejected.

$E\{w_t(t)w_t(t)^T\} = Wt(t)$ is an input to a stationary first order Gauss-Markov process that models target acceleration (see CH VI).

The following assumes a constant cycle time that defines the sampling interval and a possible delay between sampling and control of

$$\Delta t' = t_{i'} - t_i$$

The components of the controlled system are

(5)

$$x(t) = \begin{bmatrix} x(t) \\ y(t) \\ z(t) \\ \phi(t) \\ \dot{x}(t) \\ \dot{y}(t) \\ \dot{z}(t) \\ \dot{\phi}(t) \end{bmatrix} \qquad T(t) = \begin{bmatrix} Tx(t) \\ Ty(t) \\ Tz(t) \end{bmatrix} \qquad r(t) = \begin{bmatrix} r_x(t) \\ r_y(t) \\ r_z(t) \\ r_\phi(t) \\ \dot{r}_x(t) \\ \dot{r}_y(t) \\ \dot{r}_z(t) \\ \dot{r}_\phi(t) \end{bmatrix}$$

$$u(t) = \begin{bmatrix} Nx(t) \\ Ny(t) \\ Nz(t) \\ P(t) \end{bmatrix} \qquad e(t) = \begin{bmatrix} x(t) \\ y(t) \\ z(t) \\ \phi(t) \\ 0 \\ 0 \\ 0 \\ \dot{\phi}(t) \end{bmatrix} - \begin{bmatrix} r_x(t) \\ r_y(t) \\ r_z(t) \\ r_\phi(t) \\ 0 \\ 0 \\ 0 \\ \dot{r}_\phi(t) \end{bmatrix}$$

In block form, with appropriate dimensions, the system matrices are

(6)

$$F(t) = A(t) = F = \begin{bmatrix} O & I \\ O & O_w \end{bmatrix} \qquad G(t) = B(t) = G = \begin{bmatrix} O \\ I_w \end{bmatrix}$$

$$H(t) = C(t) = [\, I \quad h_w \,] \qquad L(t) = I \qquad M(t) = I$$

$$(O_w)_{ij} = \begin{cases} -w & i=j=8 \\ 0 & \text{otherwise} \end{cases}$$

$$(I_w)_{ij} = \begin{cases} +w & i=8, j=4 \\ I & \text{otherwise} \end{cases}$$

$$(h_w)_{jj} = \begin{cases} 1 & i=j=8 \\ 0 & \text{otherwise} \end{cases}$$

Sampled-data Equations

System

From the continuous system, the discrete-time sampled-data system model can be summarized in the following set of equations:

$$x(t_{i+1}) = \Phi x(\Delta t)x(t_i) + T_c(I - e^{(\Delta t/T_c)})\, T(t_i) \qquad (7)$$

$$+ G(\Delta t)u(t_i) + L(\Delta t)w_s(t_i)$$

$$y(t_i') = H\, x(t_i) + D\, u(t_i)$$

For a time invariant F with a constant sample interval:

$$\Phi_x(t_{i+i},t_i) = e^{F(t_{i+i}-t_i)} = e^{F(\Delta t)} \text{ with } \Delta t = t_{i+i} - t_i \qquad (8)$$

$$\Phi x(\Delta t) = \begin{pmatrix} 1 & 0 & 0 & 0 & \Delta t & 0 & 0 & 0 \\ 0 & 1 & 0 & 0 & 0 & \Delta t & 0 & 0 \\ 0 & 0 & 1 & 0 & 0 & 0 & \Delta t & 0 \\ 0 & 0 & 0 & 1 & 0 & 0 & 0 & \Phi x_{48} \\ 0 & 0 & 0 & 0 & 1 & 0 & 0 & 0 \\ 0 & 0 & 0 & 0 & 0 & 1 & 0 & 0 \\ 0 & 0 & 0 & 0 & 0 & 0 & 1 & 0 \\ 0 & 0 & 0 & 0 & 0 & 0 & 0 & \Phi x_{88} \end{pmatrix}$$

with

$$\Phi x_{48}(\Delta t) = (1/\omega_\phi)\cdot(1 - \exp\{-\omega_\phi(\Delta t)\})$$

$$\Phi x_{88}(\Delta t) = \exp\{-\omega_\phi(\Delta t)\}$$

Also, since G and H are time invariant and the $u(t_i)$ are piecewise continuous, the input and output matrices (allowing for non-coincident sampling and control) are

$$G = \int_{t_i}^{t_{i+1}} \Phi(t_{i+1},\tau)G(\tau)d\tau \tag{9}$$

$$H = H\,\Phi(t_i',t_i) \tag{10}$$

$$D = H \int_{t_i}^{t_i'} \Phi(t_i',\tau)G(\tau)d\tau \tag{11}$$

Therefore,

$$G = \begin{bmatrix} \Delta t^2/2 & 0 & 0 & 0 \\ 0 & \Delta t^2/2 & 0 & 0 \\ 0 & 0 & \Delta t^2/2 & 0 \\ 0 & 0 & 0 & \Delta t - \Phi x_{48}(\Delta t) \\ \Delta t & 0 & 0 & 0 \\ 0 & \Delta t & 0 & 0 \\ 0 & 0 & \Delta t & 0 \\ 0 & 0 & 0 & 1 - \Phi x_{88}(\Delta t) \end{bmatrix} \tag{12}$$

$$H = \begin{bmatrix} 1 & 0 & 0 & 0 & \Delta t' & 0 & 0 & 0 \\ 0 & 1 & 0 & 0 & 0 & \Delta t' & 0 & 0 \\ 0 & 0 & 1 & 0 & 0 & 0 & \Delta t' & 0 \\ 0 & 0 & 0 & 1 & 0 & 0 & 0 & \Phi x_{48}(\Delta t') \\ 0 & 0 & 0 & 0 & 0 & 0 & 0 & 0 \\ 0 & 0 & 0 & 0 & 0 & 0 & 0 & 0 \\ 0 & 0 & 0 & 0 & 0 & 0 & 0 & 0 \\ 0 & 0 & 0 & 0 & 0 & 0 & 0 & \Phi x_{88}(\Delta t') \end{bmatrix} \tag{13}$$

$$D = \begin{bmatrix} \Delta t'^2/2 & 0 & 0 & 0 \\ 0 & \Delta t'^2/2 & 0 & 0 \\ 0 & 0 & \Delta t'^2/2 & 0 \\ 0 & 0 & 0 & \Delta t' - \Phi x_{48}(\Delta t') \\ \Delta t' & 0 & 0 & 0 \\ 0 & \Delta t' & 0 & 0 \\ 0 & 0 & \Delta t' & 0 \\ 0 & 0 & 0 & 1 - \Phi x_{88}(\Delta t') \end{bmatrix} \tag{14}$$

Target Disturbance

For time correlated disturbances, $Wt(t) = Wt = 2\ \sigma_t^2/T_c$ where σ_t is the RMS value of the noise process $T(\cdot,\cdot)$, and T_c is the correlation time.

$$N(t) = -\ (1/T_c)[I] \tag{15}$$

The sampled data disturbance is

$$T(t_{i+1}) = \Phi_T(\Delta t)T(t_i) + \underbrace{\int_{t_i}^{t_{i+1}} \Phi_T(t_{i+1},\tau)w_t(\tau)d\tau}_{w_t(t_i)} \tag{16}$$

$w_t(t_i)$ is a sequence of zero mean mutually uncorrelated random variables, and $\Phi_T(\Delta t)$ is given by:

$$\Phi_T(\Delta t) = e^{-(\Delta t/T_c)}1 \tag{17}$$

with $\Phi_n(\Delta t) = T_c(I - \Phi_T(\Delta t))$ the sampled data impact on the system.

Minimum Control Reference

From the dual system, the sampled data minimum control reference, with average acceleration from the motor equal to $a(t_i)$, is

$$r(t_{i+1}) = \Phi r(\Delta t) r(t_i) + [B(\Delta t)] a(t_i) \qquad r(t_0) = r_0 = \begin{bmatrix} 0 \\ -Vi(0) \end{bmatrix} \tag{18}$$

$$y_r(t_i') = C\, r(t_i) + E\, a(t_i)$$

For the reference trajectory, the linear accelerations are the uncontrollable X_b axis accelerations from the rocket motor as well as preprogrammed maneuvers designed to enhance aerodynamic performance. Because this reference trajectory is a null control trajectory, the current position of the reference trajectory can be determined by reversing the direction of the current velocity and average acceleration and running the system forward in time for tgo seconds from the origin to determine the current position of the coasting trajectory.

Let:

$$\Phi r(\Delta t) = \begin{bmatrix} 1 & 0 & 0 & 0 & \Delta t & 0 & 0 & 0 \\ 0 & 1 & 0 & 0 & 0 & \Delta t & 0 & 0 \\ 0 & 0 & 1 & 0 & 0 & 0 & \Delta t & 0 \\ 0 & 0 & 0 & 0 & 0 & 0 & 0 & 0 \\ 0 & 0 & 0 & 0 & 1 & 0 & 0 & 0 \\ 0 & 0 & 0 & 0 & 0 & 1 & 0 & 0 \\ 0 & 0 & 0 & 0 & 0 & 0 & 1 & 0 \\ 0 & 0 & 0 & 0 & 0 & 0 & 0 & 0 \end{bmatrix} \tag{19}$$

$$B = \begin{bmatrix} +\Delta t^2/2 & 0 & 0 & 0 \\ 0 & +\Delta t^2/2 & 0 & 0 \\ 0 & 0 & +\Delta t^2/2 & 0 \\ 0 & 0 & 0 & 0 \\ +\Delta t & 0 & 0 & 0 \\ 0 & +\Delta t & 0 & 0 \\ 0 & 0 & +\Delta t & 0 \\ 0 & 0 & 0 & 0 \end{bmatrix} \tag{20}$$

$$C = C\,\Phi(t_i', t_i) \tag{21}$$

$$C = \begin{bmatrix} 1 & 0 & 0 & 0 & \Delta t' & 0 & 0 & 0 \\ 0 & 1 & 0 & 0 & 0 & \Delta t' & 0 & 0 \\ 0 & 0 & 1 & 0 & 0 & 0 & \Delta t' & 0 \\ 0 & 0 & 0 & 0 & 0 & 0 & 0 & 0 \end{bmatrix}$$

$$E = C \int_{t_i}^{t_i'} \Phi(t_i', \tau) B(\tau)\, d\tau \tag{22}$$

$$E = \begin{bmatrix} \Delta t'^2/2 & 0 & 0 & 0 \\ 0 & \Delta t'^2/2 & 0 & 0 \\ 0 & 0 & \Delta t'^2/2 & 0 \\ 0 & 0 & 0 & 0 \\ \Delta t' & 0 & 0 & 0 \\ 0 & \Delta t' & 0 & 0 \\ 0 & 0 & \Delta t' & 0 \\ 0 & 0 & 0 & 0 \end{bmatrix}$$

Summary

In block form, the entire system becomes: (23)

$$\begin{bmatrix} x(t_{i+1}) \\ T(t_{i+1}) \\ r(t_{i+1}) \end{bmatrix} = \begin{bmatrix} \Phi x(\Delta t) & \Phi n(\Delta t) & O \\ O & \Phi_T(\Delta t) & O \\ O & O & \Phi r(\Delta t) \end{bmatrix} \begin{bmatrix} x(t_i) \\ T(t_i) \\ r(t_i) \end{bmatrix} + \begin{bmatrix} G \\ O \\ O \end{bmatrix} u(t_i) + \begin{bmatrix} O \\ O \\ B(\Delta t) \end{bmatrix} a(t_i) + \begin{bmatrix} w_s(t_i) \\ w_t(t_i) \\ O \end{bmatrix}$$

with associated tracking error:

$$e(t_i') = [\ H\ O\ -C\ ] \begin{bmatrix} x(t_i) \\ T(t_i) \\ r(t_i) \end{bmatrix} + [\ D\ -E\ ] \begin{bmatrix} u(t_i) \\ a(t_i) \end{bmatrix} \tag{24}$$

APPENDIX C
SAMPLED DATA COST FUNCTIONS

Assume that the performance objective is to minimize an appropriate continuous-time quadratic cost.

$$J_s(t) = E\{J_d(t)|I(t)\} \tag{1}$$

where J_s is the stochastic cost, J_d a deterministic cost, and I(t) is the information set available at time t.

Let

$$J_d(t) = e_f^T P_f e_f + \int_{t_0}^{t_f} \{e(t)^T Q(t) e(t) + u(t)^T R(t) u(t)\} d\tau \tag{2}$$

Dividing the interval of interest into N+1 control intervals for discrete time control,

$$J_d(t) = e(t_{n+1})^T P_f e(t_{n+1}) + \sum_{i=0}^{N} \left[\int_{t_i}^{t_{i+1}} \{e(t)^T Q(t) e(t) + u(t)^T R(t) u(t)\} d\tau \right] \tag{3}$$

where for all $t \in [t_i, t_{i+1})$, $u(t) = u(t_i)$.

Substituting the following for e(t):

$$e(t) = \Phi(t,t_i) e(t_i) + \int_{t_i}^{t} \Phi(t,\tau) G(\tau) u(\tau) d\tau + \int_{ti}^{t} \Phi(t,\tau) L(\tau) d\beta(\tau) \tag{4}$$

the deterministic cost becomes:

$$J_d(t) = e(t_{n+1})^T P_f e(t_{n+1}) \tag{5}$$
$$+ \sum_{i=0}^{N} \left[\int_{t_i}^{t_{i+1}} \left([\Phi(t,t_i)e(t_i) + \left\{ \int_{t_i}^{t} \Phi(t,\tau)G(\tau)d\tau \right\} u(t_i) \right.\right.$$
$$+ \left\{ \int_{t_i}^{t} \Phi(t,\tau)L(\tau)d\tau \right\} w(t_i)]^T$$
$$\cdot Q(t) \cdot [\Phi(t,t_i)e(t_i) + \left\{ \int_{t_i}^{t} \Phi(t,\tau)G(\tau)d\tau \right\} u(t_i)$$
$$\left.\left. + \left\{ \int_{t_i}^{t} \Phi(t,\tau)L(\tau)d\tau \right\} w(t_i)] + u(t_i)^T R(t) u(t_i) \right) dt \right]$$

Making the following substitutions:

$$Wxx(t_i) = \int_{t_i}^{t_{i+1}} \Phi(\tau,t_i)^T Q(\tau) \Phi(\tau,t_i) d\tau \tag{6}$$

$$Wuu(t_i) = \left[\int_{t_i}^{t_{i+1}} R(t) + \left\{ \int_{t_i}^{t} \Phi(t,\tau)G(\tau)d\tau \right\}^T Q(t) \left\{ \int_{t_i}^{\tau} \Phi(\tau,t_i)G(\tau)d\tau \right\} \right] dt \tag{7}$$

$$Www(t_i) = \left[\int_{t_i}^{t_{i+1}} \left\{ \int_{t_i}^{\tau} \Phi(t,\tau)L(\tau)d\tau \right\}^T Q(t) \cdot \left\{ \int_{t_i}^{t} \Phi(t,\tau)L(\tau)d\tau \right\} \right] dt \tag{8}$$

$$Wxu(t_i) = \left[\int_{t_i}^{t_{i+1}} \Phi(t,t_i)^T Q(t) \left\{ \int_{t_i}^{t} \Phi(t,\tau)G(\tau)d\tau \right\} \right] dt \tag{9}$$

$$Wux(t_i) = \left[\int_{t_i}^{t_{i+1}} \left\{ \int_{t_i}^{t} \Phi(t,\tau)G(\tau)d\tau \right\}^T Q(t)\Phi(t,t_i) \right]dt \tag{10}$$

$$Wxw(t_i) = \left[\int_{t_i}^{t_{i+1}} \Phi(t,t_i)^T Q(t)\left\{ \int_{t_i}^{t} \Phi(t,\tau)L(\tau)d\tau \right\} \right]dt \tag{11}$$

$$Wwx(t_i) = \left[\int_{t_i}^{t_{i+1}} \left\{ \int_{t_i}^{t} \Phi(t,\tau)L(\tau)d\tau \right\}^T Q(t)\Phi(t,t_i) \right]dt \tag{12}$$

$$Wuw(t_i) = \left[\int_{t_i}^{t_{i+1}} \left\{ \int_{t_i}^{t} \Phi(t,\tau)G(\tau)d\tau \right\}^T Q(t) \cdot \left\{ \int_{t_i}^{t} \Phi(t,\tau)L(\tau)d\tau \right\} \right]dt \tag{13}$$

$$Wwu(t_i) = \left[\int_{t_i}^{t_{i+1}} \left\{ \int_{t_i}^{t} \Phi(t,\tau)L(\tau)d\tau \right\}^T Q(t) \cdot \left\{ \int_{t_i}^{t} \Phi(t,\tau)G(\tau)d\tau \right\} \right]dt \tag{14}$$

And, allowing for the fact that for all $t \in [t_i,t_{i+1})$:

$$\begin{aligned} u(t) &= u(t_i) \\ e(t) &= e(t_i) \\ w(t) &= w(t_i) \end{aligned} \tag{15}$$

the deterministic cost can be expressed as:

$$\begin{aligned} J_d = {} & e(t_{N+1})^T P_f e(t_{N+1}) + \\ & \sum_{i=0}^{N} \{ e(t_i)^T Wxx(t_i)e(t_i) + u(t_i)^T Wuu(t_i)u(t_i) \\ & + w(t_i)^T Www(t_i)w(t_i) + 2e(t_i)^T Wxu(t_i)u(t_i) \\ & + 2e(t_i)^T Wxw(t_i)w(t_i) + 2u(t_i)^T Wuw(t_i)w(t_i) \} \end{aligned} \tag{16}$$

Recall that $J_s(t) = E\{J_d(t)|I(t)\}$ and that $w(\cdot,\cdot)$ is zero mean and uncorrelated with either e or u. Since if two variables x & y are uncorrelated then $E\{x,y\} = E\{x\}E\{y\}$. Therefore,

$$E\{2e(t_i)^T W_{xw}(t_i)w(t_i)\} = 2E\{e(t_i)^T w(t_i)\}E\{w(t_i)\} = 0 \tag{17}$$

$$E\{2u(t_i)^T W_{xw}(t_i)w(t_i)\} = 2E\{u(t_i)^T w(t_i)\}E\{w(t_i)\} = 0$$

and

$$E\{w(t_i)^T W_{ww}(t_i)w(t_i)\} =$$

$$E\{w(t_i)^T[\int_{t_i}^{t_{i+1}}\{\int_{t_i}^{t}\Phi(t,\tau)L(\tau)d\tau\}^T Q(t)\{\int_{t_i}^{t}\Phi(t,\tau)L(\tau)d\tau]w(t_i)\} \tag{18}$$

$$= \int_{t_i}^{t_{i+1}} tr[Q(t)\{\int_{t_i}^{t}\Phi(t,\tau)L(\tau)W_S(\tau)L(\tau)^T\Phi(t,\tau)^T d\tau\}dt] \tag{19}$$

$$= Jw(t_i)$$

Consequently, for consideration in J_S

$$J_d = e(t_{N+1})^T P_f e(t_{N+1}) \tag{20}$$
$$+ \sum_{i=0}^{N}\{e(t_i)^T W_{xx}(t_i)e(t_i) + u(t_i)^T W_{uu}(t_i)u(t_i) + Jw(t_i)$$
$$+ 2e(t_i)^T W_{xu}(t_i)u(t_i)\}$$

$$J_d = e(t_{N+1})^T P(t_{N+1})e(t_{N+1}) + Jw(t_i) \tag{21}$$
$$+ \sum_{i=0}^{N}\begin{bmatrix} e(t_i) \\ u(t_i)\end{bmatrix}^T\begin{bmatrix} W_{xx}(t_i) & W_{xu}(t_i) \\ W_{xu}(t_i)^T & W_{uu}(t_i)\end{bmatrix}\begin{bmatrix} e(t_i) \\ u(t_i)\end{bmatrix}$$

For small sample times, the weighting functions can be approximated by:

$$Wxx \sim Q(t)\Delta t \tag{22}$$

$$Wxu \sim (1/2)Q(t)G(t)(\Delta t)^2 \tag{23}$$

$$Wuu \sim [R(t)+(1/3)G(t)^T Q(t)G(t)(\Delta t)^2](\Delta t) \tag{24}$$

In order to relate the values of the sampled data weighting terms on the system error to the state variables (using discrete variable notation), let:

$$P(t_i) = [\ H\ \ O\ \ -C\ ]^T P_f [\ H\ \ O\ \ -C\ ] \tag{25}$$

$$Q(t_i) = [\ H\ \ O\ \ -C\ ]^T Wxx(t_i) [\ H\ \ O\ \ -C\ ] \tag{26}$$

$$R(t_i) = Wuu \tag{27}$$

$$S(t_i) = [\ H\ \ O\ \ -C\ ]^T Wxu \tag{28}$$

Therefore, with the augmented state variable $\chi = [\ x\ T\ r\ ]^T$:

$$J_d = \chi(t_{N+1})^T P(t_{N+1}) \chi(t_{N+1}) + \sum_{i=0}^{N} \begin{bmatrix} \chi(t_i)^T \\ u(t_i) \end{bmatrix} \begin{bmatrix} Q(t_i) & S(t_i) \\ S(t_i)^T & R(t_i) \end{bmatrix} \begin{bmatrix} \chi(t_i) \\ u(t_i) \end{bmatrix} \tag{29}$$

Expanding Q and S^T

$$Q(t_i) = \begin{bmatrix} H^T Wxx(t_i) H & O & -H^T Wxx(t_i) C \\ O & O & O \\ -C^T Wxx(t_i) H & O & C^T Wxx(t_i) C \end{bmatrix} \tag{30}$$

$$S^T(t_i) = [\ Wxu^T H \mid\ O \mid\ -Wxu^T C\ ]$$

With non-coincident sampling and control, the penalty terms are modified as follows:

$$e(t_i') = [\ H\ \ O\ \ -C\ ] \begin{bmatrix} x \\ T \\ r \end{bmatrix}_{t_i'} + [\ D\ \ E\ ] \begin{bmatrix} u \\ \\ a \end{bmatrix}_{t_i'} \tag{31}$$

This modification adds additional terms:

$$e(t_i')^T \begin{bmatrix} Wxx(t_i) & Wxu(t_i) \\ Wxu(t_i)^T & Wuu(t_i) \end{bmatrix} e(t_i') = \tag{32}$$

$$\{\ [\ H\ \ O\ \ C\ ] \begin{bmatrix} x \\ T \\ r \end{bmatrix}_{t_i'} + [\ D\ \ E\ ] \begin{bmatrix} u \\ \\ a \end{bmatrix}_{t_i'}\}^T \cdot$$

$$\begin{bmatrix} Wxx(t_i) & Wxu(t_i) \\ Wxu(t_i)^T & Wuu(t_i) \end{bmatrix} \cdot \{\ [\ H\ \ O\ \ C\ ] \begin{bmatrix} x \\ T \\ r \end{bmatrix}_{t_i'} + [\ D\ E\ ] \begin{bmatrix} u \\ \\ a \end{bmatrix}_{t_i'}\}$$

Again with $Wxx(t_i) = Wxx(t_i')$ and $Wxu(t_i') = Wxu(t_i)$, the additional terms can be grouped with R and S to generate:

$$R(t_i') = R(t_i) + D^T Wxx(t_i) D + D^T Wxu(t_i) \tag{33}$$

$$S(t_i') = S(t_i) + D^T Wxx(t_i)[\ H\ \ O\ \ -C\ ] \tag{34}$$

APPENDIX D
LQG CONTROLLER DECOMPOSITION

The combination of the system, target disturbance, and the reference, result in a 19 state controller. However, the decoupled structure, symmetry, and the zeros in the control input and cost matrices can be exploited to streamline the calculations.

In general, the optimal solution to the LQG tracker can be expressed as:

$$u^*(t_i) = -[G^*(t_i)] \begin{bmatrix} x(t_i) \\ T(t_i) \\ r(t_i) \end{bmatrix} \tag{1}$$

where

$$G^*(t_i) = [R(t_i) + G^T(t_i)P(t_{i+1})G(t_i)]^{-1} \cdot [G^T(t_i)P(t_{i+1})\Phi(t_{i+1},t_i) + S^T(t_i)] \tag{2}$$

and

$$P(t_i) = Q(t_i) + \Phi^T(t_{i+1},t_i)P(t_{i+1})\Phi(t_{i+1},t_i) - [G^T(t_i)P(t_{i+1})\Phi(t_{i+1},t_i) + S^T(t_i)]^T G^*(t_i) \tag{3}$$

To reduce the number of calculations, partition the gain and Riccati equation such that:

$$G^*(t_i) = [\ G_1 |\ G_2 |\ G_3\ ] \tag{4}$$

Evaluating terms:

$$G^T(t_i)P(t_{i+1})G(t_i) = [\ G^T |\ O |\ O\ ] \begin{pmatrix} P_{11} & P_{12} & P_{13} \\ P_{21} & P_{22} & P_{23} \\ P_{31} & P_{32} & P_{33} \end{pmatrix} \begin{pmatrix} G \\ O \\ O \end{pmatrix}$$

$$= [\ G^TP_{11} |\ G^TP_{12} |\ G^TP_{13}] \begin{pmatrix} G \\ O \\ O \end{pmatrix}$$

$$= [\ G^TP_{11}G\ ] \tag{5}$$

Therefore,

$$[\, R(t_i) + G^T(t_i)P(t_{i+1})G(t_i)\,] = [\, R(t_i) + G^T P_{11}\, G\,] \tag{6}$$

Now consider,

$$G^T(t_i)P(t_{i+1})\Phi(t_{i+1},t_i) \tag{7}$$

$$= [\; G^T |\; O |\; O\;] \begin{pmatrix} P_{11} & P_{12} & P_{13} \\ P_{21} & P_{22} & P_{23} \\ P_{31} & P_{32} & P_{33} \end{pmatrix} \begin{pmatrix} \Phi x & \Phi n & O \\ O & \Phi_T & O \\ O & O & \Phi r \end{pmatrix}$$

$$= [\; G^T P_{11} |\; G^T P_{12} |\; G^T P_{13}] \begin{pmatrix} \Phi x & \Phi n & O \\ O & \Phi_T & O \\ O & O & \Phi r \end{pmatrix}$$

$$G^T(t_i)P(t_{i+1})\Phi(t_{i+1},t_i) = [\; G^T P_{11}\Phi x \;|\; G^T P_{11}\Phi n + G^T P_{12}\Phi_T \;|\; G^T P_{13}\Phi r\;]$$
$$O$$

From Appendix C, $S = [\, H \;\; O \;\; -C\,]^T W x u$

Substituting, the required terms for the gain computation become:

$$[G^T(t_i)P(t_{i+1})\Phi(t_{i+1},t_i) + S^T(t_i)] = \tag{8}$$

$$[\; G^T P_{11}\Phi x + W x u^T H |$$

$$| \; G^T P_{11}\Phi n + G^T P_{12}\Phi_T |$$
$$O$$

$$| \; G^T P_{13}\Phi r - W x u^T C\;]$$

Consequently, with

$$GI = -\,[\; R(t_i) \; + G^T P_{11} G\;]^{-1} \tag{9}$$

the optimal control can be expressed as:

$$G1(t_i) \;= GI \cdot [\; G^T P_{11}\Phi x + W x u^T H\,] \tag{10}$$

$$G2(t_i) \;= GI \cdot [\; G^T P_{11}\Phi n + G^T P_{12}\Phi_T\,] \tag{11}$$
$$O$$

$$G3(t_i) \;= GI \cdot [\; G^T P_{13}\Phi r - W x u^T C\,] \tag{12}$$

Partitioning equation 3:

$$\begin{bmatrix} P_{11} & P_{12} & P_{13} \\ P_{21} & P_{22} & P_{23} \\ P_{31} & P_{32} & P_{33} \end{bmatrix}_{(ti)} = \begin{bmatrix} H^T W_{xx}(t_i) H & O & -H^T W_{xx}(t_i) C \\ O & O & O \\ -C^T W_{xx}(t_i) H & O & C^T W_{xx}(t_i) C \end{bmatrix}_{(ti)} \tag{13}$$

$$+ \begin{bmatrix} \Phi_x & \Phi_n & O \\ & O & O \\ O & \Phi_T & O \\ O & O & \Phi_r \end{bmatrix}^T \begin{bmatrix} P_{11} & P_{12} & P_{13} \\ P_{21} & P_{22} & P_{23} \\ P_{31} & P_{32} & P_{33} \end{bmatrix}_{(ti+1)} \begin{bmatrix} \Phi_x & \Phi_n & O \\ & O & O \\ O & \Phi_T & O \\ O & O & \Phi_r \end{bmatrix}$$

$$- \{ [\, G^T \mid O \mid O \,] \begin{bmatrix} P_{11} & P_{12} & P_{13} \\ P_{21} & P_{22} & P_{23} \\ P_{31} & P_{32} & P_{33} \end{bmatrix}_{ti+1)} \begin{bmatrix} \Phi_x & \Phi_n & O \\ & O & O \\ O & \Phi_T & O \\ O & O & \Phi_r \end{bmatrix}$$

$$+ [\, W_{xu}^T H \mid O \mid -W_{xu}^T C \,] \}^T [\, G_1 \mid G_2 \mid G_3 \,]$$

$$= \begin{bmatrix} H^T W_{xx}(t_i) H & O & -H^T W_{xx}(t_i) C \\ O & O & O \\ -C^T W_{xx}(t_i) H & O & C^T W_{xx}(t_i) C \end{bmatrix} \tag{14}$$

$$+ \begin{vmatrix} \{\Phi_x^T P_{11}\} & \{\Phi_x^T P_{12}\} & \{\Phi_x^T P_{13}\} \\ \{[\Phi_n^T \; O] P_{11} + \Phi_x^T P_{21}\} & \{[\Phi_n^T \; O] P_{12} + \Phi_T^T P_{22}\} & \{[\Phi_n^T \; O] P_{13} + \Phi_T^T P_{23}\} \\ \{\Phi_r^T P_{31}\} & \{\Phi_r^T P_{32}\} & \{\Phi_r^T P_{33}\} \end{vmatrix} \cdot$$

$$\begin{bmatrix} \Phi_x & \Phi_n & O \\ & O & O \\ O & \Phi_T & O \\ O & O & \Phi_r \end{bmatrix}_{(ti+1)}$$

$$- \{ [G^T P_{11} \mid G^T P_{12} \mid G^T P_{13}] \begin{bmatrix} \Phi_x & \Phi_n & O \\ & O & O \\ O & \Phi_T & O \\ O & O & \Phi_r \end{bmatrix}$$

$$+ [W_{xu}^T H \mid O \mid -W_{xu}^T C \,] \}^T [\, G_1 \mid G_2 \mid G_3]$$

$$= \begin{bmatrix} H^T W_{xx}(t_i) H & O & -H^T W_{xx}(t_i) C \\ O & O & O \\ -C^T W_{xx}(t_i) H & O & C^T W_{xx}(t_i) C \end{bmatrix} \tag{15}$$

$$+ \begin{vmatrix} \{\Phi_x^T P_{11} \Phi_x\} & \{\Phi_x^T P_{11} \Phi_n + \Phi_x^T P_{12} \Phi_T\} & \{\Phi_x^T P_{13} \Phi_r\} \\ & O & \\ \{([\Phi_n \;\; O] P_{11} + \Phi_T^T P_{21}) \Phi_x\} & & \\ & \{([\Phi_n \;\; O] P_{11} + \Phi_T^T P_{21}) \Phi_n + ([\Phi_n O] P_{12} + \Phi_T^T P_{22}) \Phi_T\} & \\ & O & \\ & & \{([\Phi_n \;\; O] P_{13} + \Phi_T^T P_{23}) \Phi_r\} \\ \{\Phi_r^T P_{31} \Phi_x\} & \{(\Phi_r^T P_{31}) \Phi_n + (\Phi_r^T P_{32}) \Phi_T)\} & \{\Phi_r^T P_{33} \Phi_r\} \\ & O & \end{vmatrix}$$

$$- \begin{vmatrix} \{G^T P_{11} \Phi_x + W_{xu}^T H\}^T \\ \{G^T P_{11} \Phi_n + G^T P_{22} \Phi_T\}^T \\ O \\ \{G^T P_{13} \Phi_r - W_{xu}^T C\}^T \end{vmatrix}_{(t_{i+1})} [G_1 \mid G_2 \mid G_3]$$

For the propagation of the Riccati equation only these terms are required to generate the control gain:

$$P_{11}(t_i) = H^T W_{xx}(t_i) H + \{\Phi_x^T P_{11}(t_{i+1}) \Phi_x\} - [\{G^T P_{11}(t_{i+1}) \Phi_x + W_{xu}^T H\}^T][G_1] \tag{16}$$

$$P_{12}(t_i) = \{\Phi_x^T P_{11}(t_{i+1}) \Phi_n + \Phi_x^T P_{12}(t_{i+1}) \Phi_T\} \quad (O) - [\{G^T P_{11}(t_{i+1}) \Phi_x + W_{xu}^T H\}^T][G_2] \tag{17}$$

$$P_{13}(t_i) = -H^T W_{xx}(t_i) C + \{\Phi_x^T P_{13}(t_{i+1}) \Phi_r\} - [\{G^T P_{11}(t_{i+1}) \Phi_x + W_{xu}^T H\}^T][G_3] \tag{18}$$

APPENDIX E
CONTROLLER AND FILTER PARAMETERS

Controller

Control Delay = .21 seconds

Target Maneuver Correlation time = .21 seconds

Riccati initialization (P_f)

Linear controller::

Pf = 1E+2 for sample times < .01 second

P_f = 1E1 for sample times > .01 second

Roll rate controller: P_f = 1.0

Quadratic Cost Terms (Continuous)

Linear Accelerations Q = 320.

R = 1.

Roll Control		HI GAIN	LO GAIN
(Angle)	Q11	1E+1	1E-4
(Rate)	Q22	1E-4	1E-3
	R	1E-3	

Sample Time = integration (not sample) step for the continuous-discrete filter

System Disturbance Input = $(A_T - A_M) * (T_f - T_0)^2 / 2.$

Filter

Target Correlation Time = 2.0 seconds

Riccati initialization (P_f)

Positions : P11 = 2500

Velocities: P44 = 2.0E6

Covariance: P14 = 5.0E4

Maneuver Excitation Matrix ($2\sigma^2$) = 5120000

Seeker Measurement Noise

Azimuth & Elevation

R = (SITH*SITH/(RNG HAT*RNG HAT)+SOTH*SOTH
+SITH1*SITH1*RNG HAT**4)/MEAS ST

Range

R = (SOR*SOR+SIR*SIR*RNG HAT**4)/MEAS ST

Range Rate

R = (SODR*SODR+SIDR*SIDR*(RNG HAT**4))/MEAS ST

With

SITH = SIPH = 1.5

SOTH = SOPH = .225E-4

SITH1= SIPH1= 0.0

SOR = SODR = 3.0

SIR = 1E-8

SIDR = .2E-10

LIST OF REFERENCES

[1] A. Arrow, "Status and Concerns for Bank-To-Turn Control of Tactical Missiles," GACIAC PR-85-01, "Proceedings of the Workshop on Bank-To-Turn Controlled Terminal Homing Missiles," Vol 1, Joint Service Guidance and Control Committee, January 1985.

[2] J.R. McClendon and P.L. Verges, "Applications of Modern Control and Estimation Theory to the Guidance and Control of Tactical Air-to-Air Missiles," Technical Report RG-81-20, "Research on Furure Army Modular Missile," US Army Missile Command, Redstone Arsenal, Alabama, March 1981.

[3] N.K. Gupta, J.W. Fuller, and T.L. Riggs, "Modern Control Theory Methods for Advanced Missile Guidance," Technical Report RG-81-20, "Research on Furure Army Modular Missile," US Army Missile Command, Redstone Arsenal, Alabama, March 1981.

[4] N.B. Nedeljkovic, "New Algorithms for Unconstrained Nonlinear Optimal Control Problems," IEEE Transactions on Automatic Control, Vol. AC-26, No. 4, pp 868-884, August 1981.

[5] W.T. Baumann and W.J. Rugh, "Feedback Control of Nonlinear Systems by Extended Linearization," IEEE Transactions on Automatic Control, Vol. AC-31, No. 1, pp. 40-46, January 1986.

[6] E.D. Sontag, "Controllability and Linearized Regulation," Department of Mathematics, Rutgers University, New Brunswick, NJ (unpublished), 14 February 1097.

[7] A.E. Bryson and Y.C. Ho, Applied Optimal Control, Blaisdell Publishing Company, Waltham, Massachusetts, 1969.

[8] Y.-S. Lim, "Linearization and Optimization of Stochastic Systems with Bounded Control," IEEE Transactions on Automatic Control, Vol. AC-15, No. 1, pp 49-52, February 1970.

[9] P.-O. Gutman and P. Hagander, "A New Design of Constrained Controllers for Linear Systems," IEEE Transactions on Automatic Control, Vol. AC-30, No. 1, pp 22-33, January 1985.

[10] R.L. Kousut, "Suboptimal Control of Linear Time-Invariant Systems Subject to Control Structure Constraints," IEEE Transactions on Automatic Control, Vol. AC-15, No. 5, pp 557-562, October 1970.

[11] D.J. Caughlin, "Bank-To-Turn Control," Master's Thesis, University of Florida, 1983.

[12] J.F. Frankena and R. Sivan, "A non-linear optimal control law for linear systems," INT. J. CONTROL, Vol 30, No 1, pp 159-178, 1979.

[13] P.S. Maybeck, Stochastic Models, Estimation, and Control, Volume 3, Academic Press, New York, 1982.

[14] S.A. Murtaugh and H.E. Criel, "Fundamentals of Proportional Navigation," IEEE Spectrum, pp.75-85, December 1966.

[15] L.A. Stockum, and I.C. Weimer, "Optimal and Suboptimal Guidance for a Short Range Homing Missile," IEEE Trans. on Aerospace and Electronic Systems, Vol. AES-12, No. 3, pp 355-361, May 1976.

[16] B. Stridhar, and N.K. Gupta, "Missile Guidance Laws Based on Singular Perturbation Methodology," AIAA Journal of Guidance and Control, Vol 3, No. 2, 1980.

[17] R.K. Aggarwal and C.R. Moore, "Near-Optimal Guidance Law for a Bank-To-Turn Missile," Proceedings 1984 American Control Conference, Volume 3, pp. 1408-1415, June 1984.

[18] P.H. Fiske, "Advanced Digital Guidance and Control Concepts for Air-To-Air Tactical Missiles," AFATL-TR-77-130, Air Force Armament Laboratory, United States Air Force, Eglin Air Force Base, Florida, January 1980.

[19] USAF Test Pilot School, "Stability and Control Flight Test Theory," AFFTC-77-1, revised February 1977.

[20] L.C. Kramer and M. Athans, "On the Application of Deterministic Optimization Methods to Stochastic Control Problems," IEEE Transactions on Automatic Control, Vol. AC- 19, No. 1, pp 22-30, February 1974.

[21] Y. Bar-Shalom and E. Tse, "Dual Effect, Certainty Equivalence, and Separation in Stochastic Control," IEEE Transactions on Automatic Control, Vol. AC-19, No. 5, pp 494-500, October 1974.

[22] H. Van DE Water and J.C. Willems, "The Certainty Equivalence Property in Stochastic Control Theory," IEEE Transactions on Automatic Control, Vol. AC-26, No. 5, pp 1080-1086, October 1981.

[23] "Bank-To-Turn Configuration Aerodynamic Analysis Report" Rockwell International Report No. C77-1421/034C, date unknown.

[24] D.E Williams and B. Friedland, "Design of An Autopilot for Bank-To-Turn Homing Missile Using Modern Control and Estimation Theory," Proc Fifth Meeting of the Coordinating Group on Modern Control Theory, 15-27 October 1983, (Picatinny) Dover, New Jersey, October 1983, pp. 397-419.

[25] B. Friedland, et al., "On the "Adiabatic Approximation for Design of Control Laws for Linear, Time-Varying Systems," IEEE Transactions on Automatic Control, Vol. AC- 32, No. 1, pp. 62-63, January 1987.

[26] D.W. Tufts and D.A. Shnidman, "Optimum Waveforms Subject to Both Energy and Peak-Value Constraints," Proceedings of the IEEE, September 1964.

[27] M. Pontier and J. Szpirglas, "Linear Stochastic Control with Constraints, IEEE Transactions on Automatic Control, Vol. AC-29, No. 12, pp 1100-1103, December 1984.

[28] P.-O. Gutman and S. Gutman, "A Note on the Control of Uncertain Linear Dynamical Systems with Constrained Control Input," IEEE Transactions on Automatic Control, Vol. AC-30, No. 5, pp 484-486, May 1985.

[29] M.W. Spong, J.S. Thorp, and J.M. Kleinwaks, "The Control of Robot Manipulators with Bounded Input," IEEE Transactions on Automatic Control, Vol. AC-31, No. 6, pp 483-489, June 1986.

[30] D. Feng and B.H. Krogh, "Acceleration-Constrained Time Optimal Control in n Dimensions," IEEE Transactions on Automatic Control, Vol. AC-31, No. 10, pp 955-958, October 1986.

[31] B.R. Barmish and W.E. Schmitendorf, "New Results on Controllability of Systems of the Form $\dot{x}(t) = A(t)x(t) + F(t,u(t))$," IEEE Transactions on Automatic Control, Vol. AC-25, No. 3, pp 540-547, June 1980.

[32] W.-G. Hwang and W.E. Schmitendorf, "Controllability Results for Systems with a Nonconvex Target," IEEE Transactions on Automatic Control, Vol. AC-29, No. 9, pp 794-802, September 1984.

[33] T. Kaliath, Linear Systems, Prentice-Hall, Inc., Englewood Cliffs, New Jersey, 1980.

[34] M. Vidyasager, Nonlinear Systems Analysis, Prentice-Hall, Englewood Cliffs, New Jersey, 1978.

[35] K. Zhou, and P. Khargonekar, "Stability Robustness Bounds for Linear State-Space Models with Structured Uncertainity," Transactions on Automatic Control, Vol. AC- 32, No. 7, pp 621-623, July 1987.

[36] K.G. Shin and N.D. McKay, "Minimum Time Control of Robotic Manipulators with Geometric Path Constraints," IEEE Transactions on Automatic Control, Vol. AC-30, No. 6, pp 531-541, June 1985.

[37] A. Sabari and H. Khalil, "Stabilization and Regulation of Nonlinear Singularly Perturbed Systems - Composite Control," IEEE Transactions on Automatic Control, Vol. AC- 30, No. 8, pp. 739-747, August 1985.

[38] M. Sampei and K. Furuta, "On Time Scaling for Nonlinear Systems: Application to Linearization," IEEE Transactions on Automatic Control, Vol. AC-31, No. 5, pp 459-462, May 1986.

[39] I.J. Ha and E.G. Gilbert, "A Complete Characterization of Decoupling Control Laws for a General Class of Nonlinear Systems," IEEE Transactions on Automatic Control, Vol. AC- 31, No. 9, pp. 823-830, September 1986.

[40] H. Kwakernaak and R. Sivan, Linear Optimal Control Systems, Wiley-Interscience, New York, 1972.

[41] R.A. Singer, "Estimating Optimal Tracking Filter Performance for Manned Maneuvering Targets," IEEE Transactions on Aerospace and Electronic Systems, Vol. AES- 6, No. 4, pp 473-483, July 1970.

[42] M.E Warren and T.E. Bullock, "Development and Comparison of Optimal Filter Techniques with Application to Air-to-Air Missiles," Electrical Engineering Department, University of Florida, Prepared for the Air Force Armament Laboratory, Eglin Air Force Base, Florida, March 1980.

BIOGRAPHICAL SKETCH

Donald J. Caughlin, Jr., was born in San Pedro, California on 17 Dec. 1946. He graduated from the United States Air Force Academy, earning a B.S. in physics, and chose pilot training instead of an Atomic Energy Commission Fellowship. Since then he has flown over 3100 hours in over 60 different aircraft and completed one tour in Southeast Asia flying the A-1 Skyraider. A Distinguished Graduate of the United States Air Force Test Pilot School, Don has spent much of his career in research, development, and test at both major test facilities--Eglin AFB in Florida, and Edwards AFB in California.

Don Caughlin is a Lieutenant Colonel in the United States Air Force currently assigned as the Assistant for Senior Officer Management at Headquarters Air Force Systems Command.

In addition to the B.S. in physics, Lt. Colonel Caughlin has an M.B.A. from the University of Utah, and a masters degree in electrical engineering from the University of Florida. He is a member of the Society of Experimental Test Pilots and IEEE.

Lt. Colonel Caughlin is married to the former Barbara Schultz of Montgomery, Alabama. They have two children, a daughter, Amy Marie, age eight, and Jon Andrew, age four.